TL1A IS A CENTRAL REGULATOR OF GROUP 3 INNATE LYMPHOID CELL FUNCTION IN COLITIS

A Dissertation

Presented to the Faculty of Weill Cornell Graduate School

of Medical Sciences

in Partial Fulfillment of the Requirements for the Degree of

Doctor of Philosophy

by

Jim Gonzalez Castellanos

December 2018

TL1A IS A CENTRAL REGULATOR OF GROUP 3 INNATE LYMPHOID CELL FUNCTION IN COLITIS

Jim Gonzalez Castellanos, Ph.D.

Cornell University 2018

Inflammatory bowel disease (IBD) results from a dysregulated interaction between the microbiota and a genetically susceptible host. Genetic studies have linked *TNFSF15* polymorphisms and its protein TNF-like ligand 1A (TL1A) with IBD, but the functional role of TL1A in linking tissue homeostasis and intestinal inflammation is not known. Here, using cell-specific genetic deletion models, we report an essential role for CX_3CR1^+ mononuclear phagocyte (MNP) TL1A in signaling through its cognate receptor death receptor 3 (DR3) on group 3 innate lymphoid cell (ILC3) to promote IL-22 dependent protection during acute colitis. Induction of intestinal MNP TL1A by IBD-associated adherent microbes confers TL1A-dependent protection from acute colitis. However, in contrast to this protective role in acute colitis, colitis-induced DR3-dependent expression of OX40L enables $MHCII^+$ ILC3 to co-stimulate antigen-specific T cell proliferation and exacerbate chronic T cell-dependent colitis. Colonic biopsies from IBD patients revealed increased TL1A expression on MNPs and OX40L on ILC3 compared to healthy controls, highlighting the conserved TL1A-OX40L ILC3 axis in IBD. These results identify the mechanistic contributions of this IBD-linked pathway as a central regulator of ILC3 function in tissue homeostasis.

BIOGRAPHICAL SKETCH

Jim Gonzalez Castellanos was born on July 31st, 1983 in Santa Ana, California to Transito and Martha Castellanos. He was raised in Chino Hills, California, where he graduated from Ruben S. Ayala High School in 2001.

After high school, Jim enlisted in the United States Marine Corps as an aviation ordnance technician, where he specialized on the weapon systems for Marine Corps attack helicopters. In 2004, Jim deployed to Iraq where he completed a seven-month combat tour in support of Operation Iraqi Freedom. In 2007, Jim was honorably discharged from the Marine Corps with the rank of Corporal, having been awarded numerous medals and decorations for his service. After completing his military service, Jim enrolled at Claremont McKenna College, where he graduated with a Bachelor of Arts in Biology degree in 2009. After college, Jim completed a Master of Fine Arts in Creative Writing at the University of Arizona, where his thesis work focused on a collection of personal essays exploring the ethical and moral terror of war. So it goes…

Currently, Jim is pursuing a combined MD-PhD at the Weill Cornell/Rockefeller/Sloan-Kettering Tri-institutional MD-PhD program. Under the direction of Dr. Randy Longman, Jim is completing his doctoral research on the role for TL1A in intestinal inflammation.

ACKNOWLEDGEMENTS

First, I'd like to thank my early mentors Drs. Lawrence Steinman and Robert Axtell, who introduced me to the world of immunology; for this marriage, I blame you both.

A tremendous, heartfelt *thank you* goes to my thesis mentor, Dr. Randy Longman. I'm not sure which one of us gambled more—you taking me on as your first student or me taking you on as your first student—but the gamble paid off on unimaginable levels. You taught me immunology, you taught me about the microbiome, you expanded my concept of what it means to lead a group of scallywag scientists, but mostly you taught me how to *think*. For that, and for your friendship, I am eternally grateful. I'd like to thank all members of the Longman Lab, past and present: Drs. Lasha Gogohkia and Svetlana Lima for the reminders that if I ever fail scientifically, I can always "just" be a doctor; to Maeva Metz for reminding me that "work/life balance" really is a thing I should adopt; a special acknowledgement goes out to Dr. Monica Viladomiu for teaching me the nuances of lab life and for being gifted a level of patience that belongs among the mythological queens of Greece—you are truly a gem. Finally, I'd like to thank our technician/manager/lab mom Viola Woo for all her genotyping, gut preps, food recommendations and motivational glances—without you this Ph.D. would have truly been a struggle. To our past lab technicians Charlie Kivolowitz and Danny Victorio for feeling the early struggle.

Next, I'm grateful for all the wonderful members of the Jill Roberts Institute for Research in Inflammatory Bowel Disease for their helpful discussions, including Benji Grigg, Drs. Tanel Mahlakõiv, Nick Bessman, and Anne-Laure Flamar, especially, for teaching me flow cytometry.

I'd like to thank my thesis committee members Drs. David Artis, Daniel Mucida and Joseph Sun for all their insightful comments and for always demanding more from me as a scientist. I'd like to acknowledge the Tri-Institutional MD-PhD program for making all this possible: Drs. Olaf Andersen, Ruth Gotian and the MD-PhD administrators for running such a flawless program; also to the NIH MSTP grant T32GM07739 for their support.

Finally, I'd like to thank all my family and friends: my thirteen MD-PhD classmates—we navigated this process together and you will always have a special place in my heart. To my childhood friends Diego, Mark, Richard and Vic—you four are my sanity check when things get real. Lastly, I'd like to thank my sisters Veronica, Jenny and Kelly—words cannot explain how much your love and support has helped me through this training. Mom and dad, this Ph.D. is for you!

TABLE OF CONTENTS

LIST OF FIGURES

LIST OF TABLES

LIST OF ABBREVIATIONS

Abx	antibiotic
AIEC	Adherent-invasive E. coli
APC	antigen presenting cell
C. rodentium	*Citrobacter rodentium*
CCR6	chemokine receptor 6
CD	Crohn's disease
cDNA	complementary DNA
CFSE	carboxyfluorescein succinimidyl ester
CRE	cre recombinase
CX3CR1	CX3C chemokine receptor (a.k.a. fractalkine receptor)
DMEM	Dulbecco's modified eagles media
DMSO	dimethylsulfoxide
DR3	Death Receptor 3
DSS	dextran sodium sulfate
DTR	diptheria toxin receptor
DTT	Dithiothreitol
EDTA	ethylenediamine tetraacetic acid
ES	embryonic stem
FACS	fluorescence-activated cell sorting
FBS	fetal bovine serum
Foxp3	forkhead box P3
FRT	Flippase recognition target
GF	germ-free
GFP	green fluorescent protein
GM-CSF	granulocyte-macrophage colony-stimulating factor

GWAS	genome wide association study
IBD	Inflammatory Bowel Disease
ICOSL	ICOS Ligand
IFN-γ	interferon-γ
IgG	immunoglobulin
ILC	Innate Lymphoid Cell
ILC1	Group 1 Innate Lymphoid Cell
ILC2	Group 2 Innate Lymphoid Cell
ILC3	Group 3 Innate Lymphoid Cell
IL-1R	Interleukin-1 receptor
IL-17	Interleukin-17
IL-22	Interleukin-22
IL-23	Interleukin-23
IL-23R	Interleukin-23 receptor
KO	knockout
Lin^-	lineage negative
loxP	locus of X-over P1
IP	intraperitoneal
i.v.	intravenous
IACUC	Institutional Animal Care and Use Committee
LPMC	lamina propria mononuclear cell
LPS	lipopolysaccharide
MAPK	mitogen-activated protein kinase
MFI	mean fluorescent intensity
MHCII	major histocompatibility complex II
MLN	mesenteric lympho node

MNP	mononuclear phagocyte
mRNA	messenger RNA
MyD88	myeloid differentiation primary response 88
NKp46	natural cytotoxicity receptor
OVA	ovalbumin
OX40L	OX40 Ligand
OTII	Ovalbumin Transgenic T cell receptor II
PBS	phosphate buffered saline
PCR	polymerase chain reaction
PMA	phorbol myristate acetate
qPCR	quantitative polymerase chain reaction
RAG2	Recombination activating gene 2
RNA	ribonucleic acid
RNA-seq	ribonucleic acid sequencing
RORɣt	RAR-related orphan receptor-ɣ
RPMI	Roswell Park Memorial Institute medium
SFB	segmented filamentous bacteria
SPF	specific pathogen free
T-bet	T-box transcription factor TBX21
TL1A	TNF-like Ligand 1A
TLR	Toll-like receptor
TNFRSF25	Tumor Necrosis Factor Receptor Super Family member25
TNFSF4	Tumor Necrosis Factor Super Family member 4
TNFSF15	Tumor Necrosis Factor Super Family member 15
UC	Ulcerative colitis
WT	wild-type

CHAPTER ONE: INTRODUCTION

1.1 TL1A in Inflammatory Bowel Disease

Inflammatory bowel disease (IBD) affects over 4 million people worldwide, causing significant morbidity among patients[1]. IBD pathogenesis is thought to be multifactorial, with both intestinal dysbiosis and genetic components underlying disease pathogenesis. Characteristic alterations in the IBD-associated microbiome exist, with marked contraction of intestinal microbial diversity a hallmark of IBD[2]. Genetic studies have identified over 200 genes linked with IBD[3], but our functional understanding of how these genes contribute to intestinal homeostasis and IBD pathophysiology is incomplete, limiting the potential for diagnostic and therapeutic intervention.

Genome-wide association studies (GWAS) in IBD have revealed the strongest associations of genetic variants in *TNFSF15* with Crohn's disease, highlighting a central role for its protein, TNF-like cytokine 1A (TL1A), in mucosal immunity[4]. TL1A, also known as vascular endothelial growth factor-251, is a member of the Tumor Necrosis Factor Superfamily (TNFSF) of ligands (TL1A is *TNFSF15*). In humans, TL1A consists of 251 amino acids and it shares approximately 30% homology with other TNF super family members, with the closest homology being TNF-α. On the cellular surface, TL1A is expressed of a membrane-bound protein (192 amino acids in the

extracellular domain, 24 in the transmembrane region and 35 amino acids in the cytoplastic tail), and is released as a soluble protein via cleavage by the metalloproteinase TNF-α converting enzyme, also known as TACE[5,6].

Genetically, variants in *TNFSF15* have been linked to the pathogenesis of several autoimmune diseases—including psoriasis[7–10], rheumatoid arthritis[11–19], and multiple sclerosis[20–22]—implicating a broader role for TL1A in human inflammatory diseases. In human patients, elevated TL1A is often detected at the site of inflammation, including the joints in rheumatoid arthritis (chondrocytes)[11,23], in the intestinal tissue of IBD patients (mononuclear phagocytes)[24] and in endothelial cells[25,26]. Over the past decade, numerous studies have illustrated a role for TL1A's monogamous receptor, death receptor 3 (DR3), in regulating lymphocyte cell function, with DR3 being predominantly expressed on lymphocyte populations and contributing to disease pathophysiology at mucosal barrier sites, including the intestine (Figure 1.1)[4,24,27,28]. In IBD, *TNFSF15* variants confer higher risk for more aggressive, penetrating, fibrostenotic, and perianal disease complications[29,30], but the mechanistic impact of TL1A remains controversial. While early studies revealed a pathogenic role for TL1A in driving inflammatory T cell response[28,31] more recent reports in acute colitis models revealing a protective role for TL1A[32]. Genetic models are needed to understand the cellular mechanisms and potential therapeutic targetability of this IBD-linked pathway in intestinal inflammation.

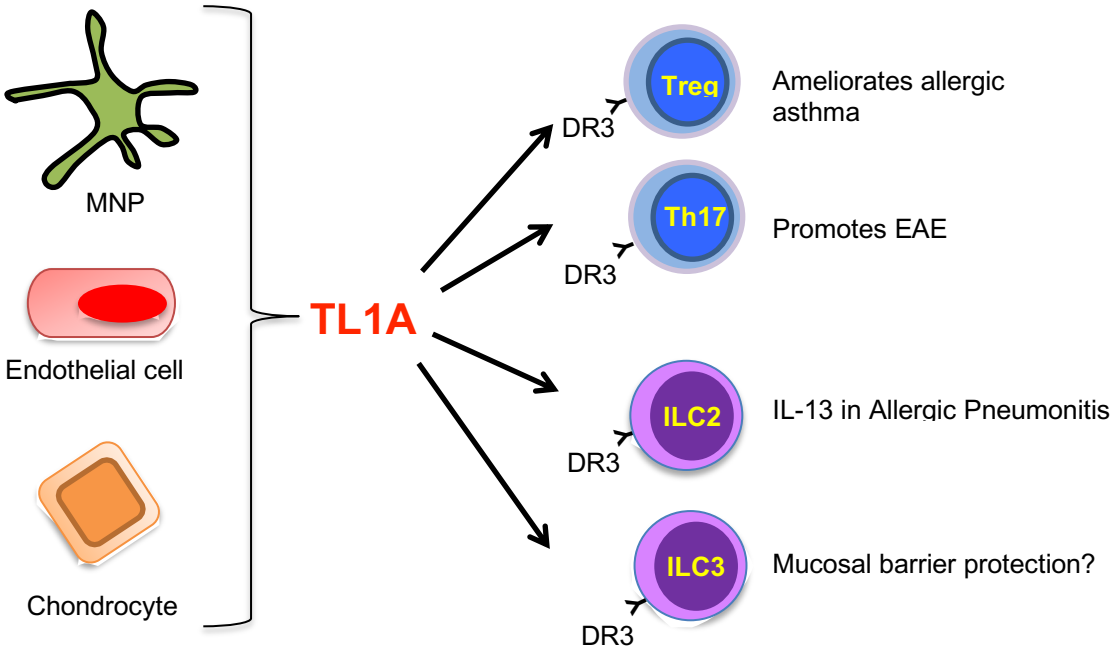

Figure 1.1. TL1A-DR3 axis regulates lymphocyte function. TL1A can be produced by a variety of cells, including MNP, endothelial cells and chondrocytes. TL1A binds to its receptor DR3 to regulate various lymphocytes functions, including ameliorating allergic asthma via T regs, promoting EAE pathophysiology via Th17, propagating allergic pneumonitis via ILC2-derived IL-13; however the role for DR3 in regulating ILC3 effector functions in the intestine has not been explored. Abbreviations: MNP (mononuclear phagocyte), TL1A (TNF-like ligand 1A), DR3 (Death Receptor 3), T reg (T regulatory cell), Th17 (T-helper 17 cell) , EAE (experimental autoimmune encephalomyelitis) ILC2 (Group 2 Innate Lymphoid Cell), ILC3 (Group 3 Innate Lymphoid Cell).

1.2 Mononuclear phagocytes and TL1A

The innate immune response plays a central role in coordinating mucosal homeostasis[24]. As sentinels of barrier immunity, CX_3CR1^+ mononuclear phagocytes (MNPs) can extend transepithelial dendrites and integrate signals from the luminal microbiota[33]. These microbial signals act to reinforce intestinal compartmentalization by restricting migration of MNPs containing non-invasive luminal microbiota to secondary lymph organs[34]. Under inflammatory colitis, MNPs producing IL-23 and IL-1β expand within the lamina[35–37]and promote both T helper cell 17 (Th17)[38] and Group 3 innate lymphocyte cell (ILC3)[24] mucosal responses (Figure 1.2). MNP production of CXCL16 promotes spatial co-localization with $CXCR6^+$ $NKp46^+$ ILC3s enabling rapid regulation of ILC3 effector cytokines to reinforce the barrier[39,40]. While recognition of stereotypical danger signals and spatial proximity within the lamina propria endows the innate immune system with the ability to swiftly respond to barrier injury, fine-tuning of this response is needed to confer selectivity and specificity. We recently showed that intestinal CX_3CR1^+ MNP produce TL1A whose gene, *TNFSF15*, encodes functional polymorphisms strongly associated with IBD[24]. Early studies showed that immune complex[41] and microbial[42] stimulation of antigen presenting cells induced TL1A *in vitro* and acted as a co-stimulator of T helper cell 1 (Th1) inflammation[28].

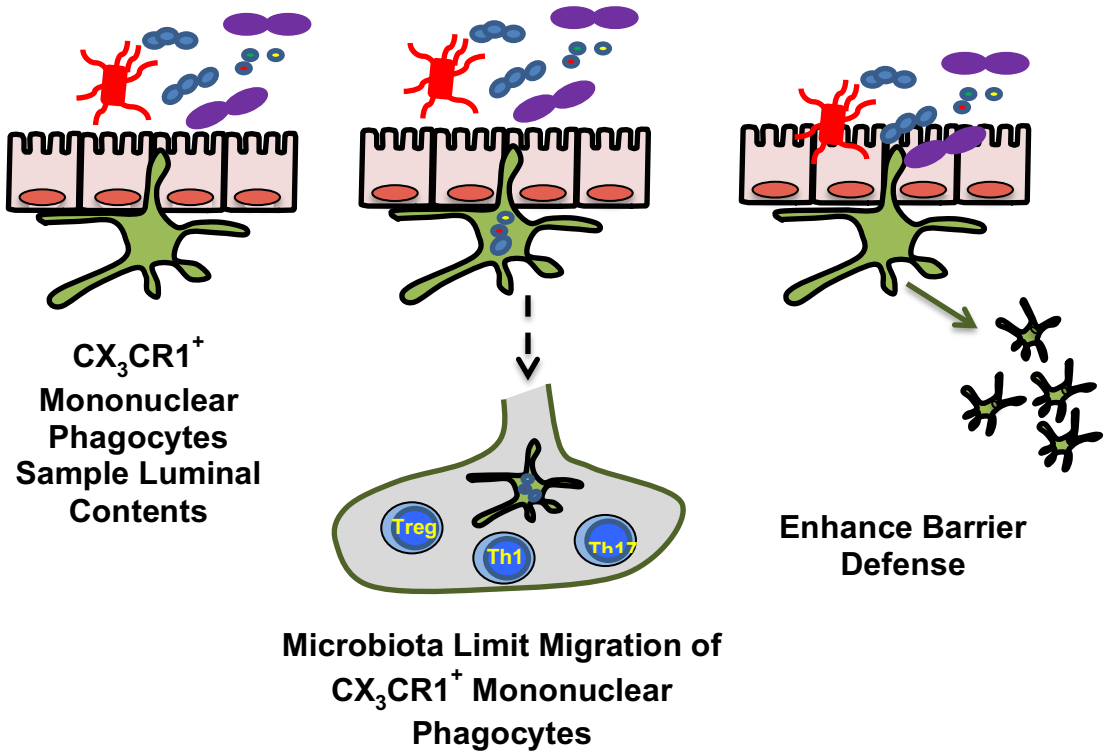

Figure 1.2. Functional roles for CX_3CR1^+ mononuclear phagocytes in intestinal barrier immunity. CX_3CR1^+ MNP reside in the intestinal lamina propria and can extend transepithelial dendrites and integrate signals from the luminal microbiota to coordinate intestinal immune responses. These microbial signals act to reinforce intestinal compartmentalization by restricting migration of MNPs containing non-invasive luminal microbiota to secondary lymph organs. During colitis, MNPs expand within the lamina and modulate lymphocyte effector functions via the secretion of IL-23 and IL-1β. Abbreviations: MNP (mononuclear phagocyte), T reg (T regulatory cell), Th1 (T helper 1 cell), Th17 (T helper 17 cell) .

Subsequent studies revealed the ability to enhance Th17 effector function[21,43] and promote T regulatory cell (T reg) ability to ameliorate allergic asthma[44].

More recent studies have illustrated a role for TL1A's monogamous receptor DR3 in regulating innate lymphoid cell function. In a helminth infection model, DR3-deficient mice show increased susceptibility to infection secondary to a reduction in IL-13 production by ILC2s[45]. Additionally, parallel to the co-stimulator effect of TL1A on T cells, *in vitro* stimulation of ILC3 with TL1A synergizes with IL-23 to enhance effector cytokine production[24]. Although sustained overexpression of TL1A leads to chronic T cell-mediated colitis in mouse model[27,31], recent studies in acute colitis models showing a protective role for DR3[32] highlight the need to understand the contribution of this pathway in innate immunity.

1.3 Group 3 Innate Lymphoid Cells and TL1A

Recent advances in sequencing technology have identified both microbial and host genetic factors with IBD and genome-wide association studies have identified over 160 genetic susceptibility loci[3,46,47]. Genetic polymorphisms at the *IL23R* locus correlate with susceptibility to both Crohn's Disease (CD) and ulcerative colitis (UC), focusing attention on IL-23-responsive lymphocytes[48–61]. An emerging group of innate lymphocyte that respond to IL-23 and express the

transcription factor RORγt have been characterized as group 3 innate lymphoid cells (ILC3).

ILC3 are innate lymphocytes that play a critical role in regulating mucosal homeostasis. In response to environmental triggers, in particular the cytokines IL-23 and IL-1β, ILC3 produce robust amounts of IL-22 and play an important role in maintaining intestinal barrier integrity and promoting mucosal healing—a major clinical endpoint in IBD[24]. Co-localization of ILC3 with CX_3CR1^+ MNPs in the lamina propria enables rapid regulation of ILC3 effector cytokines to reinforce barrier immunity and mucosal healing[40]. In response to IL-23, ILC3 produce robust amounts of IL-22, a cytokine that acts on epithelial cells to promote healing. Recently, our lab identified that IBD patients with mild to moderate colitis have significantly higher IL-22 production by ILC3. The production of IL-22 in human IBD correlated with mucosal exposure to the fecal stream[24]. Similarly, studies using germ-free mice have established that ILC3 effector cytokine function, including IL-22 production, is dependent on intestinal microbiota-derived signals[40]. At the steady-state, signaling by commensal organisms may negatively-regulate ILC3-derived IL-22 via intestinal epithelial cell production of IL-25[62]; however, during experimental infectious colitis in mouse models and human IBD, intestinal microbial signals are not only required, but may actively enhance IL-22 production by ILC3[39]. Intestinal MNPs expressing the fractalkine receptor CX_3CR1^+ interact with these intestinal microbes via their transepithelial dendrites and play a central role in integrating

the “crosstalk” between commensal microbes and effector lymphocytes, including ILC3[24,33,63]. Furthermore, CX_3CR1^+ MNPs can migrate to secondary lymphoid organs and expand in the lamina propria during human and mouse colitis[34]. These MNPs play a critical role in recruiting $CXCR6^+$ ILC3 via CXCL16 production and regulating ILC3 production of both IL-22 and GM-CSF[24,40]. While both MNP-derived IL-23 and IL-1b are potent regulators of these ILC3 effector cytokines, the mechanisms underlying the cellular dialogue between CX_3CR1^+ MNP and ILC3, and in particular, the role for TL1A in regulating ILC3 function in intestinal homeostasis, and its potential contribution to IBD pathophysiology, remain unknown (Figure 1.3). Thus, the major aim of my thesis work has been to understand the potential role for CX_3CR1^+ MNP-derived TL1A signaling through DR3 in coordinating ILC3-dependent barrier immunity.

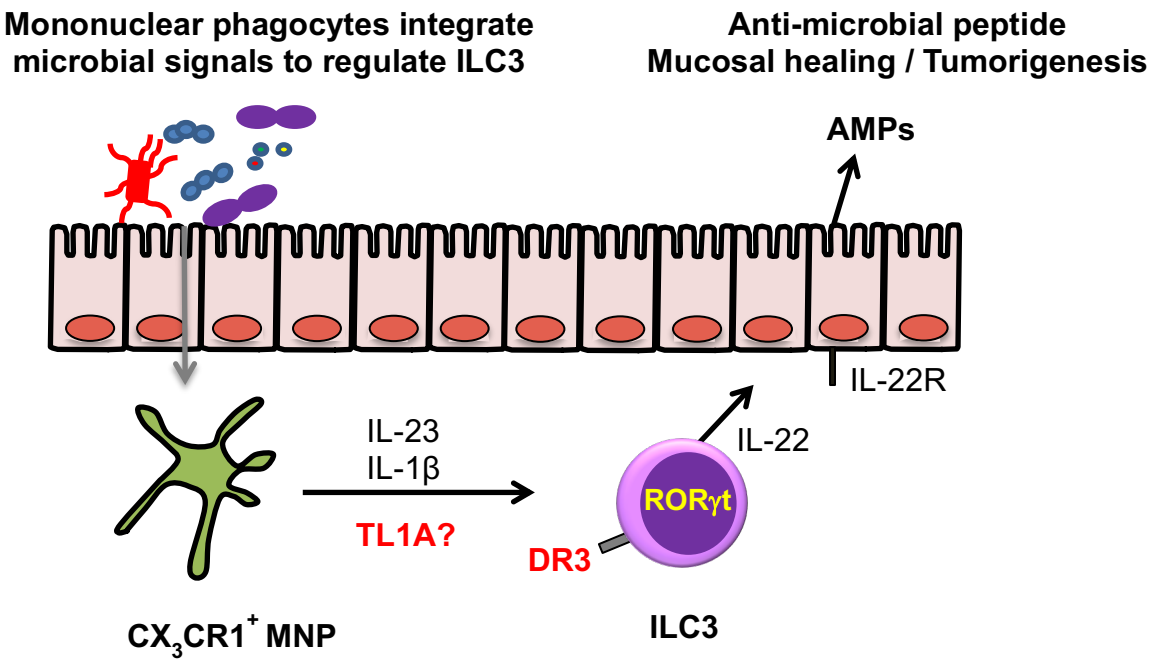

Figure 1.3. Potential role for CX_3CR1^+ MNP-derived TL1A signaling through DR3 in coordinating ILC3-dependent barrier immunity. CX_3CR1^+ MNP integrate signals from the microbiota and promote mucosal healing by regulating ILC3 production of IL-22 via IL-23 and IL-1β. Does CX_3CR1^+ MNP -derived TL1A promote intestinal barrier integrity and mucosal healing by regulating barrier immunity?

CHAPTER TWO: MONONUCLEAR PHAGOCYTE TL1A PROMOTES BARRIER PROTECTION DURING ACUTE INFLAMMATION

2.1 ABSTRACT

Inflammatory bowel disease (IBD) results from a dysregulated interaction between the microbiota and a genetically susceptible host. Genetic studies have linked *TNFSF15* polymorphisms and its protein TNF-like ligand 1A (TL1A) with IBD, but the functional role of TL1A in linking tissue homeostasis and intestinal inflammation is not known. Here, using cell-specific genetic deletion models, we identified CX_3CR1^+ mononuclear phagocytes (MNP) as the main producer of intestinal TL1A in both mouse and humans, with IBD patients upregulating TL1A during active colitis. Furthermore, we report an essential role for CX_3CR1^+ MNP TL1A in promoting IL-22 dependent protection during acute colitis. Induction of TL1A by MNP was microbiota-dependent and potently induced by IBD-associated adherent-invasive microbes, conferring TL1A-dependent protection from acute colitis.

2.2 INTRODUCTION

The innate immune response plays a central role in coordinating mucosal homeostasis[24]. As sentinels of barrier immunity, CX_3CR1^+ mononuclear phagocytes (MNPs) can extend transepithelial dendrites and integrate signals from the luminal microbiota[33]. These microbial signals act to reinforce intestinal compartmentalization by restricting migration of MNPs containing non-invasive luminal microbiota to secondary lymph organs[34]. Under inflammatory colitis, MNPs producing IL-23 and IL-1β expand within the lamina propria[35–37] and promote both Th17[38] and ILC3[24] mucosal responses. MNP production of CXCL16 promotes spatial co-localization with $CXCR6^+$ $NKp46^+$ ILC3s enabling rapid regulation of ILC3 effector cytokines to reinforce the barrier[40]. While recognition of stereotypical danger signals and spatial proximity within the lamina propria endows the innate immune system with the ability to swiftly respond to barrier injury, fine-tuning of this response is needed to confer selectivity and specificity. We recently showed that intestinal CX_3CR1^+ MNP produce TL1A whose gene, *TNFSF15*, encodes functional polymorphisms strongly associated with IBD[24]. Early studies showed that immune complex[41] and microbial[42] stimulation of antigen presenting cells induced TL1A *in vitro* and acted as a co-stimulator of Th1 inflammation[28]. Subsequent studies revealed the ability to enhance Th17 effector function[21,43] and promote T reg ability to ameliorate

allergic asthma[44]. More recent studies have illustrated a role for TL1A's monogamous receptor DR3 in regulating innate lymphoid cell function. In a helminth infection model, DR3-deficient mice show increased susceptibility to infection secondary to a reduction in IL-13 production by ILC2[45]. Additionally, parallel to the co-stimulator effect of TL1A on T cells, *in vitro* stimulation of ILC3 with TL1A synergizes with IL-23 to enhance effector cytokine production[24]. Although sustained overexpression of TL1A leads to chronic T cell-mediated colitis in mouse models[27,31], recent studies in acute colitis models have demonstrated a protective role for DR3[32], highlighting the need to understand the role of this IBD-associated pathway in innate immunity.

2.3 METHODS

Mice. C57BL/6, *CD11c-cre*, *Cx3cr1*^{GFP}, and *Cx3cr1*^{CreER} mice were purchased from The Jackson Laboratory. *MyD88*$^{-/-}$ were kindly provide by Julie Blander at Weill Cornell Medical College. CX_3CR1-DTR mice were previously described[34]. *TL1A*$^{flox/flox}$ mice were generated as follows: Tl1a endogenous locus containing 4.5 bp upstream and 3.4 bp downstream of exon 1 were generated by PCR amplification using proprietary C57BL/6J library developed at genOway. Subsequently, two loxP sites were inserted flanking Tl1a exon 1. Positive selection neomycin gene flanked by FRT sites was inserted to the intron after exons 1 to generate the targeting vector. Every step of the cloning process was validated through restriction enzyme analysis and sequencing. The Tl1a gene targeting construct was linearized and electroporated into embryonic stem (ES) cells with C57BL/6J background. Homologous recombinants were selected by G418 and confirmed by PCR and Southern blot analysis. ES clones with correct 5' and 3' recombination were microinjected into C57BL/6J blastocysts and introduced into pseudopregnant C57BL/6J mice. Male chimeric offspring were bred to obtain germ line mutant mice, which were then bred to flpe delete mouse strain to remove the neomycin cassette and were confirmed by Southern blot. For CX3CR1 depletion studies using Cx3cr1^{DTR} mice, diptheria toxin was i.p. injected (200ng/200uL) for two consecutive days and then every 72 hours to maintain depletion. All experiments were performed with 6-8 week old littermates with random and equal assignment of same sex to each

experimental group. All vertebrate work was approved by the IACUC at Weill Cornell Medicine.

Human IBD subjects. A cohort of patients was evaluated for IBD at the Jill Roberts Center for IBD under Institutional Review Board–approved protocol (1103011578) at Weill Cornell Medicine (WCM). Healthy control patients presented with abdominal pain but had normal endoscopic results; IBD patients were defined as having endoscopic inflammation with a history of ulcerative colitis or Crohn's disease. All endoscopic biopsies were taken from the colon. Endoscopic biopsies from healthy control and IBD patients were transported in ice cold PBS and processed as previously reported[24].

Preparation of LPMC. Mouse intestines were washed in PBS and 1 mM DTT with 30 mM EDTA, and then digested in collagenase 8 (Sigma-Aldrich) and DNase-containing media with 10% fetal bovine serum. Digested material was passed through a cell strainer and separated by a 40% Percoll gradient. For intracellular cytokine staining, LPMCs were cultured ex vivo in the presence of GolgiPlug (BD) for 4 h or stimulated with phorbol myristate acetate (PMA; 20 ng/ml) and ionomycin (1 μg/ml) or IL-23 (40 ng/ml; eBioscience) in the presence of GolgiPlug (BD) for 4 h before staining. All TL1A detection was done by extracellular flow cytometry staining.

Antibodies and flow cytometry. Staining of cells was performed with the following antibodies:

Table 2.1 Flow cytometry antibodies used in chapter 2.

Species	Target	Fluorophore	Clone	Manufacturer
Mouse	CD3	FITC	145-2C11	eBioscience
Mouse	CD4	eFluor780	RM4-5	eBioscience
Mouse	CD5	PE	53-7.3	eBioscience
Mouse	MHCII	Alexa700	M5/114.15.2	eBioscience
Mouse	F4/80	PE	BM8	eBioscience
Mouse	CD19	FITC	MB19-1	eBioscience
Mouse	CD11b	eFluor780	M1/70	eBioscience
Mouse	CD11c	PE-Cy7	N418	eBioscience
Mouse	CD103	APC	2E7	eBioscience
Mouse	TCR$\gamma\delta$	FITC	11-5711-82	eBioscience
Mouse	KLRG1	PE	2F1	eBioscience
Mouse	CD127	PE-Cy7	A7R34	BioLegend
Mouse	CCR6	BV421	29-2L17	BioLegend
Mouse	DR3	PE	4C12	BioLegend
Mouse	RORγt	PE	B2D	eBioscience
Mouse	T-bet	e660	eBio4B10	eBioscience
Mouse	Foxp3	e450	FJK-16s	eBioscience
Mouse	IL-22	APC	IL22JOP	eBioscience
Mouse	IL-17	PE	eBio17B7	eBioscience
Mouse	IFNγ	PE-Cy7	XMG1.2	eBioscience
Mouse	TL1A	e710	Tandys1a	eBioscience
Human	CD14	PE	61D3	eBioscience
Human	CD14	Alexa700	63D3	eBioscience
Human	HLA-DR	Alexa700	LN3	eBioscience
Human	TL1A	e710	Tandys1a	eBioscience
Human	CD45	APC	2D1	eBioscience
Human	CD3	eFluor780	UCHT1	eBioscience
Human	CD19	Alexa700	HIB19	eBioscience
Human	CD127	PE-Cy7	eBioRDR5	eBioscience
Human	CD117	efluor450	104D2	eBioscience
Human	CD5	eFluor780	UCHT1	BioLegend
Human	CD11c	Alexa700	3.9	Invitrogen

Dead cells were excluded using the Live/Dead fixable aqua dead cell stain kit (Invitrogen). Intracellular cytokine staining was performed according to the manufacturer's protocol (Cytofix/Cytoperm buffer set; BD) and transcription factor staining for was performed according to manufacturer's protocol (Intracellular Fixation and Permeabilization kit; eBioscience). Flow cytometry was performed with a BD LSRFortessa and analyzed with FlowJo software (Tree Star).

Colitis models. To induce chemical colitis in mice, 2% DSS (w/v) (M.W. 40,000-50,000; Affymetrix) was added to sterile drinking water and administered ad libitum for 7 days. After 7 days, DSS was replaced with normal drinking water. To induce infectious colitis, mice were orally gavaged with log phase growth *Citrobacter rodentium* DBS100 (ATCC 51459; American Type Culture Collection) at $1x10^{10}$ in PBS. For all colitis experiments, mice were monitored daily (DSS) or weekly (T-cell transfer) for weight loss, rectal bleeding, diarrhea and survival throughout the experiments. For *in vivo* experiments using AIEC 2A, mice were pre-treated for 21 days with a broad-spectrum antibiotic cocktail of ampicillin (1g/L), neomycin (0.5g/L), metronidazole (0.5g/L) and vancomycin (0.5g/L) in their drinking water. Mice were then orally gavaged with $2x10^{9}$ of AIEC 2A before colitis induction with 2% DSS in their drinking water.

qPCR. RNA from primary intestinal cell populations was prepared with

TRIzol (Invitrogen) and purified RNA was reverse transcribed into cDNA (Quanta qScript). qPCR was performed with a QuantStudio 6 Flex Real-time PCR (Applied Biosystems) with SYBR Green Supermix (Bio-Rad Laboratories). The following primers were used: *Tnfsf15*: 5'-ATGCTTCGGGCCATAACAGA-3' and 5'-TGAAGGCCATCCCTAGGTCA-3'. *Hprt*: 5'-GAGGAGTCCTGTTGATGTTGCCAG-3' 5'-GGCTGGCCTATAGGCTCATAGTGC-3'.

The thermocycler program was as follows: initial cycle of 95°C for 60s, followed 40 PCR cycles at 95°C for 5s, 60°C for 15s, 72°C for 15s. Relative levels of the target genes were determined by using the $\Delta\Delta C_t$ of the target gene compared to *Hprt* expression.

Statistical analysis. Statistical analysis was performed in GraphPad Prism or R software. Results represent mean ± s.e.m. and were analyzed by unpaired Student's t-test, Mann-Whitney test, one-way ANOVA, Log-rank (Mantel-Cox) test, as indicated in the figure legends. Given that mouse experiments required littermate controls and complex genotyping, experimental group allocation was not blinded. No relevant exclusion criteria were applied.

2.4 RESULTS

2.4.1 Intestinal MNPs express high levels of TL1A

Previous reports have identified MNPs as a source of intestinal TL1A in mouse and humans[64]. TL1A can be expressed by many cell types, but the highest transcriptional levels of TNFSF15 is seen in antigen presenting cells. Mouse studies from our lab have previously published that CX_3CR1^+ MNPs express higher TNFSF15 than gut derived B cells, $CD103^+$ conventional dendritic cells, or $Ly6C^+$ monocytes[24]. To evaluate TL1A expression by human intestinal lymphocyte populations, we performed flow cytometry on lamina propria mononuclear cells from endoscopic biopsies from healthy patients undergoing routine coloscopy screening. Our flow cytometric analysis of human intestinal biopsies identified $CD14^+$/HLA-DR^{hi} intestinal MNPs during colitis as having significantly higher expression of TL1A compared to $CD3^+CD4^+$ T cells or $CD19^+$ B cells, consistent with our previous mouse studies identifying MNP as a dominant source of TL1A in the intestine (Figure 2.1)[24].

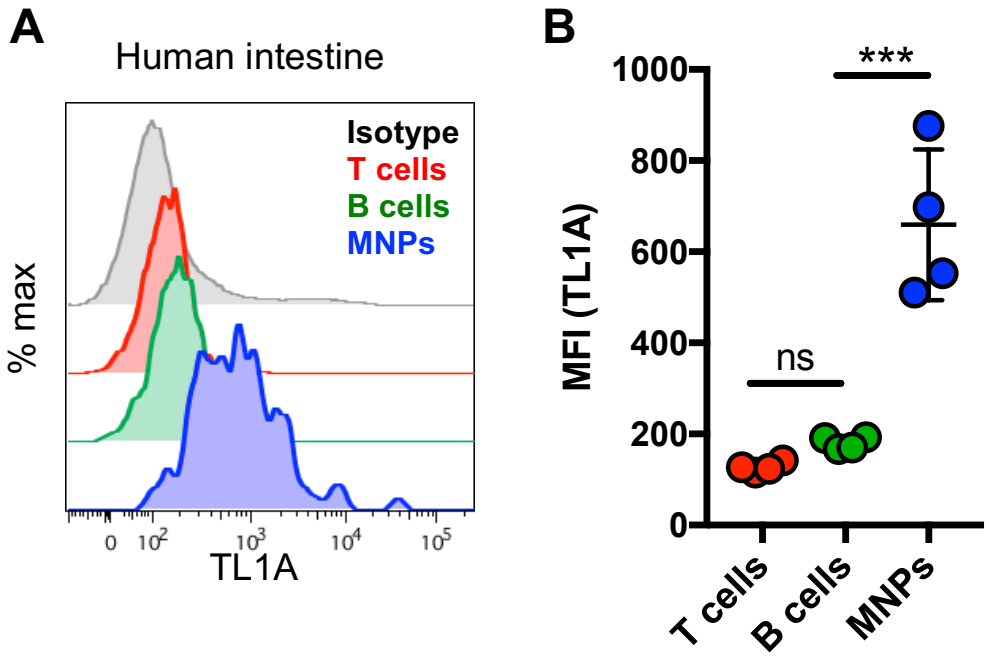

Figure. 2.1. Human MNP express TL1A. (**A, B**) T cells ($CD3^+CD4^+$), B cells ($CD19^+$) and MNPs ($CD14^+$ $HLA\text{-}DR^+$) were identified from human intestinal biopsies by flow cytometry (A) and TL1A surface expression is shown (B), (n = 4). Data in (B) are mean ± s.e.m and were analyzed by two-tailed Student's t-test; ***P<0.001.

2.4.2 Human MNP upregulate TL1A during colitis

CX_3CR1^+ MNPs play a central role in coordinating the ILC3-dependent mucosal response during colitis[24,39]. Recent studies have reported increased TL1A levels in the colonic tissue of both mouse and humans during active colitis[64]. To evaluate the contribution of TL1A expression by $CD14^+$/HLA-DR^{hi} intestinal MNPs, we performed flow cytometry on lamina propria mononuclear cells from endoscopic biopsies from healthy (N=7) and IBD patients (N=8) (Figure 2.2A). MNPs from IBD patients with active inflammation showed significantly higher surface expression of TL1A (Figure 2.2B).

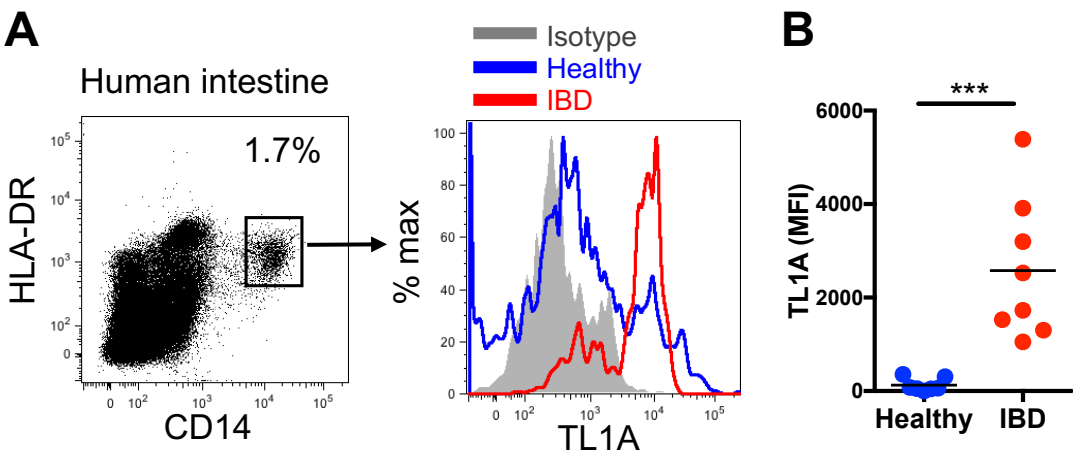

Figure. 2.2. Human MNP upregulate TL1A during colitis. (**A**, **B**) CD14^{+} HLA-DR^{+} MNPs were identified from human intestinal biopsies (IBD=8, Healthy=7) by flow cytometry and TL1A surface expression is shown. Data in (B) are mean ± s.e.m and were analyzed by two-tailed Student's t-test; ****P*<0.001.

2.4.3 CX_3CR1^+ MNPs are the dominant source of intestinal TL1A

Consistent with these data from human IBD, selective depletion of CX_3CR1^+ MNP using mice harboring a diphtheria toxin receptor insertion into the *Cx3cr1* locus ($CX3CR1^{DTR}$) following diphtheria toxin injection significantly reduced TL1A expression in the intestinal lamina propria (Figure 2.3).

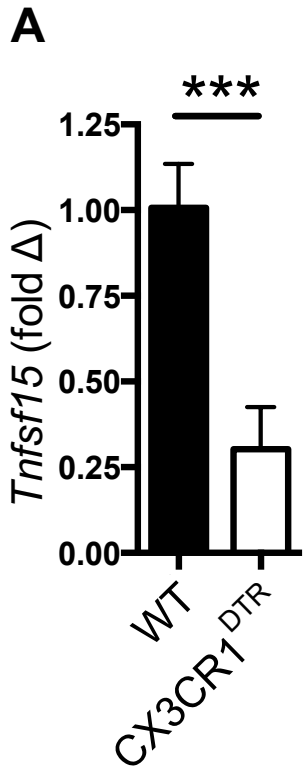

Figure. 2.3. CX_3CR1^+ MNP are the dominant source of intestinal TL1A. (**A)** TL1A expression by qPCR from intestinal lamina propria mononuclear cells from $CX3CR1^{DTR}$ mice or controls after DT toxin injection (n = 4 mice/group). Data in (B) are mean ± s.e.m and were analyzed by two-tailed Student's t-test. ****P*<0.001.

2.4.4 MNP-specific deletion of TL1A impairs wound healing

To evaluate the potential physiological role for MNP-derived TL1A in colitis, we generated a novel TL1A conditional knockout allele with *lox*P-flanked *Tnfsf15* (*TL1A*$^{flox/flox}$) and then crossed these mice to transgenic mice expressing the Cre recombinase under the CD11c promoter (*TL1A*$^{\Delta CD11c}$) (Figure 2.4A). TL1A mRNA expression in lamina propria CD11c^{+} cells was used to confirm deletion (Figure 2.4B). *TL1A*$^{\Delta CD11c}$ mice exposed *ad libitum* to 2% dextran sodium sulfate (DSS) for seven days lost significantly more weight than their littermate controls (Figure 2.4C,D).

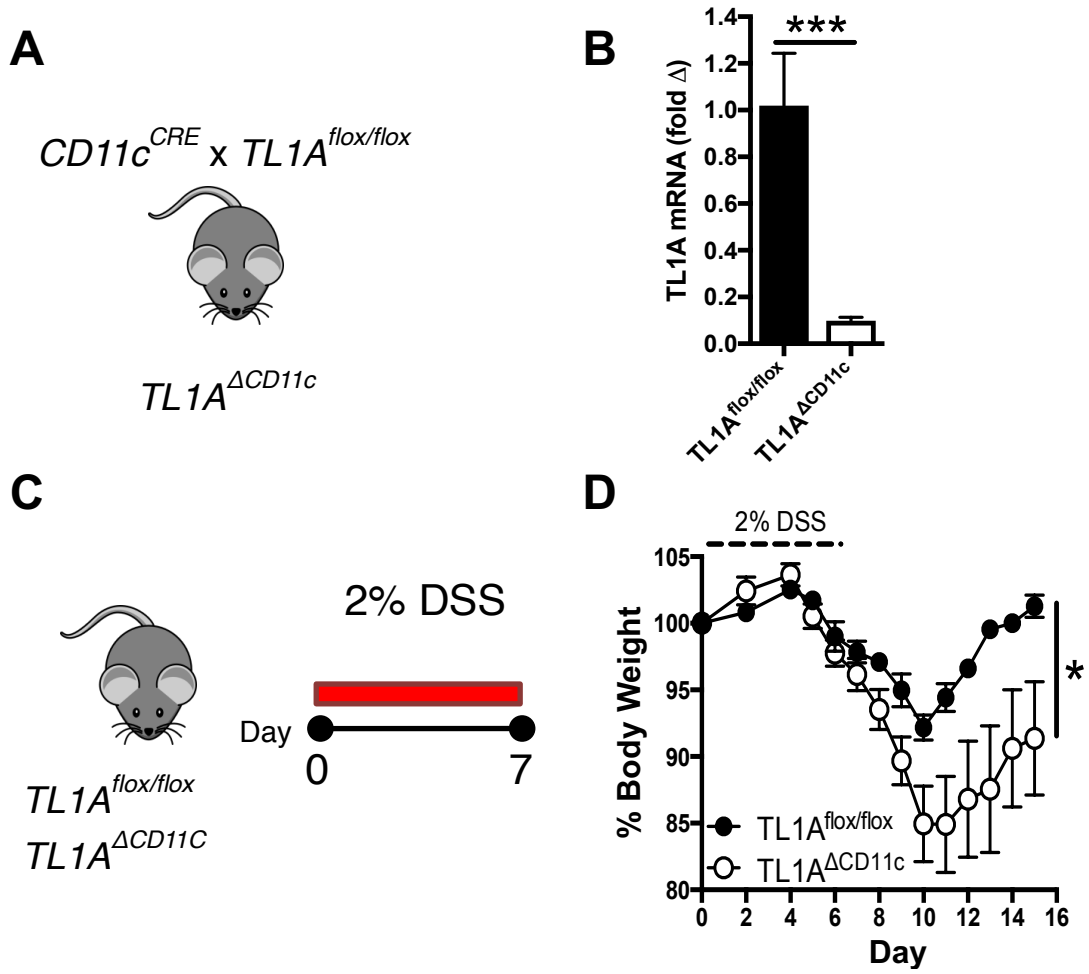

Figure 2.4. **MNP-specific deletion of TL1A impairs mucosal wound healing during acute colitis**. (**A**) Generation of MNP-specific TL1A genetic deletion model. (**B**) TL1A mRNA expression in FACS-sorted MHCII^{+}CD11c^{+} MNPs from *TL1A$^{flox/flox}$* or *TL1A$^{\Delta CD11c}$* littermate mice was determined by qPCR (n = 3, 4 mice group, respectively). (**C**) Experimental design for *TL1A$^{flox/flox}$* or *TL1A$^{\Delta CD11c}$* littermate mice treated with 2% DSS for 7 days. (**D**) Weight loss curves of 2% DSS-treated *TL1A$^{flox/flox}$* or *TL1A$^{\Delta CD11c}$* littermate mice (n = 10, 9 mice/group, respectively, pooled from two independent experiments). Data in (B) are mean ± s.e.m and were analyzed by two-tailed Student's t-test. Data in (D) are mean ± s.e.m and were analyzed by two-tailed Mann-Whitney test; *P<0.05, ***P<0.001.

2.4.5 CX_3CR1^+ MNP-specific TL1A deletion impairs barrier protection

To specifically test the role for CX_3CR1^+ MNP-derived TL1A, we crossed *TL1A*$^{flox/flox}$ mice with transgenic mice expressing a tamoxifen-inducible Cre recombinase under control of the *Cxc3cr1* promoter (*TL1A*$^{\Delta CX3CR1}$) (Figure 2.5A). Transcriptional analysis validated that *TL1A*$^{\Delta CX3CR1}$ mice selectively lacked TL1A expression on $CD11C^+MHCII^+CD11b^+$ MNPs following induction with tamoxifen (Figure 2.5B). To examine a role for CX_3CR1^+ MNP-derived TL1A *in vivo*, *TL1A*$^{\Delta CX3CR1}$ and their littermate *TL1A*$^{flox/flox}$ controls were exposed to 2% DSS for seven days (Figure 2.5C). *TL1A*$^{\Delta CX3CR1}$ mice lost significantly more weight than their littermate controls, had increased histopathological damage, and reduced IL-22 production in ILC3 (Figure 2.5C-E); however, IL-17 and IFN-γ production by ILC3 or T cells was not impaired (Figure 2.6A-C). To test the role for CX_3CR1^+ MNP-derived TL1A in a secondary colitis model, we colonized *TL1A*$^{\Delta CX3CR1}$ and their littermate *TL1A*$^{flox/flox}$ controls with *Citrobacter rodentium*. Similar to the DSS colitis experiments, *TL1A*$^{\Delta CX3CR1}$ mice lost significantly more weight than their littermate controls (Figure 2.7).

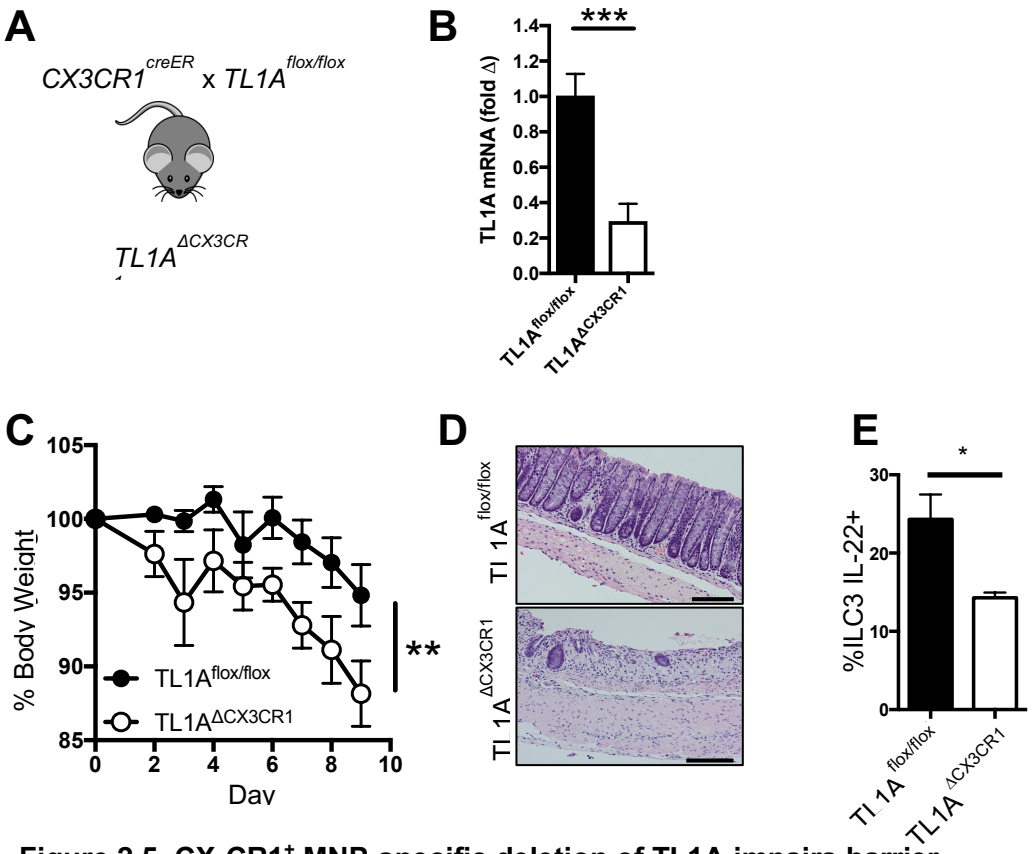

Figure 2.5. CX_3CR1^+ MNP-specific deletion of TL1A impairs barrier protection during acute colitis. (**A**) Generation of CX_3CR1^+ MNP-specific TL1A genetic deletion model. (**B**) qPCR of TL1A expression in $MHCII^+CD11c^+CD11b^+CX3CR1^{YFP}$ MNPs from 4OHT-treated *TL1A*$^{\Delta CX3CR1}$ and *TL1A*$^{flox/flox}$ littermate mice. (**C**) Weight loss curves of 2% DSS-treated *TL1A*$^{flox/flox}$ or *TL1A*$^{\Delta CX3CR1}$ littermate mice (n = 10, 7 mice/group, respectively, pooled over two experiments). (**D**) Representative colonic histology from *TL1A*$^{\Delta CX3CR1}$ or *TL1A*$^{flox/flox}$ mice littermate mice following 2% DSS treatment for 9 days. (**E**) Flow cytometric analysis of IL-22 production by ILC3 from *TL1A*$^{flox/flox}$ or *TL1A*$^{\Delta CX3CR1}$ mice on day 3 after starting 2% DSS treatment (n = 10, 5 mice/group, respectively). Data in (B) and (E) are mean ± s.e.m and were analyzed by two-tailed Student's t-test. Data in (C) are mean ± s.e.m and were analyzed by two-tailed Mann-Whitney test; **P*<0.05, ***P*<0.01, ****P*<0.001.

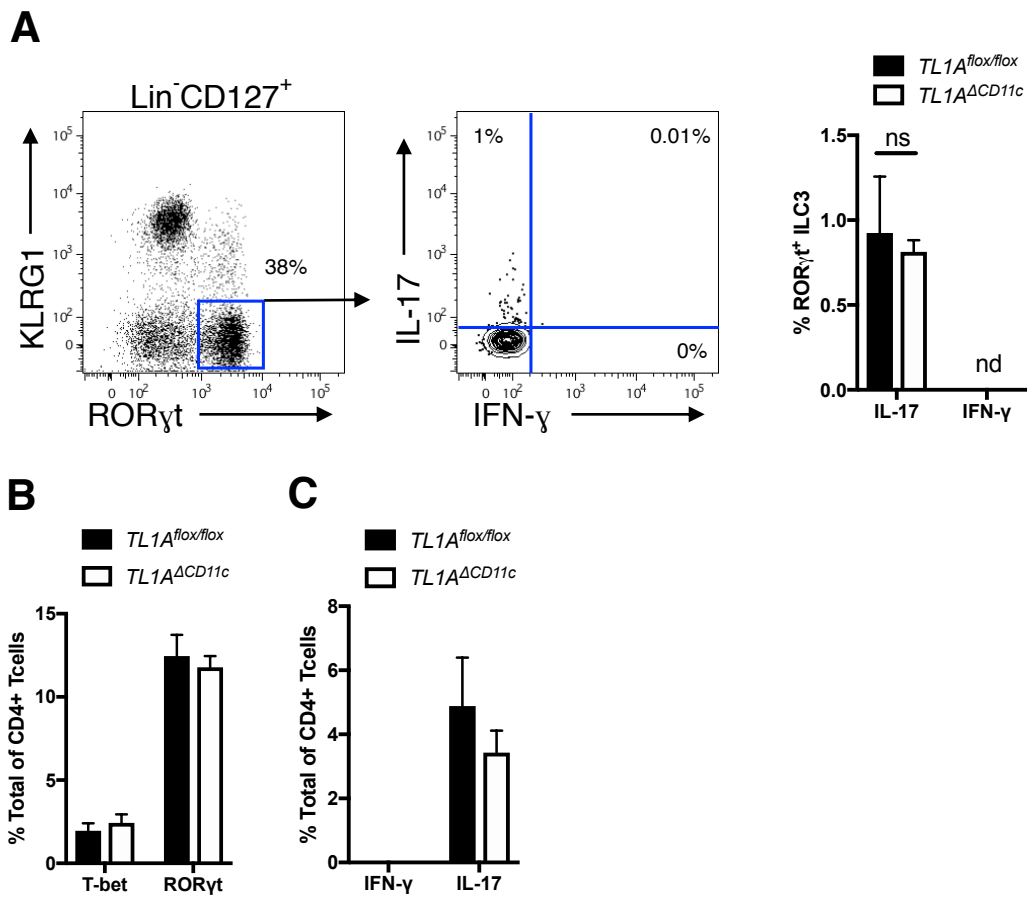

Figure 2.6. MNP-specific deletion of TL1A does not impair ILC3 or T cell IFN-γ or IL-17 production. (**A**) Flow cytometric analysis of IL-17 and IFN-γ expression in Lin$^-$CD127$^+$RORγt$^+$ ILC3 from *TL1A*$^{\Delta CD11c}$ or *TL1A*$^{flox/flox}$ control mice after 2% DSS treatment for three days (n = 4-5 mice/group); data are represented as mean ± s.e.m and were analyzed by two-tailed Student's t-test; ns = not statistically significant; nd= not detected. (**B**, **C**) Quantification of CD3$^+$CD4$^+$ T cell transcription factors (B) and cytokine expression (C) from from *TL1A*$^{\Delta CD11c}$ or *TL1A*$^{flox/flox}$ control mice after 2% DSS treatment for three days (n = 5 mice/group); data are represented as mean ± s.e.m and were analyzed by two-tailed Student's t-test; ns = not statistically significant; nd= not detected.

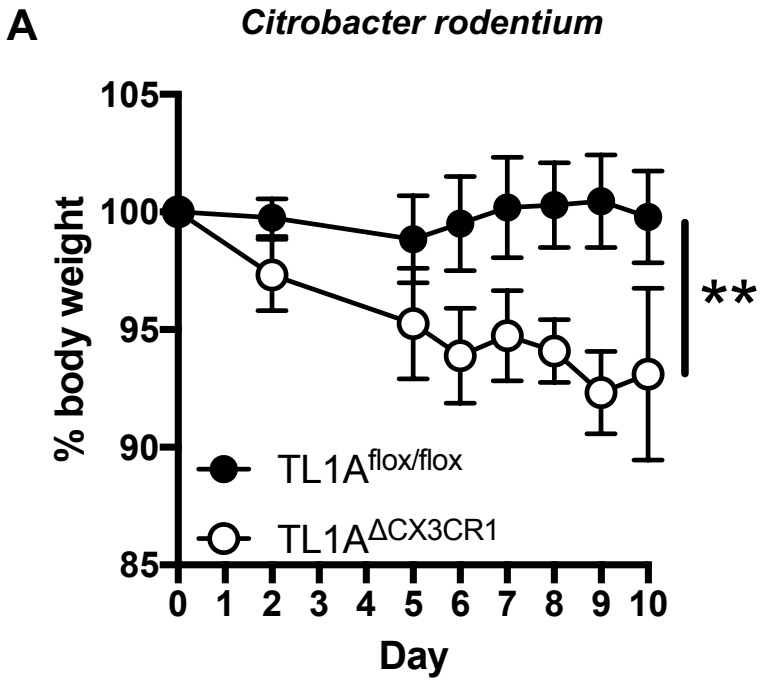

Figure 2.7 CX_3CR1^+ MNP-specific deletion of TL1A impairs barrier protection during infectious colitis. (**A**) Weight loss curves of *TL1A*$^{flox/flox}$ or *TL1A*$^{\Delta CX3CR1}$ littermate mice infected with *Citrobacter rodentium* (n = 6 mice/group, pooled over two experiments). Data are mean ± s.e.m and were analyzed by two-tailed Mann-Whitney test; $^{**}P<0.01$.

2.4.6 MNP TL1A Induction is microbiota-dependent

CX_3CR1^+ MNP are uniquely positioned at the intestinal barrier to sample luminal microbes[33]. Given the ability of bacterial signals to induce TL1A mRNA in human antigen-presenting cells[42], we evaluated the role for microbial regulation of TL1A *in vivo* using germ-free and antibiotic-treated mice compared to specific pathogen free (SPF) control mice. Flow cytometric analysis of TL1A expression in $CD11c^+$ $MHCII^+$ $CD11b^+$ MNPs showed that germ-free mice and antibiotic-treated mice had a significant reduction in intestinal TL1A compared to SPF mice (Figure 2.8).

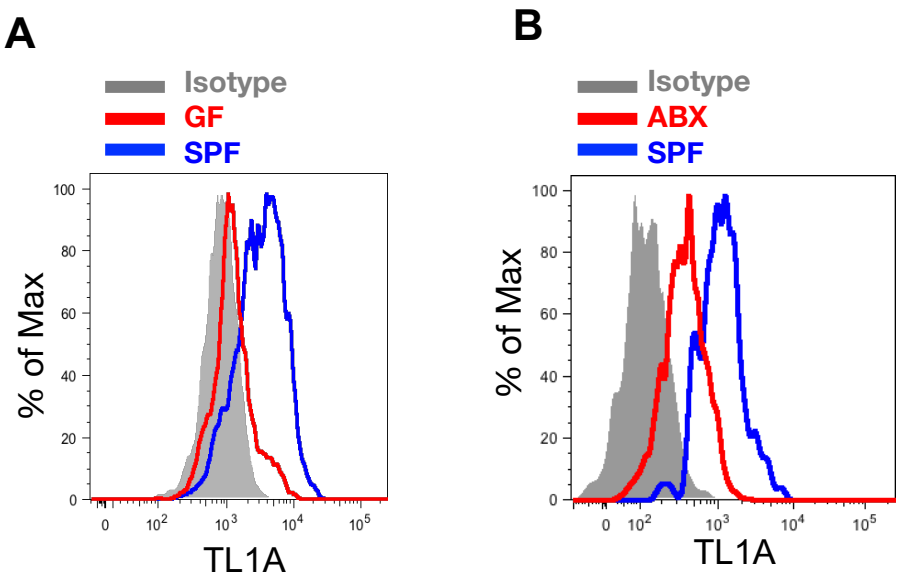

Figure 2.8. Intestinal microbes induce TL1A in MNP. (**A**) Flow cytometric analysis of TL1A expression in MHCII^{+}CD11c^{+}CD11b^{+} MNP from germ-free (GF) or specific-pathogen-free (SPF) mice. (**B**) Flow cytometric analysis of TL1A expression in MHCII^{+}CD11c^{+}CD11b^{+}GFP^{+} MNP from antibiotic-treated (ABX) or untreated specific-pathogen-free (SPF) *CX3CR1*$^{GFP/WT}$ mice.

2.4.7 IBD-associated adherent microbes induce TL1A

Previous studies have reported that microbial adherence to the intestinal epithelial surface may play a critical role in regulating immune responses in the lamina propria. Segmented filamentous bacteria (SFB), for example, adheres tightly to the ileal mucosa and induces Th17 and ILC3 effector function[65,66]. Given the importance of CX_3CR1^+ MNP in regulating this interaction[24,38], we sought to examine the role for SFB in TL1A regulation. Lamina propria MNPs from germ-free and gnotobiotic mice colonized with SFB were analyzed for TL1A expression (Figure 2.9A). SFB mono-colonized mice had significantly higher levels of intestinal TL1A compared to GF mice. To further test if this induction of TL1A was selective for adherent bacteria, we used Adherent-invasive *E. coli* (AIEC) strain 2A and a non-adherent *E. coli* control strain T75 derived from patients with Crohn's disease[67]. At 5 days following colonization, AIEC strain 2A, but not T75, induced TL1A in the colonic lamina propria (Figure 2.9B).

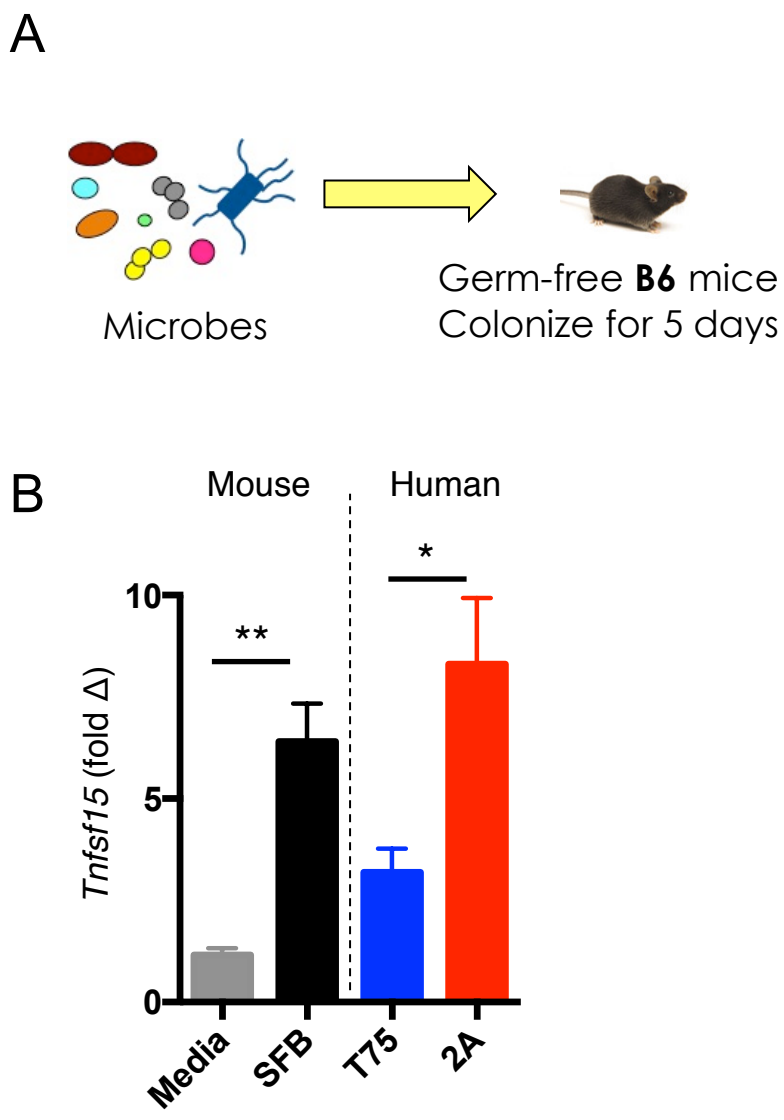

Figure 2.9. IBD-associated adherent microbiota induce TL1A in intestinal MNP. (**A**) Experimental design for colonization of germ-free mice with human IBD-associated microbes. (**B**) Germ-free mice were mono-colonized with media control, SFB, non-adherent E. coli T75, Adherent-invasive E. coli 2A for 5 days. MNPs were sorted from the lamina propria and Tnfsf15 expression determined by quantitative PCR. Data in (B) are mean ± s.e.m and were analyzed by two-tailed Student's t-test; *P<0.05, **P<0.01.

2.4.8 IBD-associated adherent microbes promote barrier protection

We recently showed that AIEC are protective during acute colitis[67], so we next asked if the protective effects of AIEC are dependent on MNP-derived TL1A. To test the role of microbe-induced MNP TL1A in acute colitis, *TL1A*$^{\Delta CD11c}$ and littermate *TL1A*$^{flox/flox}$ mice were pre-treated with broad-spectrum antibiotics and then colonized with AIEC strain 2A prior to DSS exposure (Figure 2.10A). Colonization with AIEC was sufficient to rescue the more severe weight loss and reduced survival following treatment with antibiotics, and this rescue required MNP-derived TL1A (Figure 2.10B,C). Collectively, these findings reveal a critical beneficial role for IBD-associated adherent microbiota induction of MNP-derived TL1A to promote protection from acute colitis.

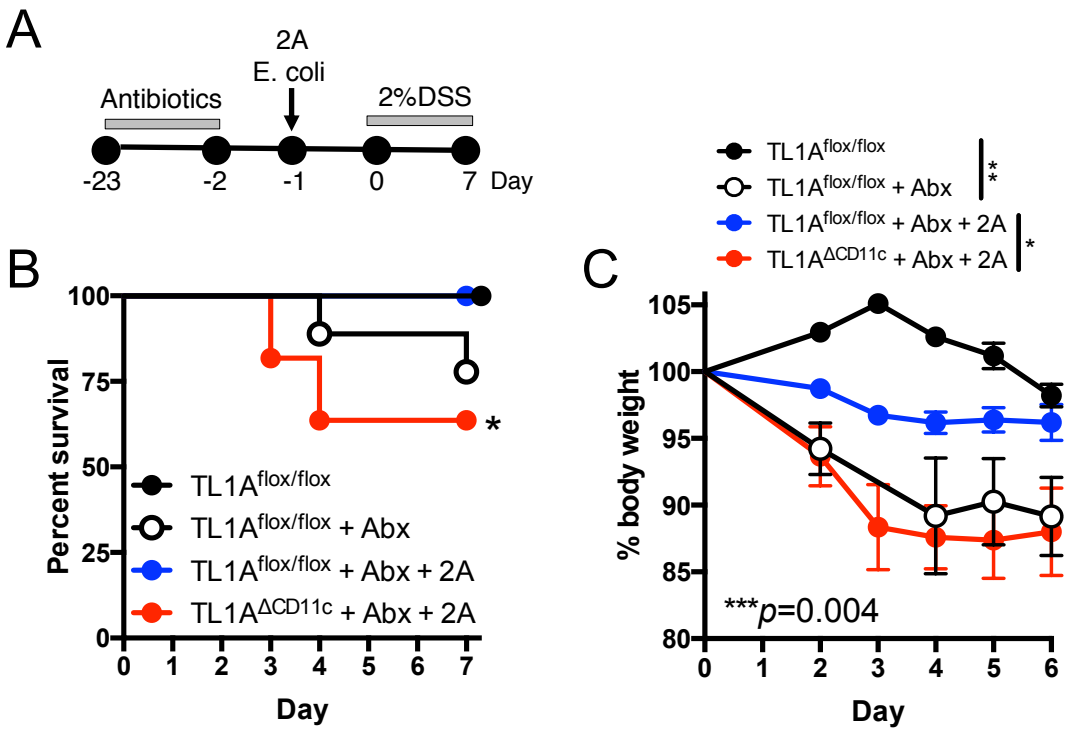

Figure 2.10. IBD-associated adherent microbiota protect from acute colitis via MNP-derived TL1A. (**A**) Experimental design for testing gene-microbe interactions during colitis. *TL1A*$^{flox/flox}$ and *TL1A*$^{\Delta CD11c}$ were treated with broad-spectrum antibiotics for three weeks before colonization with 2A *E. coli*. Mice were then mice treated with 2% DSS for 7 days. (**B, C**) Percent survival (B) and weight loss (C) is shown. Data in (B) are mean ± s.e.m and were analyzed by two-tailed Student's t-test. Data in (B) are mean ± s.e.m and were analyzed by Log-rank (Mantel-Cox) test or by one-way ANOVA with multiple comparisons test (C); *P<0.05, **P<0.01.

2.5 DISCUSSION

As sentinels of barrier immunity, MNPs integrate microbial signals and activate both innate and adaptive effector immunity. By producing IL-23 and IL-1β, as well as CXCL16, MNPs are well-positioned functionally and spatially to rapidly coordinate ILC3 effector cytokine production including IL-22[24,39]. However, if and how other MNP-derived genes regulate ILC3 functions in the intestine are currently unknown. In this chapter, we report that the IBD-associated gene *TNFSF15*, which encodes for the functional protein TL1A, is critical for ILC3-mediated intestinal barrier protection.

Here, we identify the CX_3CR1^+ MNP as the dominant producers of intestinal TL1A in both mouse and human IBD patients. Using cell-specific genetic knockout models, mice with TL1A deletion in MNPs and CX_3CR1^+ MNP, specifically, were significantly more susceptible to chemically-induced and infectious colitis damage than their littermate controls. Furthermore, MNPs from the mucosal biopsies of human IBD patients with active colitis produced robust amounts of TL1A compared to non-IBD patients, suggesting a potential role for MNP-derived TL1A during active colitis in IBD patients. However, how specific *TNFSF15* mutations (either loss-of-function or gain-of-function mutations) contribute to disease outcomes in IBD patients remains to be explored and could offer a potential avenue for therapeutic intervention.

Our results support a key role for microbial regulation of MNP-derived TL1A. Germ-free mice, or mice treated with board-spectrum

antibiotics, had remarkably decreased levels of TL1A compared to conventionally housed mice, suggesting that intestinal microbes are key regulators of lamina propria TL1A. Specifically, adherent, IBD-associated adherent microbes, including segmented filamentous bacteria (SFB) and Adherent-invasive *E. coli* enriched in Crohn's disease, robustly induced TL1A, consistent with their ability to potently induce ILC3 production of IL-22[66,67]. Furthermore, *in vivo* models using cell-specific deletion of TL1A in MNPs demonstrated that these adherent microbes were unable to rescue antibiotic-treated mice from DSS colitis, suggesting a gene-microbe link between adherent microbes and MNP-derived TL1A in mediating barrier protection. However, it remains to be seen whether this protective effect is via ILC3 IL-22 or by other mechanisms.

These findings offer a mechanism by which Crohn's disease-associated microbiota can act acutely to promote barrier immunity in wild-type hosts. The adherence and metabolic characteristics of the intestinal microbiota may offer a novel approach for regulating TL1A effects in the mucosa.

CHAPTER THREE: ILC3-SPECIFIC DR3 PROMOTES BARRIER PROTECTION DURING ACUTE COLITIS

3.1 ABSTRACT

In chapter two, we demonstrated an essential role for CX_3CR1^+ MNP-derived TL1A in mucosal barrier immunity. Deletion of CX_3CR1^+ MNP-intrinsic TL1A exacerbated intestinal inflammation by restraining ILC3 cytokine production and mucosal healing. In the intestine, CX_3CR1^+ MNP-derived TL1A was dependent on luminal microbes and potently induced by attaching/invasive bacteria. To examine the physiologic role for the TL1A:DR3 axis in mucosal healing, we generated novel genetic mouse models with targeted DR3 deletion on ILC3 ($DR3^{\Delta ILC3}$). Whole body $DR3^{-/-}$ and ILC3-specific $DR3^{\Delta ILC3}$ mice exposed to experimental colitis had more severe weight loss, pathology, and reduced survival; this phenotype correlated with reduced ILC3 production of IL-22, epithelial cell anti-microbial peptide production and was rescued by recombinant IL-22. Mechanistically, inhibition of p38-MAPK disrupted TL1A signaling on ILC3 by impairing effector cytokine. *In vivo*, mice with mice with a double deletion of DR3 and IL23R ($DR3^{-/-}$ $IL23R^{-/-}$) had decreased survival compared to mice with single deletions in either DR3 or IL23R, highlighting a synergistic role for DR3/IL23R signaling in promoting mucosal healing *in vivo*. Collectively, these data highlight a key role for ILC3-specific DR3 signaling in regulating intestinal barrier immunity *in vivo*.

3.2 INTRODUCTION

Genome-wide association studies (GWAS) in IBD have revealed the strongest associations of genetic variants in *TNFSF15* with Crohn's disease, highlighting a central role for its protein, TNF-like cytokine 1A (TL1A), in mucosal immunity[46]. Variants in *TNFSF15* have been linked to the pathogenesis of several autoimmune diseases—including psoriasis, rheumatoid arthritis, and multiple sclerosis—implicating a broader role for TL1A in human inflammatory diseases[4]. In IBD, *TNFSF15* variants confer higher risk for more aggressive, penetrating, fibrostenotic, and perianal disease complications[29,30], but the mechanistic impact of TL1A remains controversial. While early studies revealed a pathogenic role for TL1A in driving inflammatory T cell response[28,31], more recent reports in acute colitis models revealing a protective role for TL1A[32]. Genetic models are needed to understand the cellular mechanisms and potential therapeutic targetability of this IBD-linked pathway in intestinal inflammation.

Group 3 innate lymphoid cells (ILC3) are an emerging class of innate lymphocytes that play a critical role in regulating mucosal homeostasis[68–74]. In response to environmental triggers, in particular the cytokines IL-23 and IL-1β, ILC3 produce robust amounts of IL-22 and play an important role in maintaining intestinal barrier integrity and promoting mucosal healing—a major clinical endpoint in IBD[24,74,75].

Co-localization of ILC3 with CX_3CR1^+ mononuclear phagocytes (MNPs) in the lamina propria enables rapid regulation of ILC3 effector cytokines to reinforce barrier immunity and mucosal healing[39]. Both mouse and human ILC3s express Death Receptor 3 (DR3), the monogamous receptor for TL1A, on its surface, with TL1A stimulation promoting ILC3 proliferation[76] and cytokine production *in vitro*[24]*;* however, the role for TL1A in regulating ILC3 function in intestinal homeostasis, and its potential contribution to IBD pathophysiology, remains unknown.

Here, we generated mouse models with selective deletion of DR3 on ILC3 to evaluate the contribution of this critical IBD-linked genetic pathway in regulating mucosal immunity. Our data reveal a critical role for ILC3-specific DR3 acting synergistically with IL23R signaling in promoting mucosal healing in acute colitis. *In vitro*, DR3 signaling on ILC3 was dependent on TAK1 and p38-MAPK signaling. *In vivo*, mice with mice with a double deletion of DR3 and IL23R (*DR3*$^{-/-}$ *IL23R*$^{-/-}$) had decreased survival compared to mice with single deletions in either DR3 or IL23R, highlighting a synergistic role for DR3/IL23R signaling in promoting mucosal healing *in vivo*. These results highlight the central role for IBD-linked TL1A in regulating ILC3 barrier immunity.

3.3 METHODS

Mice. C57BL/6 mice were purchased from The Jackson Laboratory. . *Il23r*^{GFP} mice were obtained from M. Oukka[77]. DR3$^{-/-}$ mice were obtained from Cancer Research UK (E. Wang). Generation of *Dr3*$^{flox/flox}$ mice is previously described[78]. All experiments were performed with 6-8 week old littermates with random and equal assignment of same sex to each experimental group. All vertebrate work was approved by the IACUC at Weill Cornell Medicine.

Preparation of LPMC. Mouse intestines were washed in PBS and 1 mM DTT with 30 mM EDTA, and then digested in collagenase 8 (Sigma-Aldrich) and DNase-containing media with 10% fetal bovine serum. Digested material was passed through a cell strainer and separated by a 40% Percoll gradient. For intracellular cytokine staining, LPMCs were cultured ex vivo in the presence of GolgiPlug (BD) for 4 h or stimulated with phorbol myristate acetate (PMA; 20 ng/ml) and ionomycin (1 μg/ml) or IL-23 (40 ng/ml; eBioscience) in the presence of GolgiPlug (BD) for 4 h before staining. All TL1A detection was done by extracellular flow cytometry staining.

Antibodies and flow cytometry. Staining of cells was performed with the following antibodies:

Table 3.1. Flow cytometry antibodies used in chapter 3.

Species	Target	Fluorophore	Clone	Manufacturer
Mouse	CD3	FITC	145-2C11	eBioscience
Mouse	CD4	eFluor780	RM4-5	eBioscience
Mouse	CD5	PE	53-7.3	eBioscience
Mouse	CD45.1	APC	A20	eBioscience
Mouse	CD90.2	efluor450	53-2.1	eBioscience
Mouse	MHCII	Alexa700	M5/114.15.2	eBioscience
Mouse	F4/80	PE	BM8	eBioscience
Mouse	Ly6C	eFluor450	HK1.4	eBioscience
Mouse	CD19	FITC	MB19-1	eBioscience
Mouse	CD11b	eFluor780	M1/70	eBioscience
Mouse	CD11c	PE-Cy7	N418	eBioscience
Mouse	CD103	APC	2E7	eBioscience
Mouse	TCR$\gamma\delta$	FITC	11-5711-82	eBioscience
Mouse	KLRG1	PE	2F1	eBioscience
Mouse	NKp46	eFluor710	29A1.4	eBioscience
Mouse	OX40L	APC	RM134L	eBioscience
Mouse	ICOSL	eFluor660	HK5.3	eBioscience
Mouse	CD127	PE-Cy7	A7R34	BioLegend
Mouse	CCR6	BV421	29-2L17	BioLegend
Mouse	DR3	PE	4C12	BioLegend
Mouse	RORγt	PE	B2D	eBioscience
Mouse	T-bet	e660	eBio4B10	eBioscience
Mouse	Foxp3	e450	FJK-16s	eBioscience
Mouse	IL-22	APC	IL22JOP	eBioscience
Mouse	GMCSF	FITC	MP1-22E9	eBioscience
Mouse	IL-13	PE-Cy7	eBio13A	eBioscience
Mouse	IL-17	PE	eBio17B7	eBioscience
Mouse	IFNγ	PE-Cy7	XMG1.2	eBioscience
Mouse	TL1A	e710	Tandys1a	eBioscience

Dead cells were excluded using the Live/Dead fixable aqua dead cell stain kit (Invitrogen). Intracellular cytokine staining was performed according to the manufacturer's protocol (Cytofix/Cytoperm buffer set; BD) and transcription factor staining for was performed according to manufacturer's protocol (Intracellular Fixation and Permeabilization kit; eBioscience). Flow cytometry was performed with a BD LSRFortessa and analyzed with FlowJo software (Tree Star).

Colitis models. To induce chemical colitis in mice, 2% DSS (w/v) (M.W. 40,000-50,000; Affymetrix) was added to sterile drinking water and administered ad libitum for 7 days. After 7 days, DSS was replaced with normal drinking water. To induce infectious colitis, mice were orally gavaged with log phase growth *Citrobacter rodentium* DBS100 (ATCC 51459; American Type Culture Collection) at $1x10^{10}$ in PBS. For all colitis experiments, mice were monitored daily weight loss, rectal bleeding, diarrhea and survival throughout the experiments.

qPCR. RNA from primary intestinal cell populations was prepared with TRIzol (Invitrogen) and purified RNA was reverse transcribed into cDNA (Quanta qScript). qPCR was performed with a QuantStudio 6 Flex Real-time PCR (Applied Biosystems) with SYBR Green Supermix (Bio-Rad Laboratories). The following primers were used:

Il22: 5'-GCTCAGCTCCTGTCACATCA-3' and 5'-CAGTCCCCCAATCGCCTTGA-3'

Hprt: 5'-GAGGAGTCCTGTTGATGTTGCCAG-3' 5'-GGCTGGCCTATAGGCTCATAGTGC-3'.

The thermocycler program was as follows: initial cycle of 95°C for 60s, followed 40 PCR cycles at 95°C for 5s, 60°C for 15s, 72°C for 15s. Relative levels of the target genes were determined by using the $\Delta\Delta C_t$ of the target gene compared to *Hprt* expression.

Statistical analysis. Statistical analysis was performed in GraphPad Prism or R software. Results represent mean ± s.e.m. and were analyzed by unpaired Student's t-test, Mann-Whitney test, one-way ANOVA, Log-rank (Mantel-Cox) test, as indicated in the figure legends. Given that mouse experiments required littermate controls and complex genotyping, experimental group allocation was not blinded. No relevant exclusion criteria were applied.

3.4 RESULTS

3.4.1 DR3 signaling protects from intestinal injury

To evaluate the impact of endogenous TL1A *in vivo* using experimental colitis models, mice deficient for DR3 were exposed *ad libitum* to 2% DSS. Similar to recent results[32], DSS induced more severe acute colitis in mice deficient for DR3, as evidenced by increased weight loss with a protracted recovery (Figure 3.1A), reduced survival (Figure 3.1B) and increased histopathological damage (Figure 3.2C). Analysis of $CD4^+$ T cell population in the lamina propria did not reveal significant differences in $Foxp3^+$ regulatory $CD4^+$ T cells, IL-17 producing $ROR\gamma t^+$ Th17 cells (Figure 3.2A-C), or IL-13 producing ILC2 cells (data not shown). In contrast, Lin^- $ROR\gamma t^+$ ILC3 from the lamina propria showed a significant decrease in IL-22 (Figure 3.4A); there were no changes in the total numbers of ILC3 or in ILC3 subsets (Figure 3.3). To evaluate the contribution of reduced ILC3 production of IL-22 to this phenotype, we injected DR3-deficient mice with recombinant IL-22 following exposure to DSS; treatment with rIL-22 completely rescued DR3-deficient mice, suggesting a critical role for ILC3-derived IL-22 in mediating this colitis phenotype (Figure 3.4B).

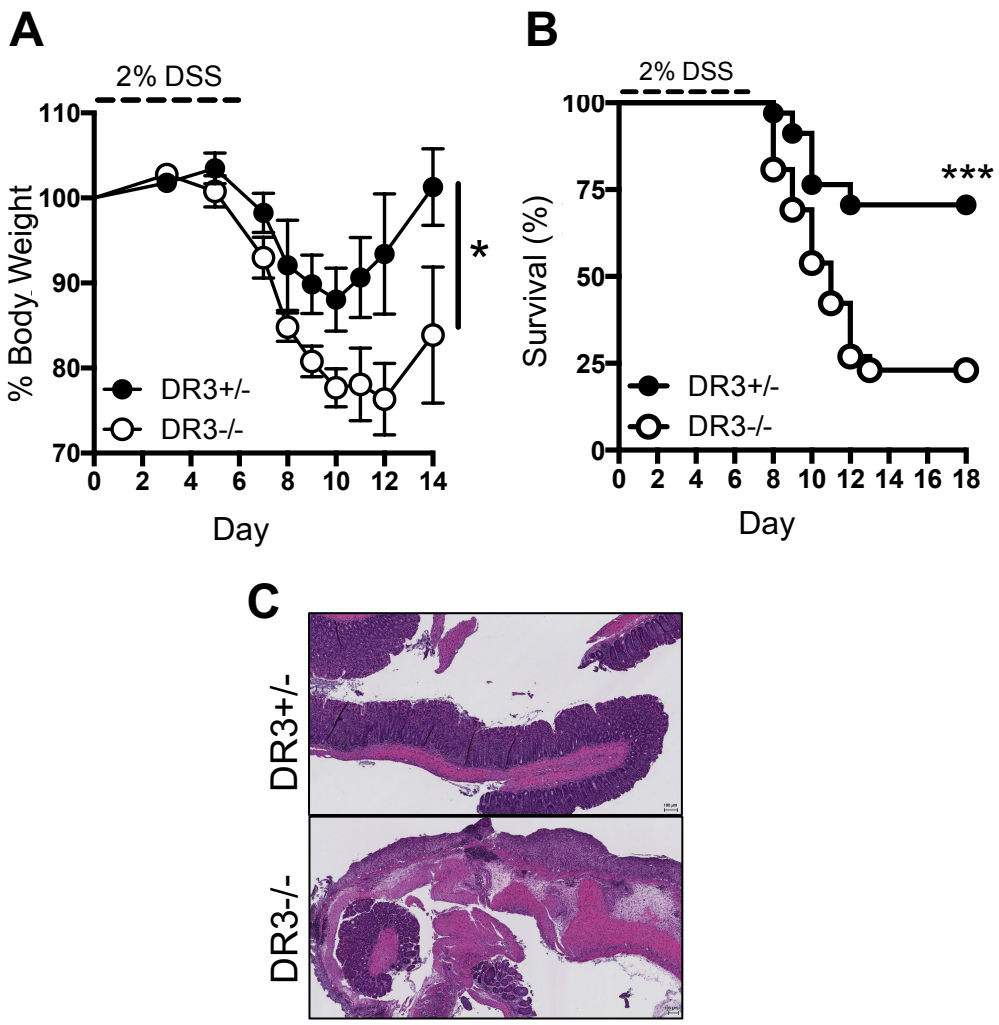

Figure 3.1. DR3 protects mice from experimental colitis. (**A**,**B**) Body weights (A) and survival curves (B,D) of *DR3*$^{+/-}$ and *DR3*$^{-/-}$ littermate mice following 7 day treatment with 2% DSS. Data are compiled from three independent experiments (with n = 34, 25 mice/group for *DR3*$^{+/-}$ and *DR3*$^{-/-}$, respectively); (**C**) Representative colonic histology and colonic scoring from *DR3*$^{+/-}$ and *DR3*$^{-/-}$ littermate mice following 2% DSS treatment for 7 days (analyzed in A, B). Data in (A) are mean ± s.e.m. and analyzed by Mann-Whitney test; data in (B) were analyzed by Log-rank (Mantel-Cox) test; *P<0.05, ***P<0.001.

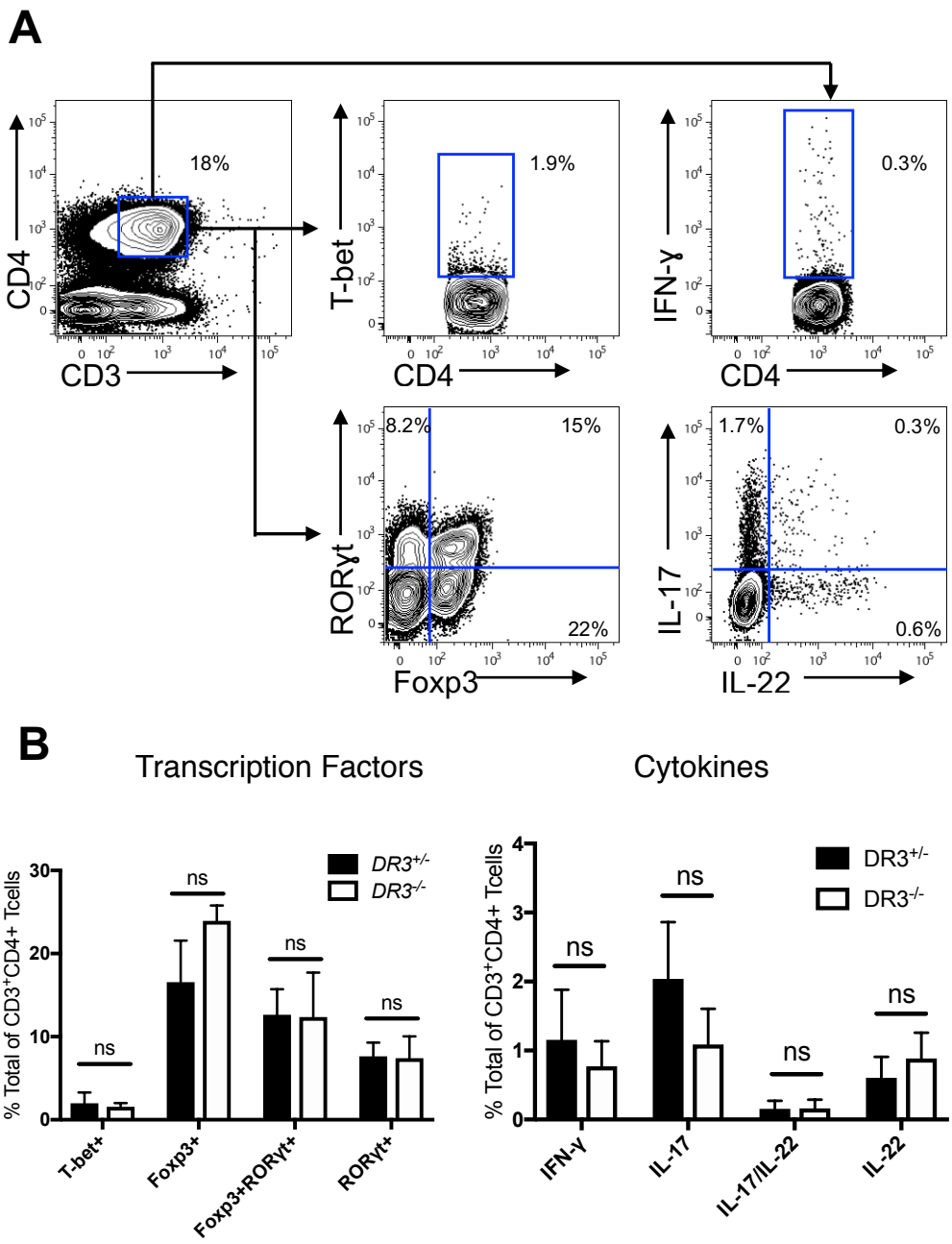

Figure 3.2. **DR3 deletion does not alter T cell function during acute colitis**. (**A**, **B**) Flow cytometric analysis (A) and quantification (B) of T cell transcription factors and cytokine production in $CD3^+CD4^+$ T cells from *DR3*$^{+/-}$ or *DR3*$^{-/-}$ control mice after 2% DSS treatment for three days (n = 8 mice/group compiled over two experiments); data are represented as mean ± s.e.m and were analyzed by two-tailed Student's t-test; ns = not statistically significant.

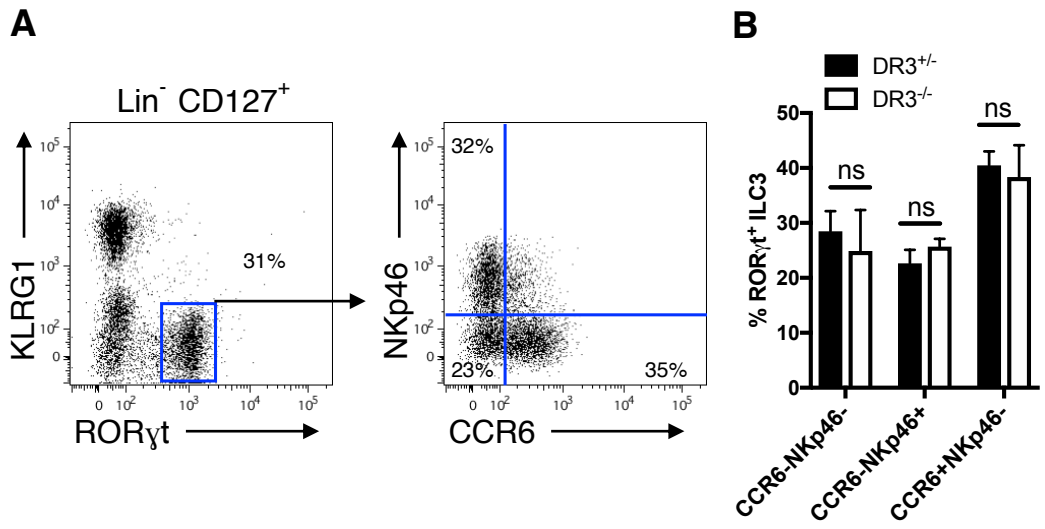

Figure 3.3. **DR3 deletion does not alter ILC3 subsets during acute colitis**. (**A**, **B**) Flow cytometric analysis (A) and quantification (B) of Lin^{-}CD127^{+}RORγt^{+} ILC3 subsets from *DR3$^{+/-}$RAG2$^{-/-}$* or *DR3$^{-/-}$RAG2$^{-/-}$* control mice after 2% DSS treatment for seven days (n = 3-4 mice/group); data are represented as mean ± s.e.m and were analyzed by two-tailed Student's t-test; ns = not statistically significant.

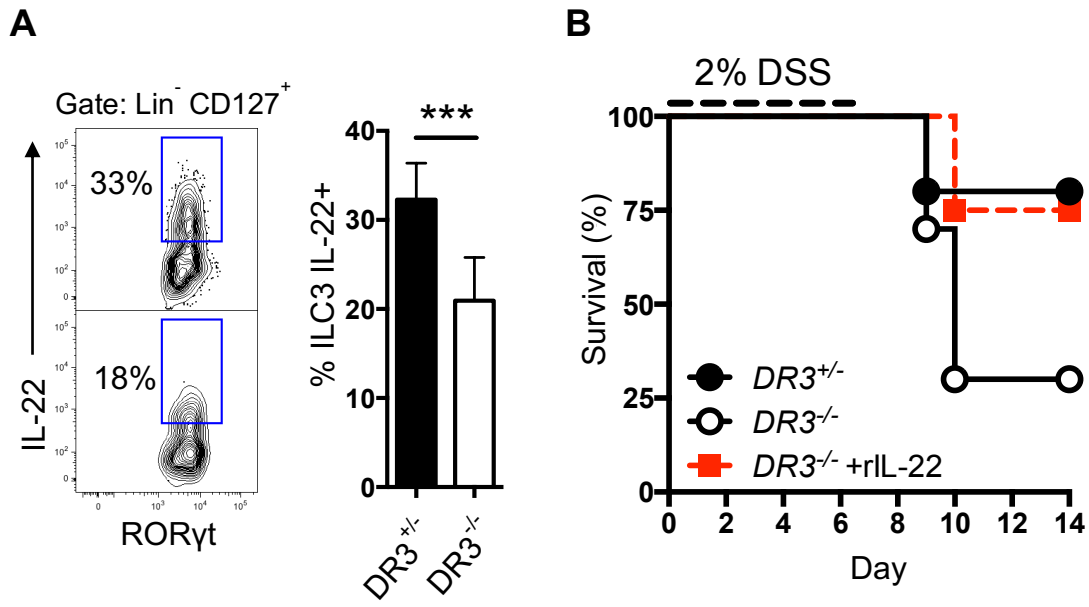

Figure 3.4. ILC3 expression of DR3 plays an essential role in regulating IL-22-dependent protection from experimental colitis. (**A**) Percentage of colonic Lin$^-$CD127$^+$CD90$^+$RORγt$^+$ ILC3s producing IL-22 from DSS-treated *DR3*$^{+/-}$ and *DR3*$^{-/-}$ co-housed littermate mice 9 days after starting DSS treatment (n = 4-5 mice/group). (**B**) Survival curves of *DR3*$^{+/-}$, *DR3*$^{-/-}$, and *DR3*$^{-/-}$ + rIL-22, mice following 7 day treatment with 2% DSS. Data are compiled from three independent experiments (with n = 34, 25, 4 mice/group for *DR3*$^{+/-}$, *DR3*$^{-/-}$, and *DR3*$^{-/-}$ + rIL-22, respectively); i.v. rIL-22 was given on days 4 and 6 following initiation DSS. Data (A) are mean ± s.e.m and analyzed by two-tailed Student's t-test; ***P<0.001.

3.4.2 Generation of ILC3-specific DR3 deletion genetic model

To specifically test the importance of ILC3-intrinsic DR3 signaling in intestinal barrier immunity, we crossed mice with a *lox*P-flanked *Tnfrsf25* (*DR3*$^{flox/flox}$) to transgenic mice expressing the Cre recombinase from the RORγt promoter (*Rorc*^{cre}) on a RAG2-deficient background (called *DR3*$^{\Delta ILC3}$). Transcriptional and flow cytometric analysis revealed that *DR3*$^{\Delta ILC3}$ mice lacked DR3 expression on ILC3, but not on ILC2, confirming cell type-specific DR3 deletion (Figure 3.5). Absence of DR3 did not change the total number or frequency of ILC3 in the small and large intestines (data not shown).

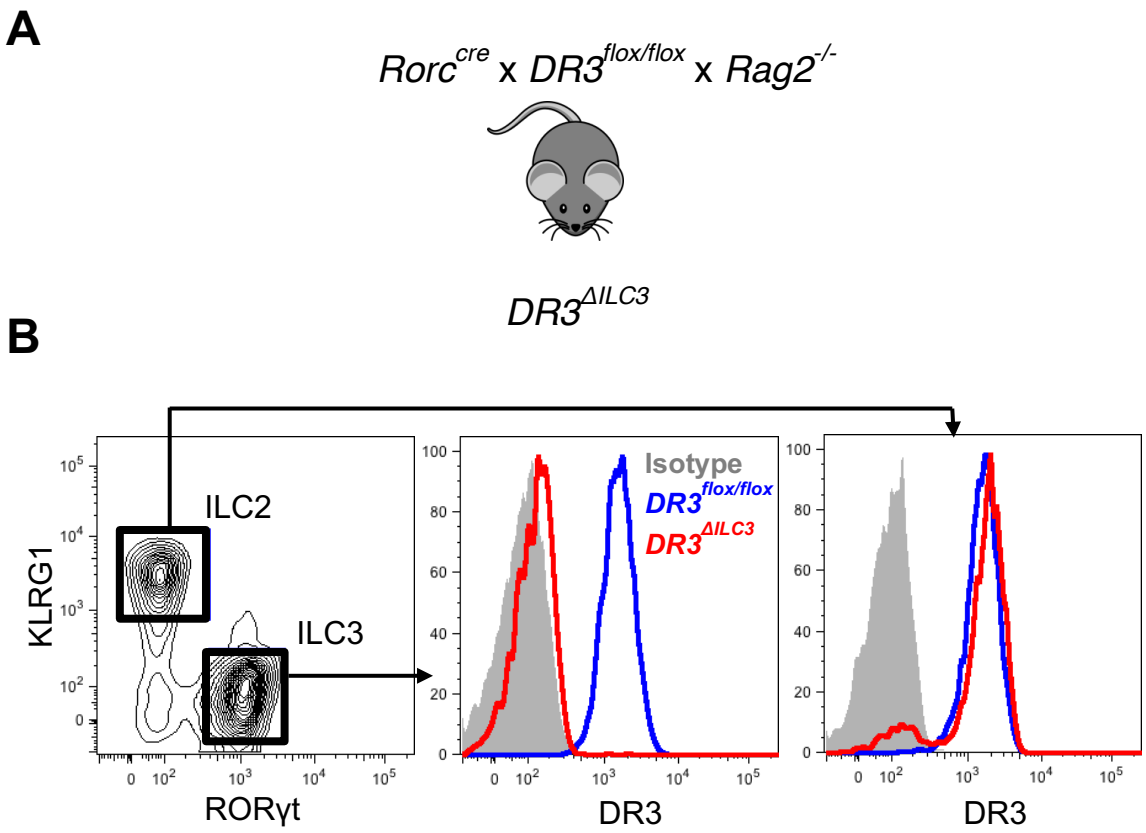

Figure 3.5. Generation of ILC3-specific DR3 genetic deletion model. (**A**) Generation of ILC3-specific DR3 genetic deletion model. (**B**) Representative flow cytometry analysis of extracellular DR3 expression on indicated mice in (A).

3.4.3 ILC3-specific DR3 signaling promotes barrier protection

To evaluate a role for ILC3-intrinsic DR3 in experimental colitis, we exposed *DR3$^{\Delta ILC3}$* mice and their littermate controls to *ad libitium* 2% DSS. Phenocopying DR3-deficient mice, *DR3$^{\Delta ILC3}$* mice lost significantly more weight (Figure 3.6A) and had more severe colitis histopathology (Figure 3.6B) than their littermate controls. Flow cytometry analysis revealed lower production of IL-22 by ILC3s from *DR3$^{\Delta ILC3}$* mice compared to littermates controls (Figure 3.6C). Similar to DR3-deficient animals, treatment with rIL-22 completely rescued *DR3$^{\Delta ILC3}$* mice (Figure 3.6A). Since IL-22 is critical for inducing intestinal epithelial cell production of antimicrobial peptides[79] and acute phase reactants[66], we evaluated *Reg3g* and *Saa1* expression in intestinal epithelial cells isolated from these mice (Figure 3.6D). Reduced expression of both *Reg3g* and *Saa1* reflects the decreased production of IL-22 in *DR3$^{\Delta ILC3}$* mice during colitis compared to littermate controls.

To test the role for DR3 in an alternate colitis model, we used the *Citrobacter rodentium* infectious colitis model, which is dependent on ILC3 during the acute response[75]. Similar to the response in DSS colitis, *DR3$^{\Delta ILC3}$* mice lost significantly more weight and had reduced survival than their littermate controls (Figure 3.7). Collectively, these experiments demonstrate a key role for cell-intrinsic DR3 in regulating ILC3 production of IL-22 and protection from acute experimental colitis.

Figure 3.6. ILC3 expression of DR3 plays an essential role in regulating IL-22-dependent protection from experimental colitis. (**A**) Body weights of 2% DSS-treated *DR3*$^{flox/flox}$ and *DR3*$^{\Delta ILC3}$ littermate mice compared with *DR3*$^{\Delta ILC3}$ mice treated with rIL-22 i.v. on days 4 and 6 of DSS treatment (with n = 13, 13, 4 mice/group for *DR3*$^{flox/flox}$, *DR3*$^{\Delta ILC3-}$, and *DR3*$^{\Delta ILC3}$ + rIL-22, respectively). (**B**) Representative colonic histology and colonic scoring from *DR3*$^{flox/flox}$ and *DR3*$^{\Delta ILC3}$ littermate mice following 2% DSS treatment for 7 days (analyzed in A). (**C**) Percentage of colonic Lin^{-}CD127^{+}CD90^{+}RORγt^{+} ILC3s producing IL-22 from 2% DSS-treated *DR3*$^{flox/flox}$ and *DR3*$^{\Delta ILC3}$ littermate mice 9 days after starting DSS treatment (n = 4-5 mice/group; LPMC were stimulated *ex vivo* with rIL-23 and brefeldin for 4 hours before intracellular IL-22 staining). (**D**) Epithelial cell REG3γ and SAA1 mRNA expression in 2% DSS-treated *DR3*$^{flox/flox}$ and *DR3*$^{\Delta ILC3}$ littermate mice 9 days after starting 2% DSS treatment (n = 4 mice/group). Data in (A) are mean ± s.e.m. and were analyzed by ANOVA with multiple comparisons; data in (C, D) are mean ± s.e.m and were analyzed by two-tailed Student's t-test; **P*<0.05, ***P*<0.01.

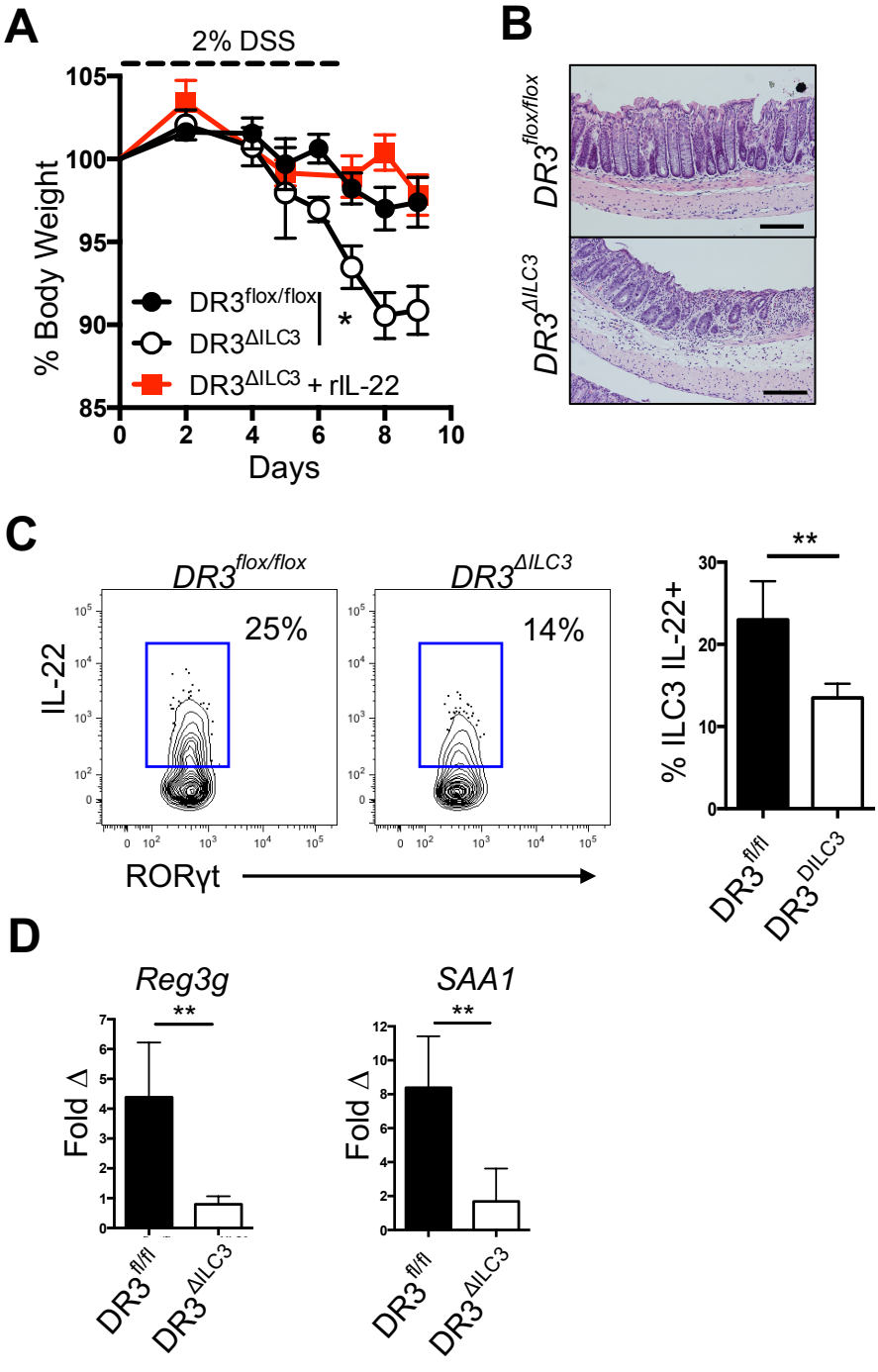

Figure 3.6. ILC3 expression of DR3 plays an essential role in regulating IL-22-dependent protection from experimental colitis.

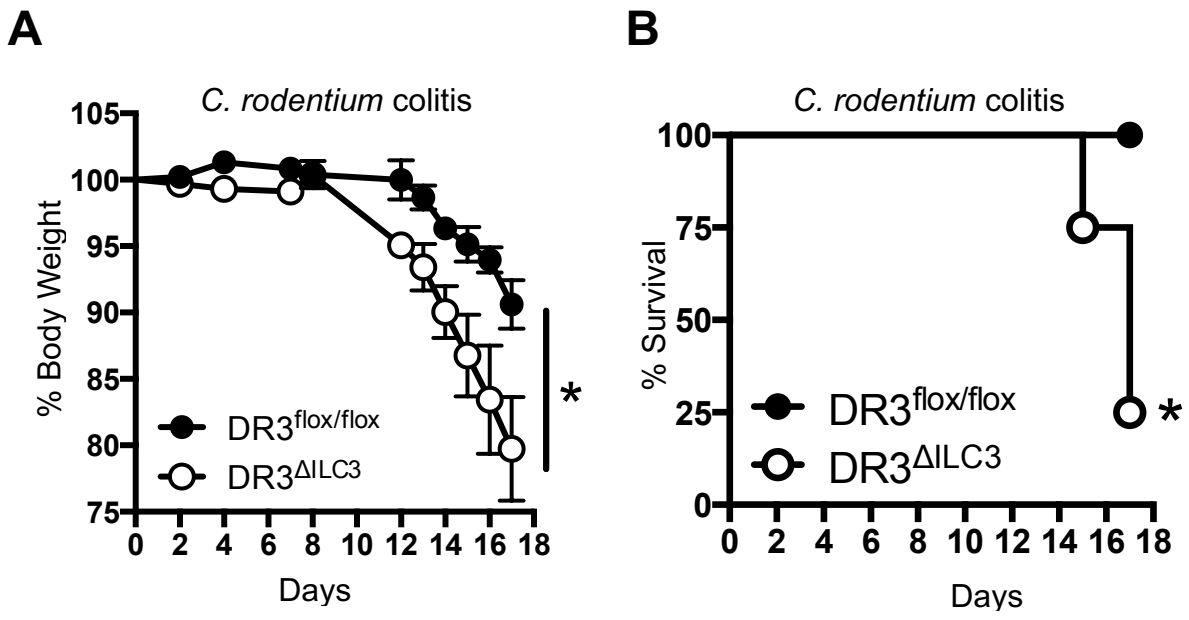

Figure 3.7. ILC3 expression of DR3 protects from *Citrobacter rodentium* colitis. (**A, B)** Body weights (A) and survival curves (B) of *C. rodentium*-infected *DR3$^{flox/flox}$* and *DR3$^{\Delta ILC3}$* littermate mice (n = 5, 4 mice/group, respectively). Data in (A) are mean ± s.e.m. and analyzed by Mann-Whitney test; data in (B) were analyzed by Log-rank (Mantel-Cox) test; *P<0.05.

3.4.4 TL1A/IL-23 synergize via p38 MAPK to mediate barrier protection

To investigate the mechanism for TL1A regulation of ILC3-derived IL-22, we sorted Lin$^-$ CD127$^+$ IL-23R^{GFP} ILC3s from the small intestinal lamina propria and stimulated *ex vivo* with either recombinant TL1A, IL-23, or TL1A+IL-23. Although both IL-23 and TL1A induce IL-22 transcription, concomitant stimulation with both IL-23 and TL1A induced a robust synergistic response in IL-22 (Figure 3.8A). To confirm that TL1A synergy signaled through its monogamous receptor DR3, we sorted ILC3 from DR3-deficient mice or WT littermates. TL1A synergy with IL-23 required ILC3 expression of DR3 (Figure 3.8B).

Distinct ILC3 subsets expressing either the natural cytotoxicity receptor NKp46 (called NCR$^+$ ILC3) or chemokine receptor 6 (CCR6) (called lymphoid tissue-inducer-like ILC3) share significant functional overlap in the intestine.[72] Surface DR3 expression was equivalent across all ILC3 subsets (Figure 3.9A). Additionally, *ex vivo* TL1A stimulation of sorted intestinal ILC3 revealed synergistic induction of IL-22 in all subsets (Figure 3.9B)

In monocyte-derived macrophages, TL1A synergy with muramyl dipeptide to induce inflammatory cytokines requires autocrine, non-canonical caspase-8-dependent IL-1β[80]. To test the

potential contribution of autocrine IL-1β by ILC3, we sorted ILC3s from WT and IL1R-deficient mice. While IL1R was required for both IL-1β-dependent induction of IL-22, the TL1A/IL23 synergy remained intact suggesting that autocrine IL-1β is dispensable for the TL1A/IL23 synergistic enhancement of IL-22 (Figure 3.10).

In contrast to the non-canonical caspase pathway used in macrophages, conventional signaling downstream of DR3 can occur through mitogen-activated protein kinase (MAPK) or NF-κB pathways[81]. To evaluate the role for these signaling pathways in ILC3, we profiled protein phosphorylation by flow cytometry. Our results revealed significant phosphorylation of IκBα and p38-MAPK but not ERK following TL1A stimulation of sorted intestinal ILC3 (Figure 3.11A). To test the dependence on MAPK or NF-κB signaling, we sorted ILC3 and pre-treated with soluble inhibitors prior to *ex vivo* TL1A stimulation. Although the NF-κB inhibitor NBD did not affect IL-22 production, pre-treatment with TAK1 or p38 MAPK inhibitors (5Z-7-Oxozeaenol and SB203580, respectively) completely blocked TL1A and IL-23 synergistic induction of IL-22 (Figure 3.11B). To evaluate a physiologic role for IL-23 and TL1A synergy *in vivo*, we generated DR3- and IL23R-deficient double knock-out mice (*DR3*$^{-/-}$*IL23R*$^{-/-}$). *DR3*$^{-/-}$*IL23R*$^{-/-}$ mice showed significantly reduced survival following acute DSS-induced colitis (Figure 3.12). Collectively, these data

reveal the direct synergy of these IBD-linked pathways in regulating ILC3 production of effector cytokines and protection from acute colitis.

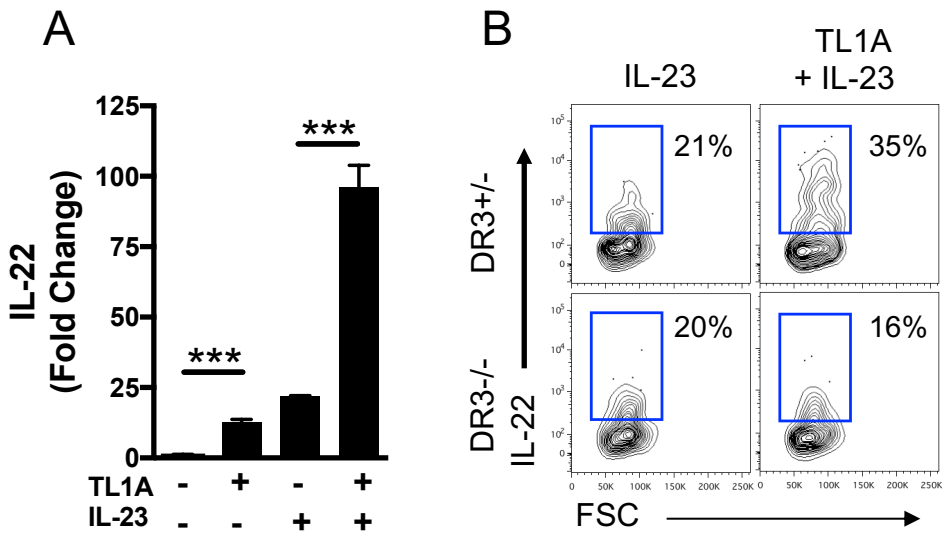

Figure 3.8. TL1A potently and selectively synergizes with IL-23 via DR3 to induce IL-22 production in ILC3 *in vitro*. (**A**, **B**) Sorted ILC3 from the intestinal lamina propria from *WT* or *DR3*$^{-/-}$ mice were stimulated *ex vivo* with media (-), rIL-23 and/or rTL1A. Quantitative PCR (A) or intracellular cytokine staining for IL-22 (B) was performed after 18h stimulation. Data in (A) are mean ± s.e.m; ***P<0.001; two-tailed Student's t-test with Bonferroni correction.

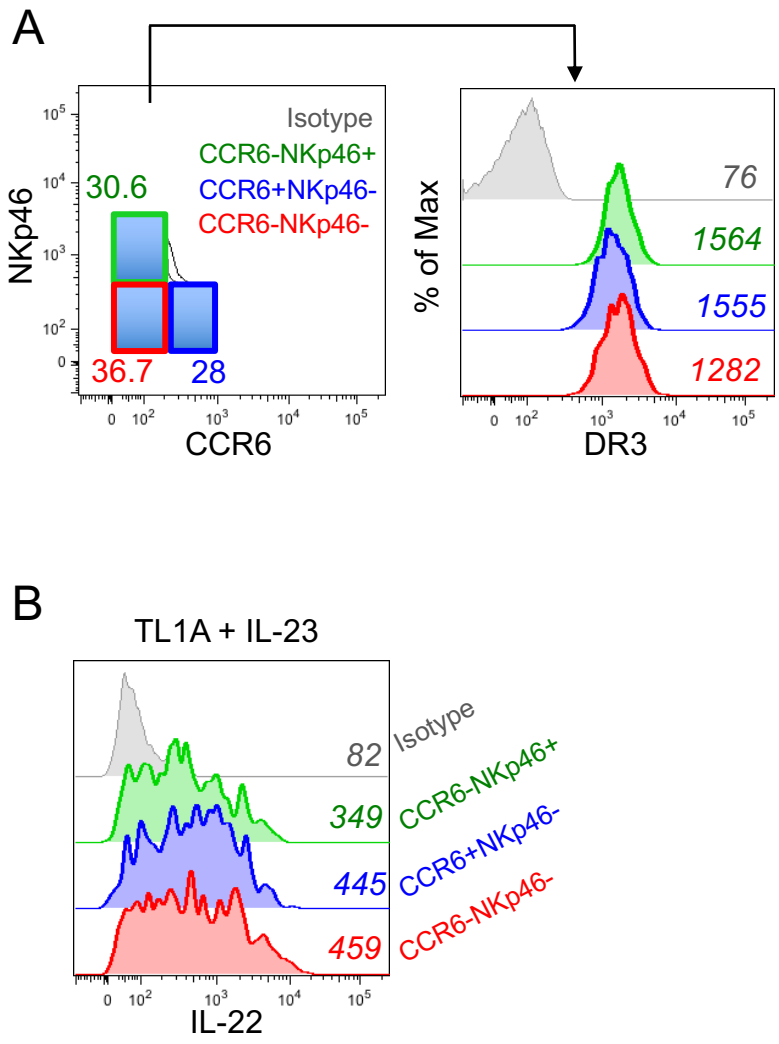

Figure 3.9. TL1A synergizes with IL-23 to induce IL-22 production in ILC3 subsets. (**A**) ILC3 (Lin-CD127^{+}IL23R-GFP^{+}) subsets were evaluated for extracellular DR3 expression by flow cytometric analysis. (**B**) IL-22 production by sorted ILC3 subsets was measured by intracellular flow cytometry after 18h stimulation. Brefeldin was added to the cultures 4h before intracellular cytokine staining.

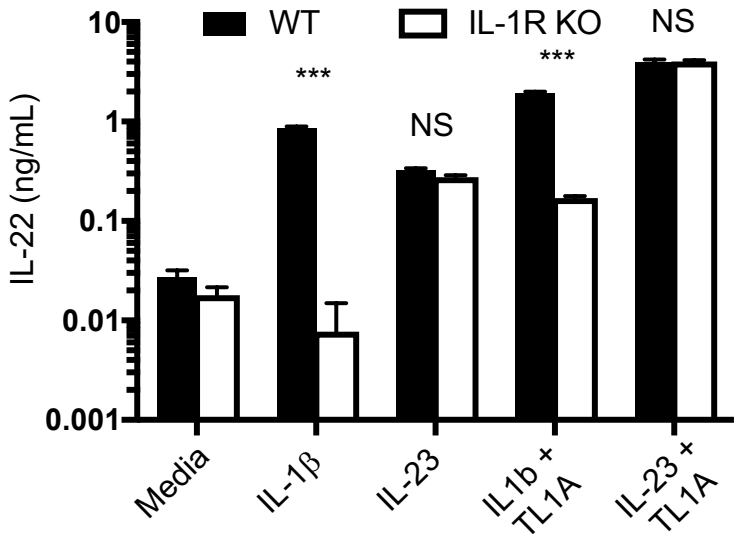

Figure 3.10. TL1A synergy with IL-23 is independent of IL1R. IL-22 production by sorted ILC3 from WT or IL1R$^{-/-}$ mice after 18h stimulation with media, rIL-1b, rTL1A, or rIL-23 (or in combinations).

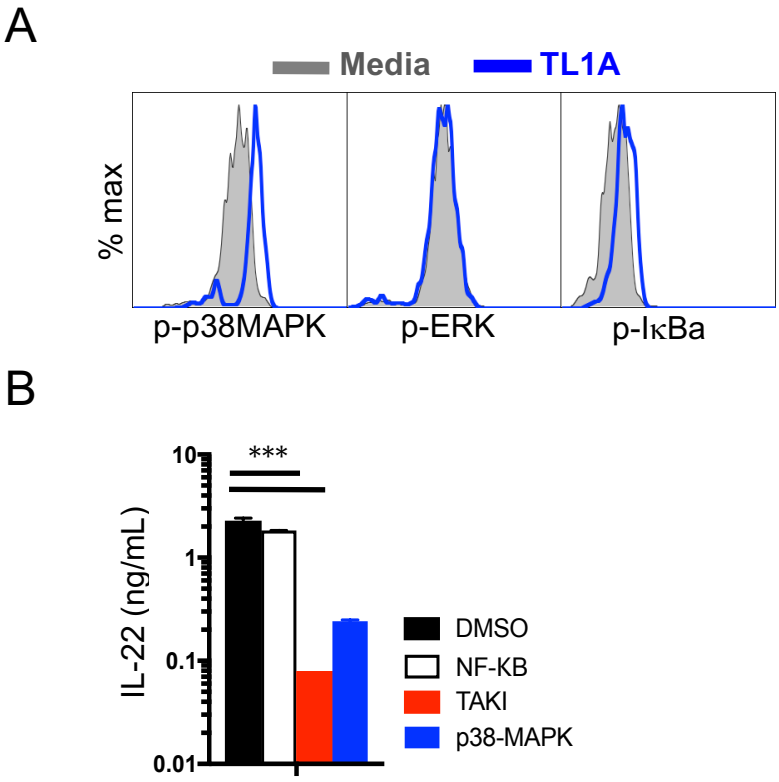

Figure 3.11. TL1A synergizes with IL-23 via p38-MAPK to induce IL-22 production in ILC3 *in vitro*. (**A**) Intracellular phosphoflow analysis was performed on sorted ILC3 for phosphorylation of p38-MAPK, ERK and IkBa 30 minute following stimulation. (**B**) Sorted ILC3 were stimulated for with r23 and rTL1A in the presence of soluble inhibitors. IL-22 production was evaluated by ELISA. Data in (B) are mean ± s.e.m; ****P*<0.001; two-tailed Student's t-test with Bonferroni correction.

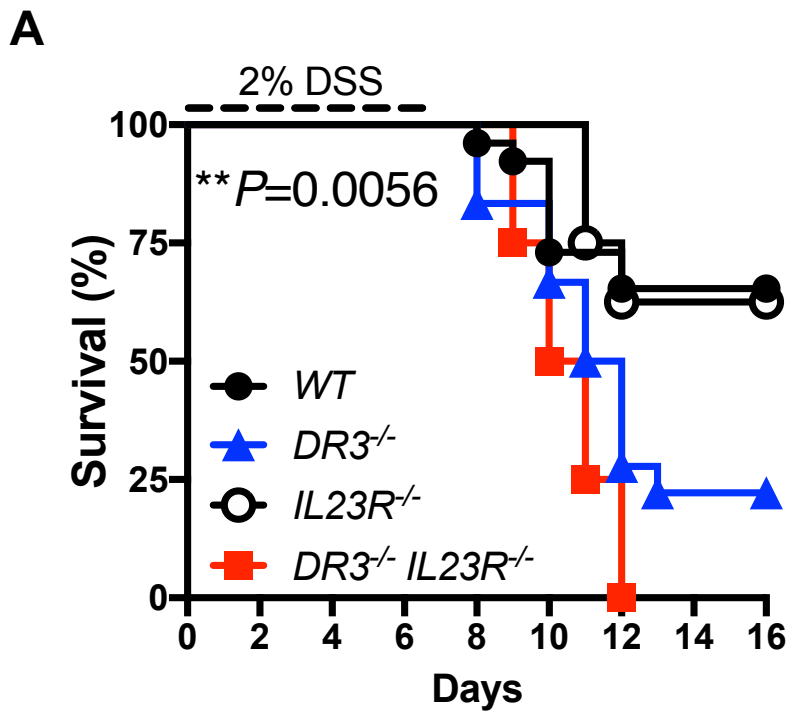

Figure 3.12. TL1A potently synergizes with IL-23 to protect from experimental colitis. (**A**) Survival curves of *WT*, *DR3*$^{-/-}$, *IL23R*$^{-/-}$ and *DR3*$^{-/-}$*IL23R*$^{-/-}$ mice following 7 day treatment with 2% DSS. Data in are compiled from two independent experiments (with n = 26, 18, 7, and 4 mice/group for *WT*, *DR3*$^{-/-}$, *IL23R*$^{-/-}$ and *DR3*$^{-/-}$*IL23R*$^{-/-}$, respectively). Data in (A) are $^{**}P<0.01$; Log-rank (Mantel-Cox) test.

3.5 DISCUSSION

Our results in Chapter 2 shed light on the mechanisms underlying how CX_3CR1^+ MNP-derived TL1A promotes barrier protection during acute inflammation. Furthermore, our data offer insights into how TL1A protects from IBD-associated microbes, a potentially evolutionary trait that evolved to protect hosts from pathogenic intestinal infections. These experiments focused on the cellular source of TL1A, identifying lamina propria MNPs as the dominant producer of intestinal TL1A, but how TL1A regulates cellular effector functions had not been thoroughly explored.

Here, using cell-specific genetic deletion models, we evaluated the contribution of this critical IBD-linked genetic pathway in regulating mucosal innate immunity during acute colitis. Our data reveal a critical role for ILC3-specific DR3 acting synergistically with IL23R signaling in promoting mucosal healing in acute colitis. *In vitro*, DR3 signaling on ILC3 was dependent on TAK1 and p38-MAPK signaling. *In vivo*, mice with mice with a double deletion of DR3 and IL23R (*DR3*$^{-/-}$ *IL23R*$^{-/-}$) had decreased survival compared to mice with single deletions in either DR3 or IL23R, highlighting a synergistic role for DR3/IL23R signaling in promoting mucosal healing *in vivo*.

Previous studies have focused predominantly on TL1A regulation of the adaptive immune system, and in particular T cells, our data demonstrate that during acute colitis, TL1A promotes barrier protection and mucosal healing via the regulation of ILC3s. A recent study reported that during acute colitis, TL1A was critical for promoting

mucosal healing via Foxp3^{+} Tregs[32]. Although we did not see changes in T cell numbers, subsets or cytokine production, our data are not entirely discordant with these findings since we looked at the early stages of acute colitis (days 7-9), whereas other studies noted T cell differences during the wound healing phase (days 10-22), but did not report significant changes during the earlier colitis stages. Here, I propose a revised model in which TL1A acts as a critical regulator of innate immunity during the early stages of colitis but can modulate the adaptive immune system during the recovery/wound healing stages of colitis.

CHAPTER FOUR: TL1A ENABLES ILC3 CO-STIMULATION OF T CELLS VIA OX40L

4.1 ABSTRACT

In previous chapters, we demonstrated an essential role for CX_3CR1^+ MNP-derived TL1A in promoting mucosal barrier protection during acute colitis. However, the mechanisms of how TL1A alters ILC3 effector functions to regulate effector T cell functions during chronic colitis are not known. Here, we used RNA-seq analysis to identify TL1A-dependent upregulation of the co-stimulatory molecule OX40L on ILC3, which enabled ILC3 to co-stimulate antigen-specific T cells proliferation *in vitro*. This data suggest a revised model in which inducible ILC3 expression of OX40L co-stimulation may trigger local T cell activation.

4.2 INTRODUCTION

Group 3 innate lymphoid cells (ILC3) are an emerging class of innate lymphocytes that play a critical role in regulating mucosal homeostasis. In response to environmental triggers, in particular the cytokines IL-23 and IL-1β, ILC3 produce robust amounts of IL-22 and play an important role in maintaining intestinal barrier integrity and promoting mucosal healing—a major clinical endpoint in IBD[24]. Co-localization of ILC3 with CX_3CR1^+ mononuclear phagocytes (MNPs) in the lamina propria enables rapid regulation of ILC3 effector cytokines to reinforce barrier immunity and mucosal healing[40]. Both mouse and human ILC3s express Death Receptor 3 (DR3), the monogamous receptor for TL1A, on its surface, with TL1A stimulation promoting ILC3 proliferation[76] and cytokine production *in vitro*[24]; however, the role for TL1A in regulating ILC3 function in intestinal homeostasis, and its potential contribution to IBD pathophysiology, remains unknown.

Beyond reinforcing the intestinal barrier via effector cytokines, ILC3 have been reported to play an important role in the regulation of the of adaptive immunity[82–85]. In the previous chapter, we identified a pathogenic role for TL1A during chronic colitis. In a chronic T cell transfer model, ILC3-specific DR3 signaling promoted the generation of T-bet$^+$ T cells *in vivo*. However, how ILC3 regulate T cell effector function via DR3 is currently unknown. To identify novel targets of TL1A on ILC3, we performed RNA-seq analysis of TL1A-stimulated ILC3, revealing an upregulation of the co-stimulatory molecule OX40L upon TL1A stimulation. In ILC3:T cell co-culture assays, TL1A

stimulation enabled MHCII^{+} ILC3 to co-stimulate OTII antigen-specific T cells *in vitro*, which was dependent on DR3 signaling, antigen presentation by MHC Class II and the costimulatory molecule OX40L, but not other co-stimulatory molecules like ICOSL. This data suggest a revised model in which inducible ILC3 expression of OX40L co-stimulation may trigger local T cell activation.

4.3 METHODS

Mice. C57BL/6, Rorc-cre, and OT-II mice were purchased from The Jackson Laboratory. *Il23r*^{GFP} mice were obtained from M. Oukka[77]. *MHCII*$^{\Delta ILC3}$ mice were obtained from Gregory Sonnenberg[86]. Generation of *Dr3*$^{flox/flox}$ mice is previously described[78]. *OX40L*$^{flox/flox}$ mice were obtained from David Withers[87]. All vertebrate work was approved by the IACUC at Weill Cornell Medicine.

Antibodies and flow cytometry. Staining of cells was performed with the following antibodies:

Table 4.1. Flow cytometry antibodies used in chapter 4.

Species	Target	Fluorophore	Clone	Manufacturer
Mouse	CD3	FITC	145-2C11	eBioscience
Mouse	CD4	eFluor780	RM4-5	eBioscience
Mouse	CD5	PE	53-7.3	eBioscience
Mouse	CD45.1	APC	A20	eBioscience
Mouse	CD90.2	efluor450	53-2.1	eBioscience
Mouse	MHCII	Alexa700	M5/114.15.2	eBioscience
Mouse	CD19	FITC	MB19-1	eBioscience
Mouse	CD11b	eFluor780	M1/70	eBioscience
Mouse	CD11c	PE-Cy7	N418	eBioscience
Mouse	CD103	APC	2E7	eBioscience
Mouse	TCR$\gamma\delta$	FITC	11-5711-82	eBioscience
Mouse	KLRG1	PE	2F1	eBioscience
Mouse	NKp46	eFluor710	29A1.4	eBioscience
Mouse	OX40L	APC	RM134L	eBioscience
Mouse	ICOSL	eFluor660	HK5.3	eBioscience
Mouse	CD127	PE-Cy7	A7R34	BioLegend
Mouse	CCR6	BV421	29-2L17	BioLegend
Mouse	DR3	PE	4C12	BioLegend

Dead cells were excluded using the Live/Dead fixable aqua dead cell stain kit (Invitrogen). Intracellular cytokine staining was performed according to the manufacturer's protocol (Cytofix/Cytoperm buffer set; BD) and transcription factor staining for was performed according to manufacturer's protocol (Intracellular Fixation and Permeabilization kit; eBioscience). Flow cytometry was performed with a BD LSRFortessa and analyzed with FlowJo software (Tree Star).

Preparation of LPMC. Mouse intestines were washed in PBS and 1 mM DTT with 30 mM EDTA, and then digested in collagenase 8 (Sigma-Aldrich) and DNase-containing media with 10% fetal bovine serum. Digested material was passed through a cell strainer and separated on a discontinuous 40%/80% Percoll gradient.

Co-culture assays. For antigen-specific T-cell proliferation assays, $2x10^5$ sort-purified, CFSE-labeled naïve $CD4^+$ T-cells from OTII transgenic mice were co-cultured with either $2.5x10^4$ sort-purified ILC3 from $IL23R^{GFP/wt}$ mice or $2x10^4$ $MHCII^+CD11c^+CD11b^+$ MNPs, with 20ug/mL OVA peptide (OVA 323-339; InvivoGen) and 200ng/mL rTL1A, as indicated, in a 96-well flat bottom plate for six days. For co-stimulatory blocking assays, ILC3/T cell co-cultures were blocked with 20ug/mL anti-mouse ICOSL antibody (LEAF purified anti-mouse

CD275; BioLegend) or 15ug/mL anti-mouse OX40L antibody (Biotin anti-mouse CD252; BioLegend).

RNA-seq analysis. Mouse RNA-Seq data was aligned to the mm9 assembly of the mouse genome using the STAR aligner[1]. Read counts for genes across all BAM files were computed using the HTSeq software[2]. Differential analysis of RNA-Seq samples utilized the DESeq package for gene expression analysis[3]. False discovery rate correction of P-values used for all bioinformatics analyses of this study utilized the Benjamini-Hochberg procedure[4]. Heatmap clustering and production was done using the heatmap function within the NMF package in **R**[5]**.** Principal components analysis plots were visualized using the ggbiplot package in **R.**

Statistical analysis. Statistical analysis was performed in GraphPad Prism or R software. Results represent mean ± s.e.m. and were analyzed by unpaired Student's t-test or one-way ANOVA, as indicated in the figure legends. Given that mouse experiments required littermate controls and complex genotyping, experimental group allocation was not blinded. No relevant exclusion criteria were applied.

4.4 RESULTS

4.4.1 TL1A induces co-stimulatory molecules on ILC3

To identify novel genes and pathways regulated by TL1A, we performed RNA-seq of TL1A-stimulated intestinal ILC3. ILC3 were sort-purified from *IL23R*$^{GFP/WT}$ mice and stimulated for 18 hours with or without recombinant TL1A (Figure 4.1A). In addition to induction of *Csf2* and *Il22,* RNA-seq analysis revealed significant induction of the co-stimulatory molecules OX40L and ICOSL following TL1A stimulation (Figure 4.1B), which was confirmed by quantitative PCR of its gene *Tnfsf4* and flow cytometric analysis of surface expression of OX40L (Figure 4.1C). Furthermore, TL1A stimulation of sort-purified ILC3 revealed upregulation of OX40L across all ILC3 subsets (Figure 4.2).

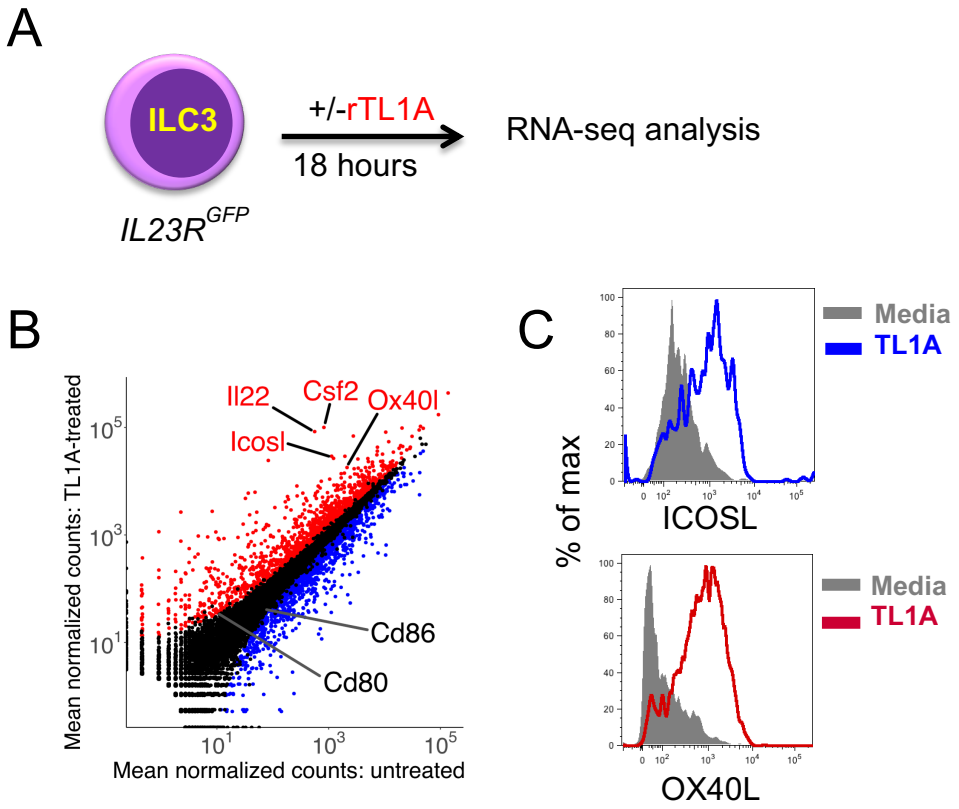

Figure 4.1. TL1A induces ILC3 expression of OX40L *in vitro*. (**A**) Experimental design for sort-purified ILC3 from *IL23R*$^{GFP/WT}$ mice treated with media or rTL1A for 18 h prior to RNA-seq analysis. (**B**) Scatterplot of global gene expression profiles of media- or rTL1A-stimulated sorted Lin^{-}CD127^{+}IL23R^{GFP+} ILC3 from IL23R$^{GFP/WT}$ mice. Red and blue dots indicate significantly up- or down-regulated genes, respectively, after FDR correction for multiple hypothesis testing. (**C**) ICOSL and OX40L surface protein in sorted Lin^{-}CD127^{+}IL23R^{GFP+} ILC3 from IL23R$^{GFP/WT}$ mice stimulated for 18h with rTL1A or media alone. Data in C are mean ± s.e.m and were analyzed by two-tailed Student's t-test; ***P<0.001.

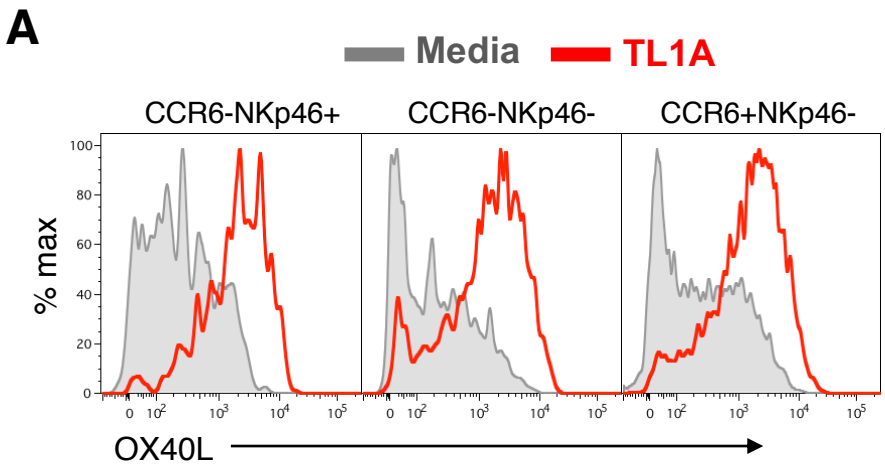

Figure 4.2. **TL1A induces OX40L expression across all ILC3 subsets.** (**A**) Sorted Lin$^-$CD127$^+$IL23R^{GFP+} ILC3 from the intestinal lamina propria of *IL23R*$^{GFP/WT}$ mice were stimulated *ex vivo* with media or rTL1A for 18 hours and extracellular OX40L levels were quantified in ILC3 subsets by flow cytometry.

4.4.2 TL1A enables ILC3 co-stimulation of OTII transgenic T cells *in vitro*

Previous studies have shown that MHCII^{+} ILC3 lacking surface expression of classical co-stimulatory molecules negatively regulate T-cell responses to commensal bacteria[86]. To test if TL1A-induced expression of co-stimulation could promote antigen-specific T-cell responses, MHCII^{+} and MHCII^{-} ILC3 were sort-purified from IL23R$^{GFP/WT}$ mice and co-cultured with CFSE-labeled naïve OTII CD4^{+} T-cells in the presence or absence of OVA peptide or recombinant TL1A stimulation (Figure 4.3A). OVA peptide and TL1A stimulation of MHCII^{+} ILC3 induced multiple rounds of ovalbumin-specific T-cell proliferation, similar to the proliferative levels seen in OVA-loaded dendritic cells (Figure 4.3B).

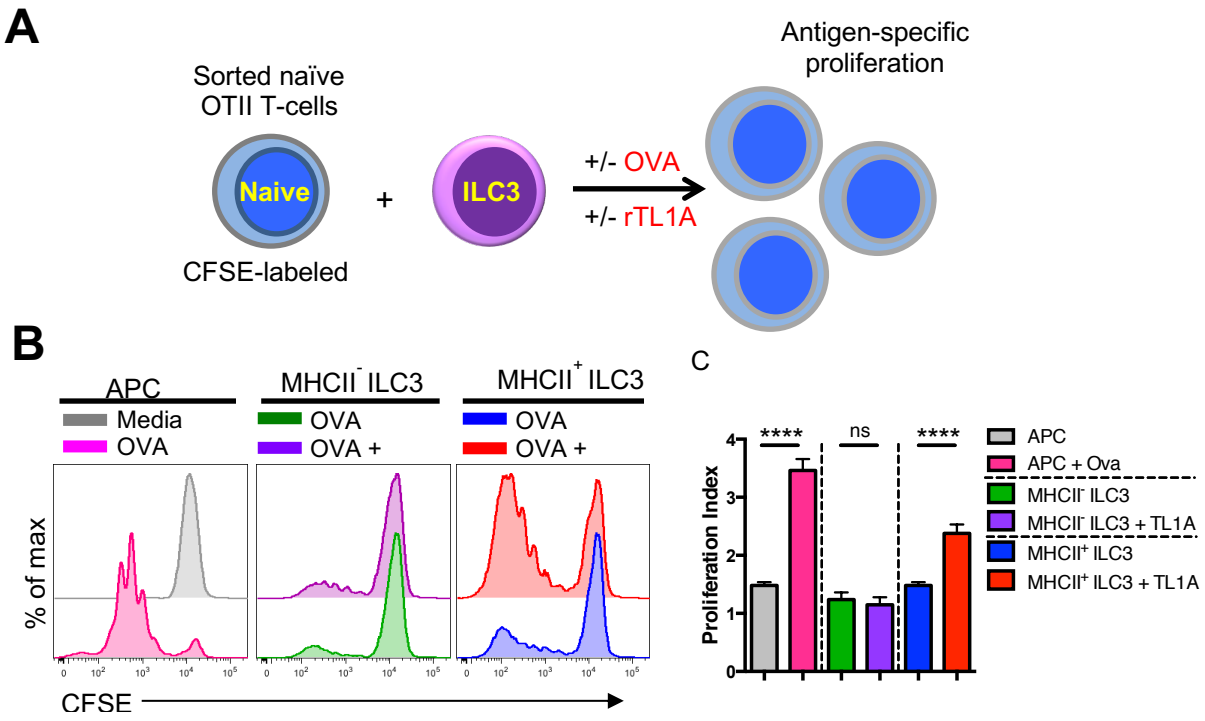

Figure 4.3. TL1A stimulation of MHCII$^+$ ILC3 enables ILC3 co-stimulation of CD4$^+$ T cells. (**A**) Experimental design for ILC3:T cell co-culture assay. (**B**) Sort-purified, CFSE-labeled CD4$^+$ T-cells from OT-II transgenic mice were cultured for 6 days with sort-purified MHCII$^+$ DCs, MHCII$^-$ ILC3 or MHCII$^+$ ILC3, from either with media alone, OVA peptide, or OVA peptide and rTL1A, as indicated. (**C**) Quantification of antigen-specific T cell proliferation from (B). Data in C are mean ± s.e.m and were analyzed by Student's t-test; ****P<0.0001, ns= not significant.

4.4.3 ILC3 co-stimulation of T cells is DR3-dependent

To test the genetic dependency of DR3 in promoting TL1A-induced ILC3 co-stimulation of antigen-specific T cells, sort-purified ILC3 from *DR3*$^{\Delta ILC3}$ *RAG2*$^{-/-}$ or *DR3*$^{flox/flox}$ *RAG2*$^{-/-}$ littermates were co-cultured with sorted, CFSE-labeled OTII T cells in the presence of OVA and with/without TL1A stimulation (Figure 4.4A). In contrast, to the proliferation seen in co-cultures with WT ILC3, DR3-deficient ILC3 did not induce proliferation of OTII T cells (Figure 4.4B).

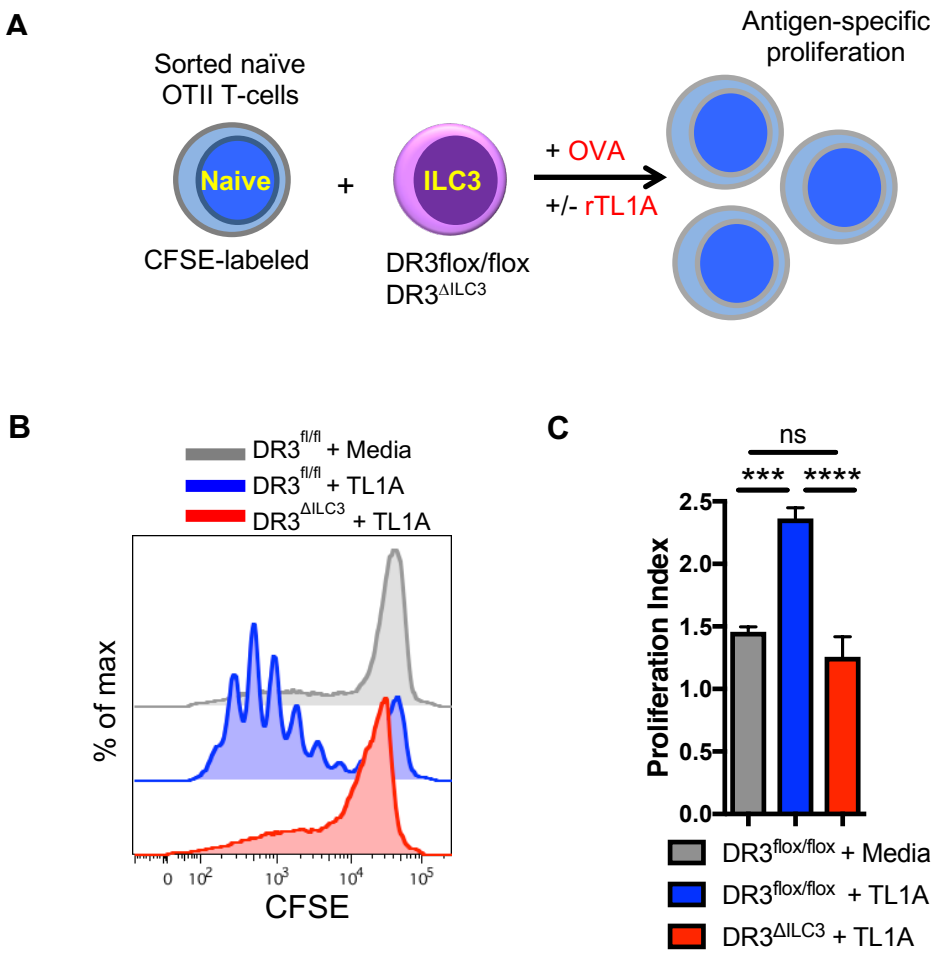

Figure 4.4. TL1A stimulation of MHCII$^+$ ILC3 enables DR3-dependent co-stimulation of CD4$^+$ T cells. (**A**) Experimental design for ILC3:T cell co-culture assay. (**B**) Sort-purified, CFSE-labeled CD4$^+$ T-cells from OT-II transgenic mice were cultured for 6 days with sort-purified ILC3, from either *DR3$^{flox/flox}$* or *DR3$^{\Delta ILC3}$* mice with media alone, OVA peptide, or OVA peptide and rTL1A, as indicated. (**C**) Quantification of antigen-specific T cell proliferation from (B). Data in C are mean ± s.e.m and were analyzed by one-way ANOVA; ***P<0.001, ****P<0.0001, ns= not significant.

4.4.4 OX40L blocking inhibits TL1A-mediated ILC3 co-stimulation of T cells

To evaluate the potential contribution of ICOSL and OX40L in promoting ILC3 co-stimulation of T-cells, ILC3s were cultured with CFSE-labeled naïve OTII $CD4^+$ T-cells in the presence of OVA, recombinant TL1A, and α-OX40L or α-ICOSL blocking antibodies (Figure 4.5A). OX40L, but not ICOSL, blockade completely inhibited *in vitro* proliferation, suggesting a key role for OX40L co-stimulation in regulation ILC3-driven T-cell proliferation (Figure 4.5B,C).

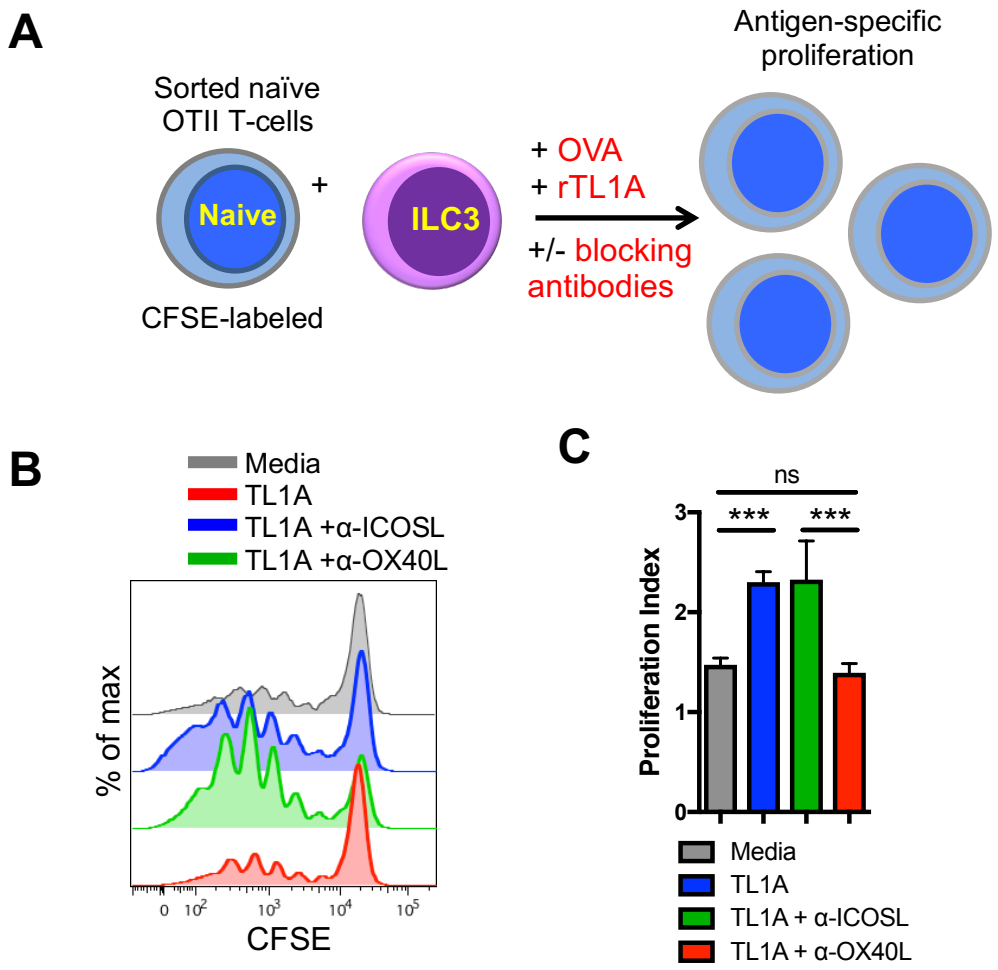

Figure 4.5. OX40L blocking inhibits TL1A-mediated ILC3 co-stimulation of CD4⁺ T cells. (A) Experimental design for ILC3:T cell co-culture assay. (B) Sort-purified, CFSE-labeled CD4⁺ T-cells from OT-II transgenic mice were cultured for 6 days with sort-purified ILC3 in the presence of media alone, rTL1A, or with rTL1A plus co-stimulatory molecule blocking antibodies. All samples received OVA peptide in culture. (C) Quantification of antigen-specific T cell proliferation from (B). Data in C are mean ± s.e.m and were analyzed by one-way ANOVA; ****P*<0.001, ns= not significant.

4.4.5 Generation of ILC3-specific OX40L deletion genetic model

To specifically test the importance of ILC3-intrinsic OX40L signaling in intestinal barrier immunity, we crossed mice with a *lox*P-flanked *Tnfsf4* (*OX40L*$^{flox/flox}$) to transgenic mice expressing the Cre recombinase from the RORγt promoter (*Rorc*^{cre}) on a RAG2-deficient background (called *OX40L*$^{\Delta ILC3}$) (Figure 4.6A). Transcriptional and flow cytometric analysis revealed that *OX40L*$^{\Delta ILC3}$ mice lacked O40L expression on ILC3 after TL1A stimulation, confirming OX40L deletion (Figure 4.6B).

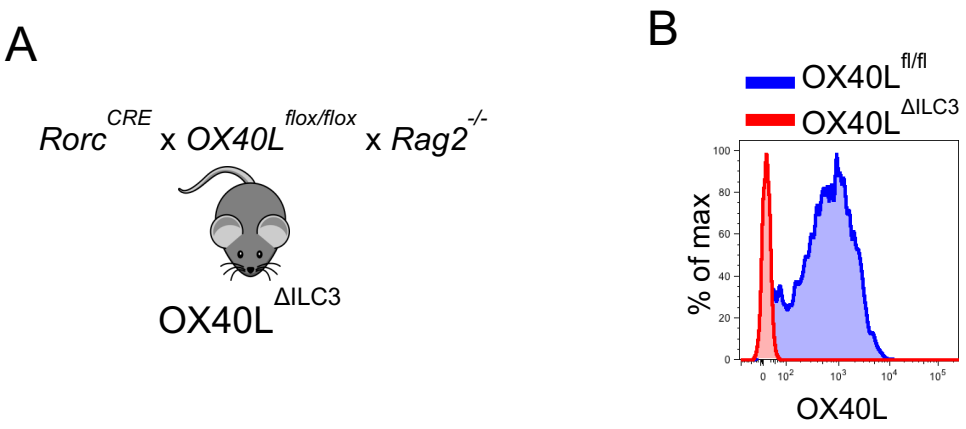

Figure 4.6. Generation of ILC3-specific OX40L genetic deletion model. (**A**) Generation of ILC3-specific OX40L genetic deletion model. (**B**) Representative flow cytometry analysis of extracellular OX40L expression in sort-purified ILC3 from indicated mice stimulated for 18 h with rTL1A.

4.4.6 ILC3 co-stimulation of T cells is OX40L-dependent

To test the genetic dependency of OX40L in promoting TL1A-induced ILC3 co-stimulation of antigen-specific T cells, sort-purified ILC3 from *OX40L*$^{\Delta ILC3}$ *RAG2*$^{-/-}$ or *OX40L*$^{flox/flox}$ *RAG2*$^{-/-}$ littermates were co-cultured with sorted, CFSE-labeled OTII T cells in the presence of OVA and with/without TL1A stimulation (Figure 4.7A). In contrast, to the proliferation seen in co-cultures with WT ILC3, OX40L-deficient ILC3 did not induce proliferation of OTII T cells (Figure 4.7B,C).

Given the previous data showing that ILC3 co-stimulation was dependent on the co-stimulatory molecule OX40L, we hypothesized that, mechanistically, ILC3 were promoting T cell proliferation via antigen presentation via MHCII with OX40L being the dominant co-stimulatory signal. To test the genetic dependency of antigen-presentation in promoting TL1A-induced ILC3 co-stimulation of antigen-specific T cells, sort-purified ILC3 from *MHCII*$^{\Delta ILC3}$ or *MHCII*^{WT} mice were co-cultured with sorted, CFSE-labeled OTII T cells in the presence of OVA and with/without TL1A stimulation (Figure 4.8A). In contrast, to the proliferation seen in co-cultures with WT ILC3, MHCII-deficient ILC3 did not induce proliferation of OTII T cells (Figure 4.8B,C).

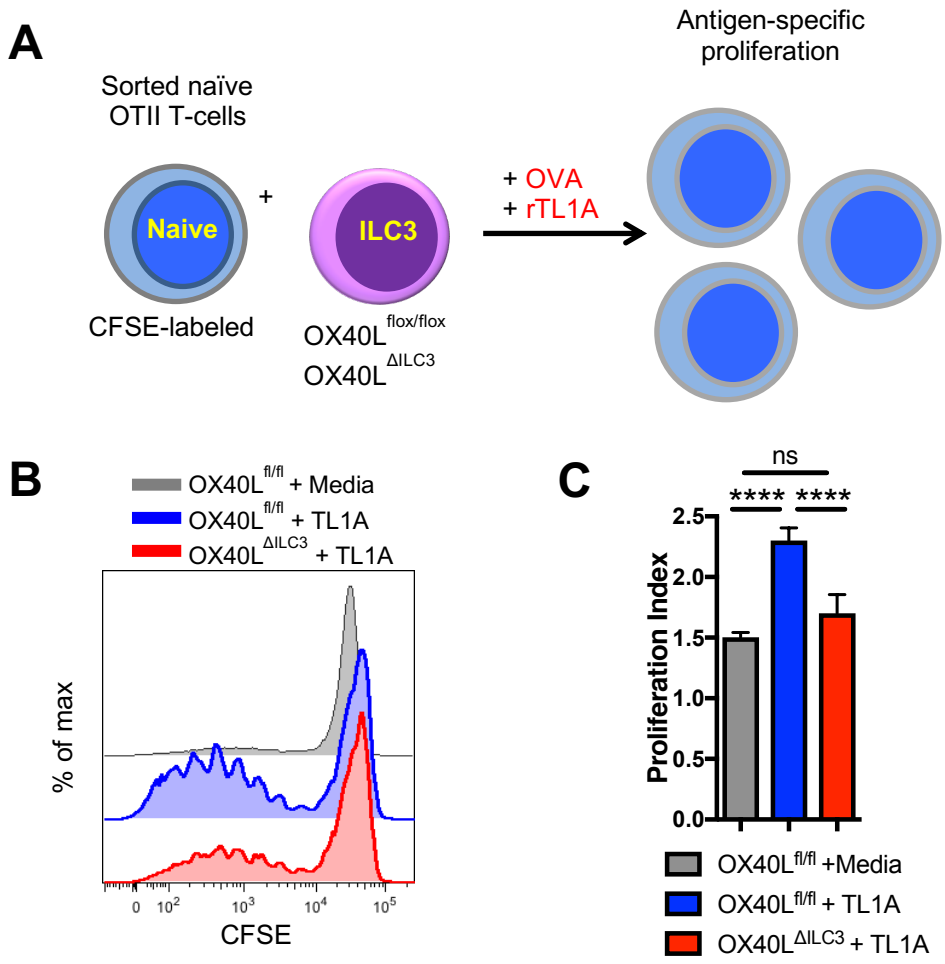

Figure 4.7. TL1A stimulation of MHCII^{+} ILC3 enables OX40L-dependent co-stimulation of CD4^{+} T cells. (A) Experimental design for ILC3:T cell co-culture assay. (B) ILC3 sorted from mice with a conditional deletion of OX40L (OX40L$^{\Delta ILC3}$) or littermate controls OX40L$^{flox/flox}$ were stimulated with TL1A and co-cultured with sort-purified, CFSE-labeled OTII CD4+ T cells for 6 days. All samples received OVA peptide in culture. (C) Quantification of antigen-specific T cell proliferation from (B). Data in C are mean ± s.e.m and were analyzed by one-way ANOVA; ***P<0.001, ns= not significant.

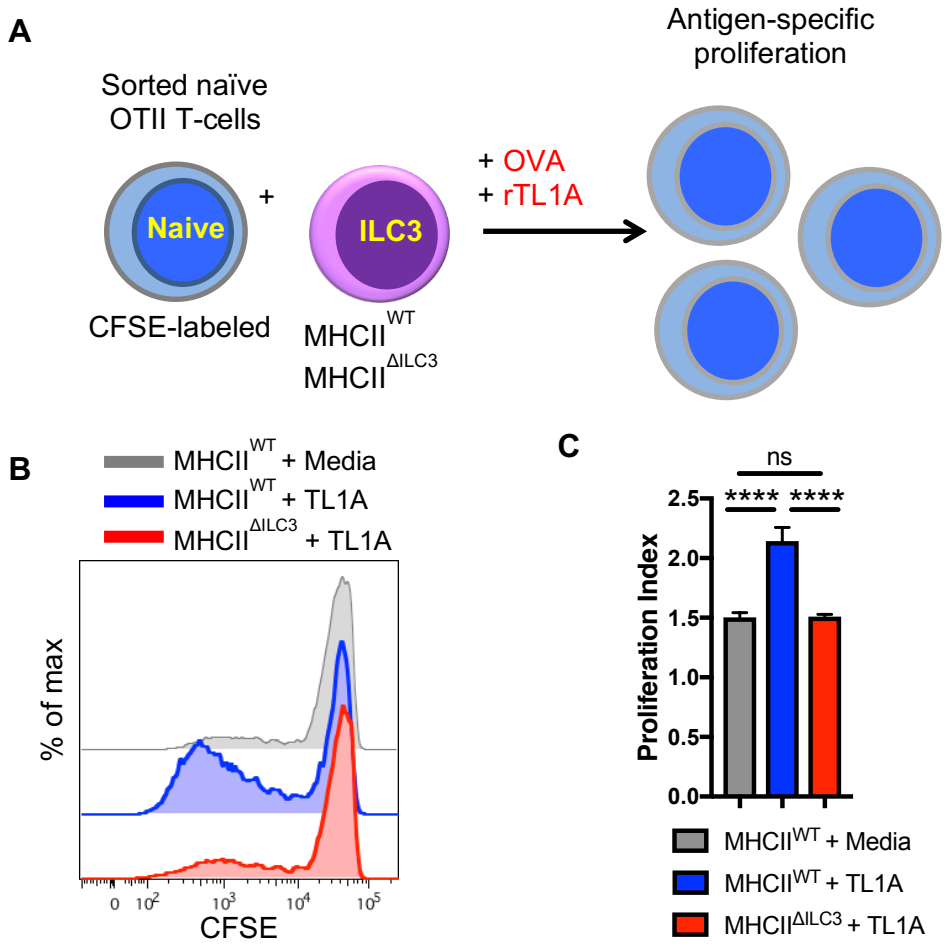

Figure 4.8. TL1A stimulation of ILC3 enables MHCII-dependent co-stimulation of CD4⁺ T cells. (A) Experimental design for ILC3:T cell co-culture assay. (B) ILC3 sorted from mice with a conditional deletion of MHCII ($MHCII^{\Delta ILC3}$) or WT ILC3 ($MHCII^{WT}$) were stimulated with TL1A and co-cultured with sort-purified, CFSE-labeled OTII CD4+ T cells for 6 days. All samples received OVA peptide in culture. (C) Quantification of antigen-specific T cell proliferation from (B). Data in C are mean ± s.e.m and were analyzed by one-way ANOVA; ***P<0.001, ns= not significant.

4.5 DISCUSSION

In the previous chapter, we identified a pathogenic role for TL1A during chronic colitis. In a chronic T cell transfer model, ILC3-specific DR3 signaling promoted the generation of T-bet$^+$ T cells *in vivo*. However, how ILC3 regulate T cell effector function via DR3 is currently unknown. Here, we used RNA-seq analysis to identify TL1A-dependent upregulation of the co-stimulatory molecules on ILC3, which enabled ILC3 to co-stimulate antigen-specific T cells proliferation *in vitro*. Mechanistically, ILC3 co-stimulation of OTII T cells *in vitro* was dependent on DR3 signaling, antigen presentation by MHC Class II and the costimulatory molecule OX40L, suggesting that ILC3 co-stimulation of naïve T cells is dependent on ILC3 antigen presentation with both signal 1 and signal 2 present after TL1A stimulation. However, it remains to be explored whether the induction of these co-stimulatory molecules, and OX40L specifically, is unique to TL1A stimulation or if it can also be induced by other cytokines, like IL-1β or IL-23. Furthermore, whether ILC3 can co-stimulate antigen-specific T cells via DR3 and OX40L *in vivo*, and any potential contribution to intestinal pathophysiological, remains unknown.

The discovery of antigen processing and presentation by intestinal ILC3 highlights a central role for these cells in linking innate and adaptive immunity[86]. Although splenic ILC3 can upregulate conventional co-stimulatory molecules CD80 and CD86 following IL-1β stimulation[88], the absence of these co-stimulatory molecules, even following stimulation, on intestinal ILC3 lead to a model in which they

limit bacteria-specific inflammatory T-cell responses in the gut[89]. By showing that TL1A induced expression of co-stimulatory molecule OX40L on the surface of $MHCII^+$ ILC3 support *in vitro* proliferation of naïve antigen specific T cells, our data suggest a revised model in which inducible ILC3 expression of OX40L co-stimulation may trigger local T cell activation.

CHAPTER FIVE: DR3-OX40L AXIS PROMOTES ILC3 CO-STIMULATION OF T CELLS IN VIVO

5.1 ABSTRACT

Previous studies have suggested a pathogenic role for chronic TL1A expression in IBD. However, the mechanisms by which TL1A contributes to chronic colitis are not known. Here, we report an essential role for ILC3-intrinsic DR3-OX40L axis in regulating T cell function *in vivo*. During colitis, ILC3 upregulated OX40L in a DR3-dependent manner. In contrast to this protective role in acute colitis, colitis-induced DR3-dependent expression of OX40L enabled $MHCII^+$ ILC3 to co-stimulate dietary and microbial antigen-specific T cell proliferation and exacerbate chronic T cell-dependent colitis. Colonic biopsies from IBD patients revealed increased OX40L on ILC3 compared to healthy controls, highlighting the conserved TL1A-OX40L ILC3 axis in IBD. These data reveal a pro-inflammatory role for the ILC3 DR3-OX40L axis in chronic T cell colitis and a novel role in the regulation of antigen-specific T cells *in vivo*.

5.2 INTRODUCTION

MHCII$^+$ ILC3s play in a central role in regulating T cell homeostasis in the intestine[84]. Previous studies have reported that at the steady state, MHCII$^+$ ILC3 lack the expression of co-stimulatory molecules and can limit T cell responses to commensal antigens via anergy[84,86], suggesting a protective role for ILC3 in limiting the generation of autoreactive T cells. In the previous chapter, we reported that TL1A stimulation induced the expression of the co-stimulatory molecule OX40L, which enabled ILC3 to co-stimulate antigen-specific T cells in vitro; the co-stimulatory capacity of ILC3 was dependent on TL1A signaling via DR3, antigen presentation by MHCII, and the co-stimulatory molecule OX40L. However, the functional role for ILC3-intrinsic OX40L in regulating T cell function *in vivo* has not been explored.

Here, using genetic mouse models with selective deletion of DR3 and OX40L on ILC3, we evaluated a role of this critical IBD-linked axis in regulating T cell-mediated mucosal immunity. Our data reveal a central role for the DR3-OX40L axis on ILC3 in regulating dietary and microbial antigen-specific T cell proliferation *in vivo* and a functional role in promoting chronic T cell-dependent colitis.

5.3 METHODS

Mice. C57BL/6, Rorc-cre, and OT-II mice were purchased from The Jackson Laboratory. *Il23r*^{GFP} mice were obtained from M. Oukka[77]. *Dr3*$^{flox/flox}$ mice is previously described[78]. *OX40L*$^{flox/flox}$ mice were obtained from David Withers[87]. *Helicobacter hepaticus* transgenic TCR mice were obtained from D. Littman[90]. Generation of All vertebrate work was approved by the IACUC at Weill Cornell Medicine.

Human IBD subjects. A cohort of patients was evaluated for IBD at the Jill Roberts Center for IBD under Institutional Review Board–approved protocol (1103011578) at Weill Cornell Medicine (WCM). Healthy control patients presented with abdominal pain but had normal endoscopic results; IBD patients were defined as having endoscopic inflammation with a history of ulcerative colitis or Crohn's disease. All endoscopic biopsies were taken from the colon. Endoscopic biopsies from healthy control and IBD patients were transported in ice cold PBS and processed as previously reported (JEM, Longman).

Antibodies and flow cytometry. Staining of cells was performed with the following antibodies:

Table 5.1. Flow cytometry antibodies used in chapter 5.

Species	Target	Fluorophore	Clone	Manufacturer
Mouse	CD3	FITC	145-2C11	eBioscience
Mouse	CD4	eFluor780	RM4-5	eBioscience
Mouse	CD5	PE	53-7.3	eBioscience
Mouse	CD45.1	APC	A20	eBioscience
Mouse	CD90.2	efluor450	53-2.1	eBioscience
Mouse	MHCII	Alexa700	M5/114.15.2	eBioscience
Mouse	CD19	FITC	MB19-1	eBioscience
Mouse	CD11b	eFluor780	M1/70	eBioscience
Mouse	CD11c	PE-Cy7	N418	eBioscience
Mouse	CD103	APC	2E7	eBioscience
Mouse	TCR$\gamma\delta$	FITC	11-5711-82	eBioscience
Mouse	KLRG1	PE	2F1	eBioscience
Mouse	OX40L	APC	RM134L	eBioscience
Mouse	CD127	PE-Cy7	A7R34	BioLegend
Mouse	CCR6	BV421	29-2L17	BioLegend
Mouse	DR3	PE	4C12	BioLegend
Mouse	RORγt	PE	B2D	eBioscience
Mouse	T-bet	e660	eBio4B10	eBioscience
Mouse	Foxp3	e450	FJK-16s	eBioscience
Mouse	IL-22	APC	IL22JOP	eBioscience
Mouse	TL1A	e710	Tandys1a	eBioscience
Human	CD14	PE	61D3	eBioscience
Human	CD14	Alexa700	63D3	eBioscience
Human	HLA-DR	Alexa700	LN3	eBioscience
Human	TL1A	e710	Tandys1a	eBioscience
Human	CD45	APC	2D1	eBioscience
Human	CD3	eFluor780	UCHT1	eBioscience
Human	CD19	Alexa700	HIB19	eBioscience
Human	CD127	PE-Cy7	eBioRDR5	eBioscience
Human	CD117	efluor450	104D2	eBioscience
Human	OX40L	PE	11C3.1	BioLegend
Human	CD5	eFluor780	UCHT1	BioLegend
Human	ST2L	FITC	B4E6	mdbioproducts
Human	CD11c	Alexa700	3.9	Invitrogen

Dead cells were excluded using the Live/Dead fixable aqua dead cell stain kit (Invitrogen). Intracellular cytokine staining was performed according to the manufacturer's protocol (Cytofix/Cytoperm buffer set; BD) and transcription factor staining for was performed according to manufacturer's protocol (Intracellular Fixation and Permeabilization kit; eBioscience). Flow cytometry was performed with a BD LSRFortessa and analyzed with FlowJo software (Tree Star).

Preparation of LPMC. Mouse intestines were washed in PBS and 1 mM DTT with 30 mM EDTA, and then digested in collagenase 8 (Sigma-Aldrich) and DNase-containing media with 10% fetal bovine serum. Digested material was passed through a cell strainer and separated on a discontinuous 40%/80% Percoll gradient.

Colitis models. To induce chemical colitis in mice, 2% DSS (w/v) (M.W. 40,000-50,000; Affymetrix) was added to sterile drinking water and administered ad libitum for 7 days. After 7 days, DSS was replaced with normal drinking water. For T-cell transfer colitis, $5x10^5$ $CD4^+$ $CD45RB^{high}$ $CD25^-$ $CD62L^-$ T-cells were transferred i.p. into *OX40L*$^{\Delta ILC3}$ *RAG2*$^{-/-}$ or *OX40L*$^{flox/flox}$ *RAG2*$^{-/-}$ mice or in a separate experiment, into *DR3*$^{\Delta ILC3}$ *RAG2*$^{-/-}$ or *DR3*$^{flox/flox}$ *RAG2*$^{-/-}$ mice, as indicated in the figure legends. To induce infectious colitis, *Helicobacter hepaticus* were cultured as previously described[90]; for oral infection, mice were orally gavaged with *Helicobacter hepaticus*

every four days for a total of two inoculations, as previously described[90]. For all colitis experiments, mice were monitored daily weight loss, rectal bleeding, diarrhea and survival throughout the experiments. For all colitis experiments, mice were monitored daily (DSS) or weekly (T-cell transfer) for weight loss, rectal bleeding, diarrhea and survival throughout the experiments.

Antigen-specific T-cell transfer. For OVA-specific T cell transfer experiments, CD45.2$^+$ *OX40L$^{flox/flox}$* and CD45.2$^+$ *OX40L$^{\Delta ILC3}$* were fed *ad libitum* 1% ovalbum and to 2% dextran sodium sulfate for five days prior to the transfer of 5x10^5 CFSE-labeled CD45.1$^+$ CD3$^+$CD4$^+$ Vα2 OTII T-cells (i.p.) from OVA TCR transgenic mice. Transferred T-cells were analyzed seven days post-transfer. For *Helicobacter hepaticus*-specific T cell transfer experiments, mice were orally gavaged with *Helicobacter hepaticus* every four days for a total of two inoculations, as previously described[90]; eight days post *Helicobacter hepaticus* inoculation, 3x10^4 sort-purified naïve CD3$^+$CD4$^+$CD44^{lo}CD62L^{hi}CD25$^-$ Vβ6$^+$ T cells from CD45.1$^+$ *Helicobacter hepaticus* transgenic TCR mice were administered by retro-orbital injection into CD45.2$^+$ *OX40L$^{flox/flox}$* and CD45.2$^+$ *OX40L$^{\Delta ILC3}$* mice. After fourteen days, the CD45.1+ *Helicobacter hepaticus*-specific T cells were analyzed by flow cytometry.

Statistical analysis. Statistical analysis was performed in GraphPad Prism or R software. Results represent mean ± s.e.m. and were analyzed by unpaired Student's t-test or one-way ANOVA, as

indicated in the figure legends. Given that mouse experiments required littermate controls and complex genotyping, experimental group allocation was not blinded. No relevant exclusion criteria were applied.

5.4 RESULTS

5.4.1 ILC3 upregulation of OX40L during colitis is DR3-dependent

To evaluate the ability of ILC3 to express OX40L *in vivo* during colitis, we performed flow cytometry on lamina propria ILC3 at steady state and following DSS-induced colitis. Although low OX40L was seen on ILC3 at steady state, colitis induced robust expression of OX40L (Figure 5.1A). Expression of OX40L on ILC3 following DSS-induced colitis in $DR3^{\Delta ILC3}$ mice was significantly reduced compared to $DR3^{flox/flox}$ littermate controls, revealing a key role for DR3 in ILC3 expression of OX40L *in vivo* (Figure 5.2B).

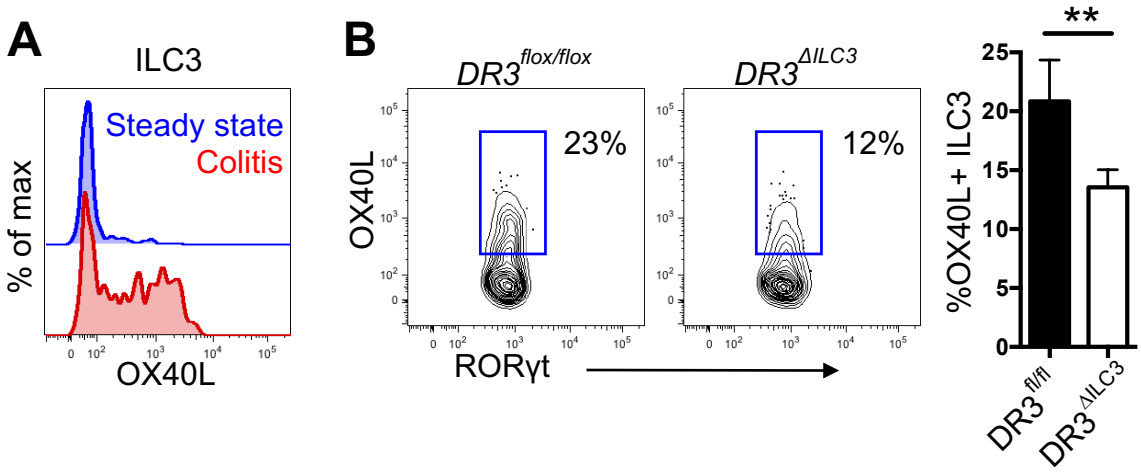

Figure. 5.1. TL1A induces ILC3 expression of OX40L during colitis *in vivo*. (**A**) OX40L expression on Lin$^-$CD127$^+$ RORgt$^+$ ILC3 at the steady-state or following 2% DSS-induced colitis. (**E**) OX40L expression on Lin$^-$CD127$^+$ RORgt$^+$ ILC3 from *DR3$^{flox/flox}$* and *DR3$^{\Delta ILC3}$* littermate mice following 2% DSS-induced colitis (n = 4 mice/group). Data in (B) are mean ± s.e.m and were analyzed by two-tailed Student's t-test; ***P*<0.01.

5.4.2 Human IBD patients upregulate OX40L on ILC3 during colitis

To determine if ILC3 express OX40L during inflammatory bowel disease (IBD), we profiled ILC3 from human intestinal biopsy samples. Lin- CD127+ c-kit+ ILC3 from patients with active IBD showed significantly higher levels of surface OX40L expression (Figure 5.2). Collectively, these results reveal TL1A- and colitis-dependent OX40L expression by intestinal ILC3 in mouse and human.

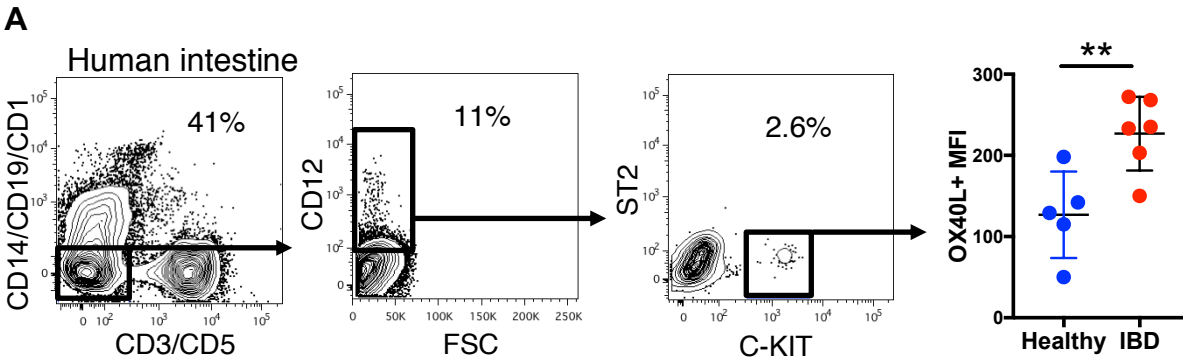

Figure 5.2. Human IBD patients upregulate ILC3 expression of OX40L during active colitis. (**A**) Human OX40L expression on Lin$^-$ CD127$^+$c-KIT$^+$ ILC3 from colonic biopsies of healthy patients or IBD patients with active inflammation (n=6 patients/group). Data in (A) are mean ± s.e.m and were analyzed by two-tailed Student's t-test; $^{**}P<0.01$.

5.4.3 ILC3-specific OX40L deletion attenuates chronic T cell transfer colitis

To evaluate the potential role for ILC3 expression of OX40L in a chronic colitis model, we used the transfer T cell colitis model by transferring sort-purified $CD4^+CD45RB^{high}$ naïve T-cells from WT mice into *OX40L*$^{\Delta ILC3}$ *RAG2*$^{-/-}$ or *OX40L*$^{flox/flox}$ *RAG2*$^{-/-}$ littermate mice (Figure 5.3A). The characteristic weight loss consistent with chronic T cell-mediated colitis developed within 4 weeks in the *OX40L*$^{flox/flox}$ *RAG2*$^{-/-}$ littermate controls (Figure 5.3B); however, in contrast to the effects seen in acute models, *OX40L*$^{\Delta ILC3}$ *RAG2*$^{-/-}$ were significantly protected (Figure 5.3B). Analysis of colonic tissue in these mice revealed decreased histopathologic damage in the *OX40L*$^{\Delta ILC3}$ mice compared to littermate controls (data not shown) and transferred T-cells revealed an expansion of IFN-γ^+ $CD4^+$ T cells in the *OX40L*$^{flox/flox}$ *RAG2*$^{-/-}$ controls compared to *OX40L*$^{\Delta ILC3}$ *RAG2*$^{-/-}$ mice (Figure 5.4B). Thus, in contrast to the protective role in acute colitis, these data reveal a pro-inflammatory role for ILC3-intrinsic OX40L in chronic T cell colitis.

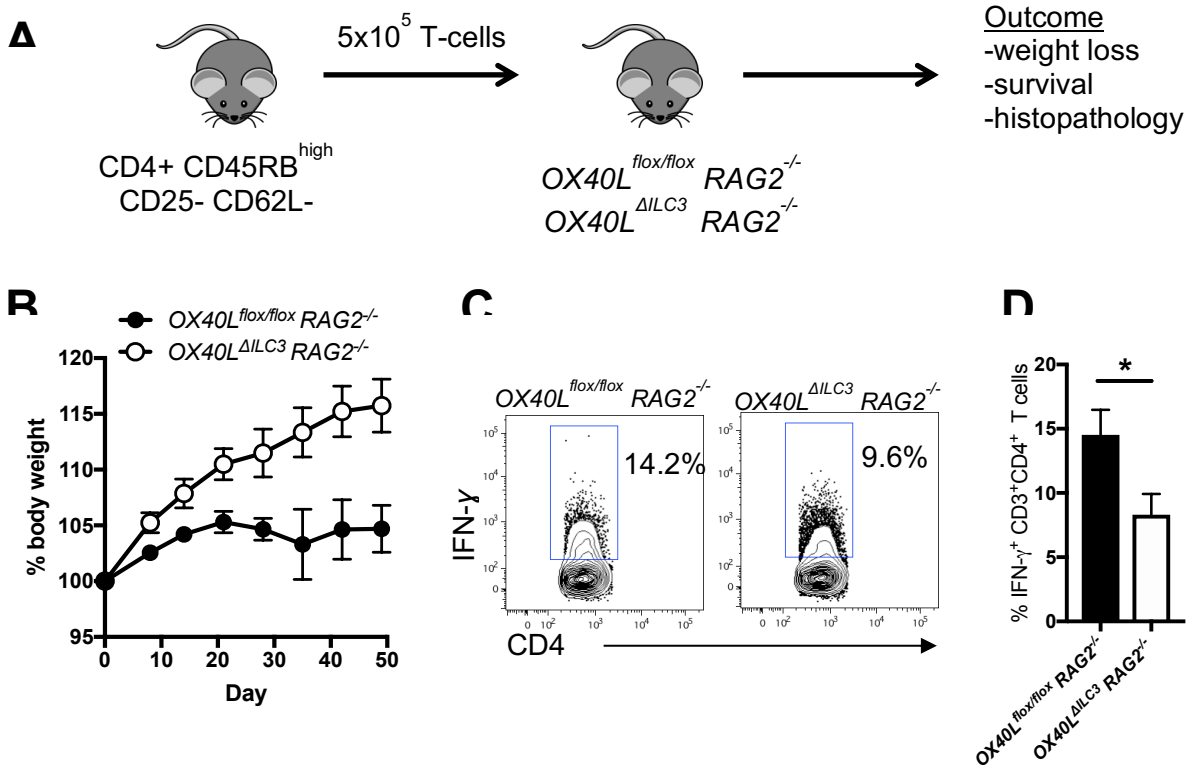

Figure 5.3. ILC3-specific deletion of OX40L attenuates chronic transfer T cell colitis and prevents expansion of pro-inflammatory colonic Th1 cells. (**A**) Experimental design for induction of transfer T cell colitis in *OX40L*$^{flox/flox}$ *RAG2*$^{-/-}$ or *OX40L*$^{\Delta ILC3}$ *RAG2*$^{-/-}$ littermate mice. (**B**-**D**) Analysis of *OX40L*$^{\Delta ILC3}$*RAG2*$^{-/-}$ *and OX40L*$^{flox/flox}$*RAG2*$^{-/-}$ littermate mice following adoptive transfer of CD4^{+}CD45RB^{high} T-cells for induction of T cell transfer colitis. Body weights (B) and cytokine induction (C, D) from *OX40L*$^{\Delta ILC3}$*RAG2*$^{-/-}$ *and OX40L*$^{flox/flox}$*RAG2*$^{-/-}$ littermate mice following adoptive transfer of CD4^{+}CD45RB^{high} T-cells (n = 8 mice/group); for (C), mice from (B) were euthanized on day 50 and CD3^{+}CD4^{+} T cell production of IFN-*γ* was analyzed by flow cytometry (n = 4 mice/group). Data in (B) are mean ± s.e.m and were analyzed by two-tailed Mann-Whitney test; data in (D) were analyzed two-tailed Student's t-test; **P*<0.05.

5.4.4 ILC3-specific DR3 deletion attenuates chronic colitis

In contrast to our findings for an essential role for TL1A and DR3 in protection from acute colitis, previous studies have suggested a pathogenic role for constitutive TL1A overexpression in IBD[31]. However, the mechanisms for TL1A-mediated intestinal damage during chronic colitis are unknown. Our previous RNA-seq analysis revealed that TL1A stimulation potently upregulated OX40L expression on ILC3 and our *in vivo* data using mouse colitis models demonstrated that ILC3-intrisic OX40L was essential for induction of T cell transfer colitis. Next, we asked if the ILC3-intrinsic DR3, which we have shown is essential for the upregulation of OX40L on ILC3, was important for mediating this OX40L-depndent T cell transfer colitis phenotype.

To evaluate the potential dependence for ILC3-intrinsic DR3 in promoting chronic colitis , we used the transfer T cell colitis model by transferring sort-purified $CD4^+CD45RB^{high}$ naïve T-cells from WT mice into $DR3^{\Delta ILC3}$ $RAG2^{-/-}$ or $DR3^{flox/flox}$ $RAG2^{-/-}$ littermates (Figure 5.4A). The characteristic weight loss (Figure 5.4B) and reduced survival (Figure 5.4C) consistent with chronic T cell-mediated colitis developed within 4 weeks in the $DR3^{flox/flox}$ $RAG2^{-/-}$ littermate controls; however, in contrast to the effects seen in acute models, $DR3^{\Delta ILC3}$ $RAG2^{-/-}$ were significantly protected. Analysis of colonic tissue in these mice revealed decreased histopathologic damage in the $DR3^{\Delta ILC3}$ mice compared to littermate controls (Figure 5.4D) and transferred T-cells revealed an expansion of T-bet$^+$ CD4$^+$ T cells in the $DR3^{flox/flox}$ $RAG2^{-/-}$

controls compared to *DR3*$^{\Delta ILC3}$ *RAG2*$^{-/-}$ mice (Figure 5.4E). Thus, in contrast to the protective role in acute colitis, these data reveal a pro-inflammatory role for ILC3-intrinsic DR3 in chronic T cell colitis.

Figure 5.4. ILC3-specific deletion of DR3 attenuates chronic transfer T cell colitis and prevents expansion of pro-inflammatory colonic Th1 cells. (**A**) Experimental design for induction of transfer T cell colitis in *DR3*$^{flox/flox}$ *RAG2*$^{-/-}$ or *DR3*$^{\Delta ILC3}$ *RAG2*$^{-/-}$ littermate mice. (**B-D**) Analysis of *DR3*$^{flox/flox}$ *RAG2*$^{-/-}$ or *DR3*$^{\Delta ILC3}$ *RAG2*$^{-/-}$ littermate mice following adoptive transfer of CD4^{+}CD45RB^{high} T-cells to induce transfer T cell colitis. Body weights (B), survival curves (C) and representative colonic histology (D) from *DR3*$^{flox/flox}$ *RAG2*$^{-/-}$ or *DR3*$^{\Delta ILC3}$ *RAG2*$^{-/-}$ littermate mice adoptive transfer of CD4^{+}CD45RB^{high} T-cells; for (B), n = 6, 7 mice/group, respectively, pooled from two independent experiments; for (C), n = 8, 10 mice/group, respectively, pooled from three independent experiments. (**E**) Flow cytometric analysis of T-bet induction in transferred T-cells from *DR3*$^{flox/flox}$ *RAG2*$^{-/-}$ or *DR3*$^{\Delta ILC3}$ *RAG2*$^{-/-}$ littermate mice in (B) and (C). Data in (B) are mean ± s.e.m and were analyzed by two-tailed Mann-Whitney test. Data in (B) were analyzed by Log-rank (Mantel-Cox) test; $^{**}P<0.01$, $^{***}P<0.001$. Data in (E) are mean ± s.e.m and were analyzed by two-tailed Student's t-test.

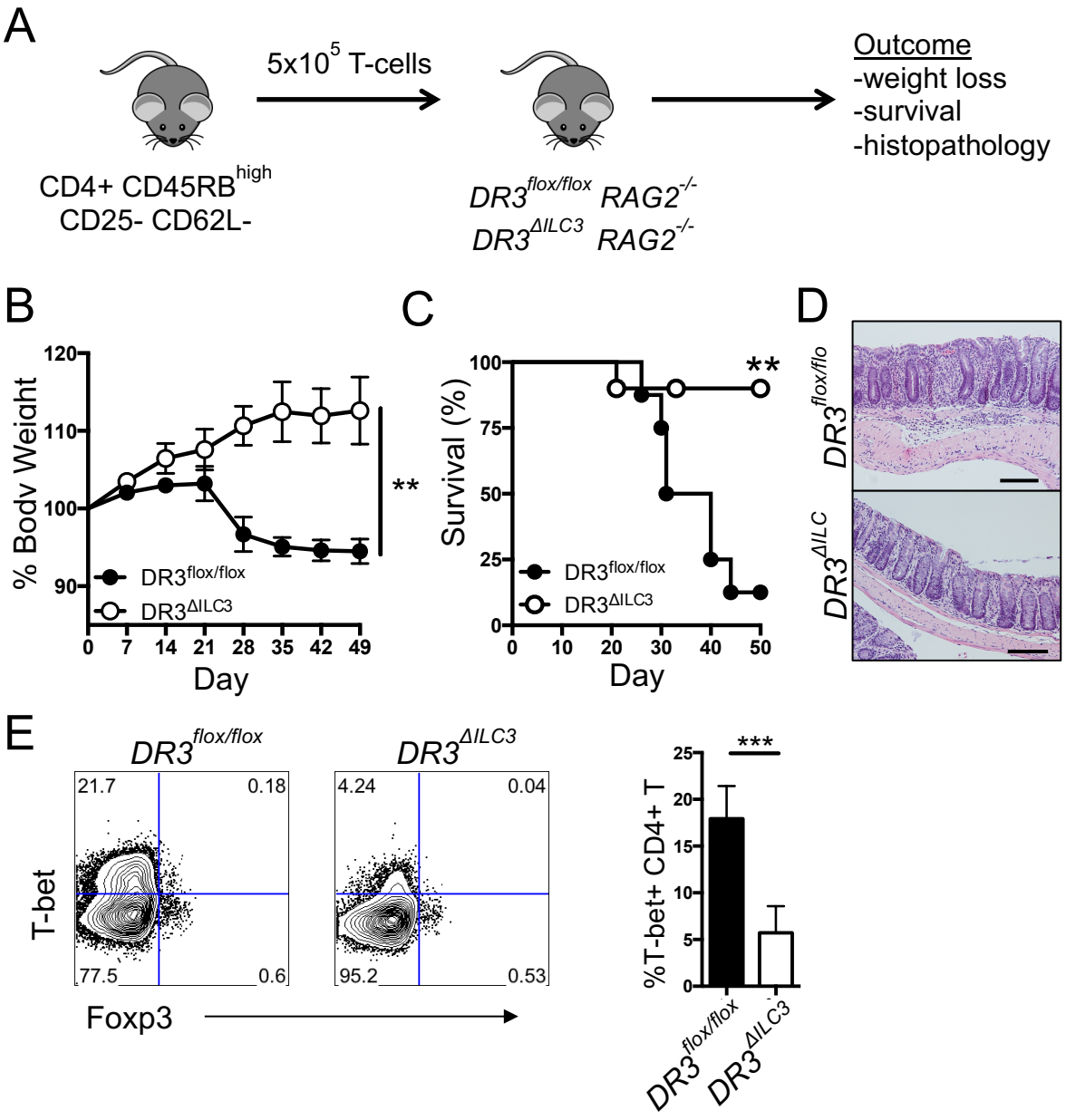

Figure 5.4. ILC3-specific deletion of DR3 attenuates chronic transfer T cell colitis and prevents expansion of pro-inflammatory colonic Th1 cells.

5.4.5 ILC3 OX40L generates intestinal T cells during colitis

To investigate a role for ILC3 OX40L signaling in regulating intestinal T cell function, we analyzed T cell subsets in *OX40L*$^{\Delta ILC3}$ and *OX40L*$^{flox/flox}$ littermate mice. At the steady state, *OX40L*$^{\Delta ILC3}$ and *OX40L*$^{flox/flox}$ had similar levels of Th1 and Th17, but *OX40L*$^{\Delta ILC3}$ had reduced regulatory T cell populations. Furthermore, under *Helicobacter hepaticus*-induced colitis, *OX40L*$^{\Delta ILC3}$ mice had significant impairment in intestinal T-bet^{+} and Foxp3^{+} T cell populations. There were no differences in mesenteric lymph node or splenic T cell populations of *OX40L*$^{\Delta ILC3}$ and *OX40L*$^{flox/flox}$ mice (data not shown).

5.4.6 ILC3 OX40L promotes dietary and microbial antigen-specific T cells

Previous studies have reported that ILC3 negatively regulate commensal antigen-specific T cells via MHCII at the steady state[86,89], but our *in vitro* data demonstrate that ILC3 can promote T cell effector function via OX40L co-stimulation; however, the a role for ILC3 OX40L co-stimulation of T cells *in vivo* has not been explored. To test the role for ILC3 expression of OX40L on dietary antigen-specific gut T-cells *in vivo*, sorted naïve CD45.1^{+} OTII cells were adoptively transferred into *OX40L*$^{\Delta ILC3}$ mice and littermate controls (Figure 5.5A). Mice were exposed to DSS for 5 days (to induce OX40L) and provided ovalbumin

antigen *ad lib*. One week following T-cell transfer, CD45.1$^+$ CD4$^+$ T cells were significantly lower in the mesenteric lymph node of *OX40L$^{\Delta ILC3}$* mice compared to *OX40L$^{flox/flox}$* littermates (Figure 5.5B).

We next asked if ILC3 could regulate microbial antigen-specific T cells. A recent study has reported that *Helicobacter hepaticus*-specific T cells are characterized by the dual expression of RORγt and Foxp3[90]. Since *OX40L$^{\Delta ILC3}$* mice were deficient in RORγt$^+$Foxp3$^+$ T cells during *Helicobacter hepaticus*-induced colitis, we investigated whether ILC3 OX40L was necessary for the generation of RORγt$^+$Foxp3$^+$ *Helicobacter hepaticus*-specific T cells. To test the role for ILC3 expression of OX40L on the generation of *Helicobacter hepaticus*-specific gut T-cells *in vivo*, *OX40L$^{\Delta ILC3}$* and *OX40L$^{flox/flox}$* littermate mice were colonized with *Helicobacter hepaticus* for seven days before the transfer of congenically-marked, sort-purified naïve CD3$^+$CD4$^+$CD44^{lo}CD62L^{hi}CD25$^-$Vβ6$^+$ T cells from CD45.1$^+$ *Helicobacter hepaticus* transgenic TCR mice (Figure 5.6A). Fourteen days after transfer, CD45.1$^+$ RORγt$^+$Foxp3$^+$ HH-Tg T cells were significantly lower in the large intestine of *OX40L$^{\Delta ILC3}$* mice compared to their *OX40L$^{flox/flox}$* littermates (Figure 5.6B). However, there were no differences in CD45.1$^+$ RORγt$^+$Foxp3$^+$ T cells HH-Tg T cells in the mesenteric lymph node or spleens of *OX40L$^{\Delta ILC3}$* and *OX40L$^{flox/flox}$* mice (data not shown).

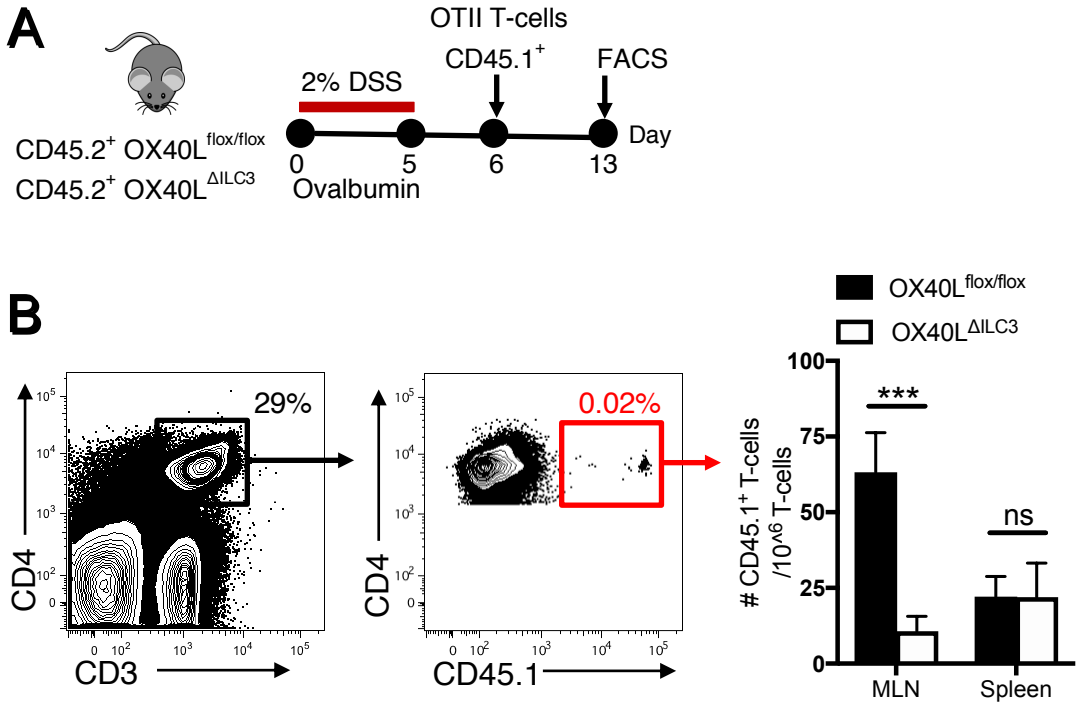

Figure 5.5. TL1A stimulation of MHCII$^+$ ILC3 enables OX40L-dependent co-stimulation of CD4$^+$ T cells. (**A)** Experimental design for transfer of CD45.1$^+$ CD3$^+$CD4$^+$Vα2$^+$ OTII T-cells into CD45.2$^+$ OX40L$^{flox/flox}$ or CD45.2$^+$ OX40L$^{\Delta ILC3}$ mice treated with 2% DSS and ovalbumin for 5 days. (**B**) Flow cytometric analysis of CD45.1$^+$ CD3$^+$CD4$^+$Vα2$^+$ OTII T-cells from (A) compiled over two independent experiments (n= 6-8 mice/group). Data in G are mean ± s.e.m and were analyzed by Student's t-test; ***P<0.001.

Figure 5.6. ILC3 promote the generation of *Helicobacter hepaticus*-specific T cells via OX40L. (**A)** Experimental design for transfer of $CD3^+CD4^+CD44^{lo}CD62L^{hi}CD25^-V\beta6^+$ HH-Tg T cells from $CD45.1^+$ *Helicobacter hepaticus* transgenic TCR mice into $CD45.2^+$ $OX40L^{flox/flox}$ or $CD45.2^+$ $OX40L^{\Delta ILC3}$ mice colonized for 7 days with *Helicobacter hepaticus*. (**B**) Flow cytometric analysis of transferred $CD45.1^+$ HH-Tg and $CD45.2^+$ endogenous T-cells from (A). (**C**) Quantification of transferred $CD45.1^+$ HH-Tg and $CD45.2^+$ endogenous T-cells from (A-B) (n= 10 mice/group compiled over two experiments). Data in C are mean ± s.e.m and were analyzed by Student's t-test; ns = not significant, **P*<0.05, ***P*<0.01, ****P*<0.001.

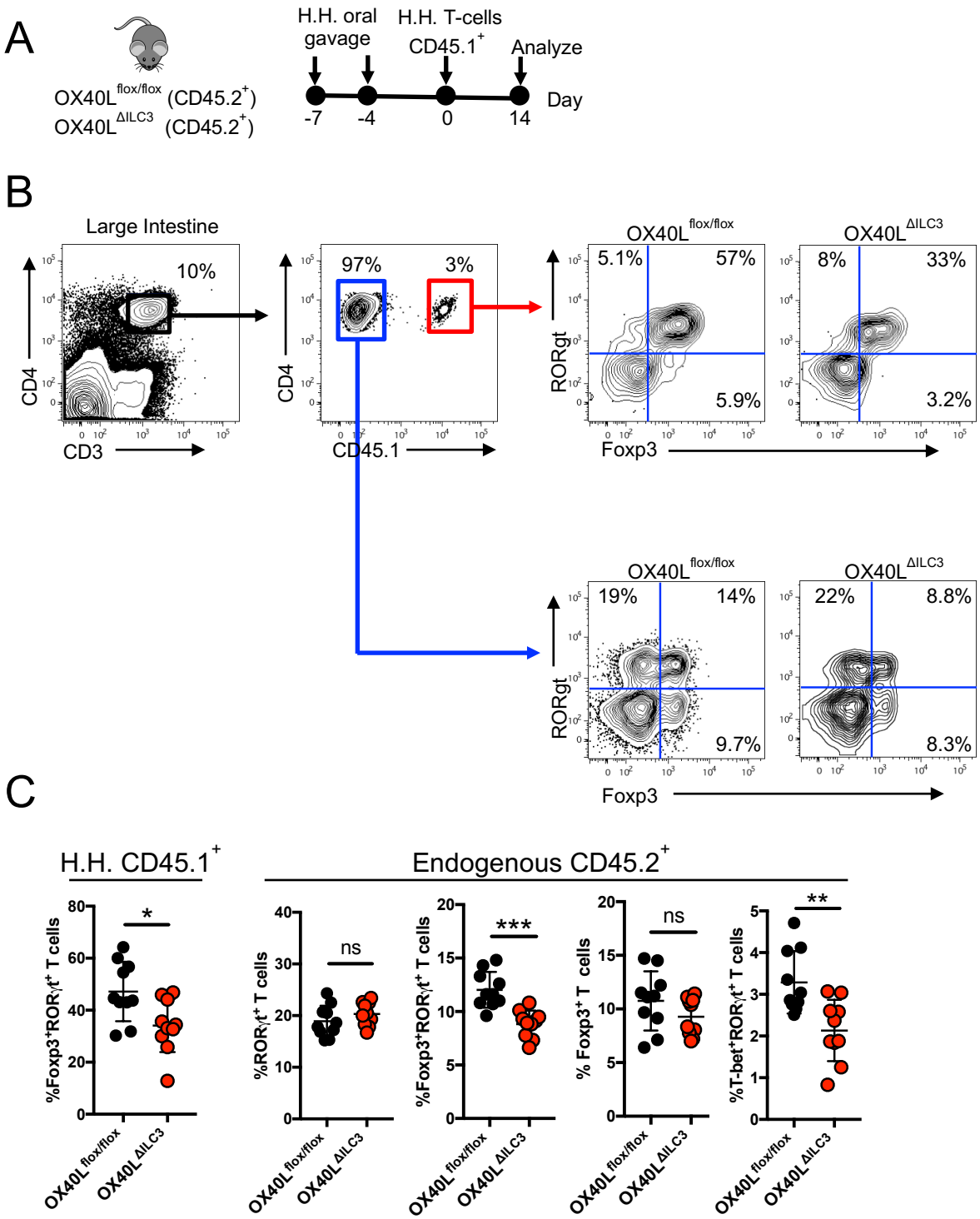

Figure 5.6. ILC3 promote the generation of *Helicobacter hepaticus*-specific T cells via OX40L.

5.5 DISCUSSION

In previous chapters, we demonstrated a protective role for MNP-derived TL1A and DR3 signaling on ILC3 during acute colitis. Here, our data demonstrate how ILC3-specific DR3 and OX40L signaling promotes chronic colitis via the regulation of pathogenic T-bet^{+}/IFN-γ^{+} T cells. This discovery offers mechanistic data on how the TL1A-OX40L axis serves as a critical link between the innate and adaptive immune systems via ILC3 regulation of T cells

The discovery of antigen processing and presentation by intestinal ILC3 highlights a central role for these cells in linking innate and adaptive immunity[86]. Although splenic ILC3 can upregulate conventional co-stimulatory molecules CD80 and CD86 following IL-1β stimulation[88], the absence of these co-stimulatory molecules, even following stimulation, on intestinal ILC3 lead to a model in which they limit bacteria-specific inflammatory T-cell responses in the gut.[89] Our data highlight the expression of OX40L by ILC3 in inflammatory colitis in mouse models and human IBD. Specifically, during chemically-induced DSS colitis, ILC3 upregulate surface OX40L in a DR3-dependent manner. Similarly, mucosal biopsies form IBD patients demonstrate that human ILC3 also upregulate OX40L during active colitis. *In vivo*, mice with a ILC3 cell-specific deletion of either DR3 or OX40L were unable to support T cell transfer colitis, demonstrating that the DR3-OX40L axis plays a significant role in ILC3 regulation of

T cell effector functions *in vivo*. Lastly, our data demonstrate that ILC3 can regulate both dietary and microbial antigen-specific T cells *in vivo* via OX40L. This data offer the exciting possibility that ILC3 may contribute to the generation of peripheral T cells that are autoreactive to intestinal microbial antigens. Whether TL1A or OX4OL contribute to this process, if true, and whether it contributes to the pathophysiology of IBD remains unknown.

In humans, how and/or if ILC3 regulate T cells in human remains to be explored. Specifically, do MNP TL1A or ILC3 OX40L levels correlate with Th1 T cells in the inflamed tissue of IBD patients? Do levels of TL1A or OX40L correlate with disease outcomes in these patients? These are valid questions that should be pursued in future studies.

Expression of OX40L by ILC3 plays a critical role in regulating gut antigen-specific and effector T-cell responses. These data, therefore, extend the model by which MHCII+ ILC3 regulate the gut T cell response, which may reflect OX40L-dependent regulatory responses under homeostatic conditions[91]. However, in IBD patients with genetic susceptibility or animal models of T-cell transfer colitis, ILC3 co-stimulation can support pathogenic, inflammatory T-cell activation. Further studies are needed to decipher the mechanisms of how TL1A alters ILC3 effector functions to regulate the adaptive immune system.

CHAPTER 6: DISCUSSION

6.1 Summary

Genetic studies have linked *TNFSF15* polymorphisms and its protein TL1A with IBD, but the functional role of TL1A in tissue homeostasis and intestinal inflammation is not known. Previous studies had pointed at a pathogenic role for TL1A, particularly via the regulation of T cells at epithelial barrier sites, but more recent studies had implicated TL1A in the promotion of mucosal healing and barrier integrity. These contradictory studies poised an important question for this IBD-associated molecule: what is the role for TL1A in maintaining intestinal homeostasis and how does it contribute to the pathophysiology of IBD? By generating novel cell-specific genetic deletion models, our data reconcile and offer mechanistic insights into the various functions of TL1A during intestinal inflammation. During acute colitis, CX_3CR1^+ MNP-derived TL1A plays an essential role in promoting barrier protection and mucosal healing via the regulation of ILC3 IL-22. However, during chronic colitis, sustained TL1A signaling results in the upregulation of co-stimulatory molecules on ILC3, in particular OX40L, which enables ILC3 to directly promote antigen-specific T cell effector functions, including the propagation of IFN-γ-producing pathogenic T cells leading to increased intestinal tissue

damage. These data implicate TL1A as a central regulator of the innate and adaptive functions of ILC3 in maintaining intestinal tissue homeostasis, but further studies are needed to better therapeutically target TL1A in clinical settings.

6.2 Microbial regulation of CX_3CR1^+ MNP-derived TL1A

Previous studies had identified a role for immune complexes/microbial signaling in promoting TL1A production by macrophages *in vitro*[42]. However, the potential role for commensal intestinal microbes in regulating macrophage TL1A had not been thoroughly investigated. Here, we identified a key role for intestinal bacteria in promoting CX_3CR1^+ MNP-derived TL1A. In particular, adherent microbiota, including segmented filamentous bacteria (SFB) and Adherent-invasive *E. coli* enriched in Crohn's disease (AIEC), robustly induced TL1A. These findings offer a mechanism by which Crohn's disease-associated microbiota can act acutely to promote barrier immunity in wild-type hosts.

Although signals from the intestinal microbiota were essential for TL1A induction during acute colitis, it remains to be explored how microbial signals might contribute to TL1A induction during chronic colitis. Extrapolation of our acute colitis data suggests that AIEC-induced TL1A could contribute to the adaptive functions of ILC3 via the TL1A-OX40L axis. T cell transfer colitis using AIEC colonized germ-free mice with anti-TL1A blocking antibodies would be an

interesting experiment to test the hypothesis that adherent intestinal microbes contribute to chronic colitis via TL1A induction. If true, targeting specific microbes that robustly induce TL1A, such as IBD-associated adherent/invasive *E. coli*, might offer a viable therapeutic modality for IBD patients.

6.3 ILC3 as antigen-presenting cells during colitis: a revised model

The discovery of antigen processing and presentation by intestinal ILC3 highlights a central role for these cells in linking innate and adaptive immunity[86]. Although splenic ILC3 can upregulate conventional co-stimulatory molecules CD80 and CD86 following IL-1β stimulation[88], the absence of these co-stimulatory molecules on intestinal ILC3 at the steady state lead to a model in which they limit bacteria-specific inflammatory T-cell responses in the gut[89]. Here, we demonstrate that TL1A stimulation enabled MHCII$^+$ ILC3 to promote antigen-specific T cell proliferation via MHCII/OX40L co-stimulation *in vitro*. These findings can be extended to our *in vivo* experiments where we demonstrated that ILC3-specific OX40L can promote T cell effector functions in chronic colitis models. Our data suggest a revised model in which inducible ILC3 expression of OX40L co-stimulation may trigger local T cell activation (Figure 6.1).

6.4 Therapeutic Targeting of TL1A

In IBD patients, there are numerous clinical trials aimed at inhibiting the function of TL1A. Our data, and in particular the role for TL1A in acute vs chronic colitis, may guide therapeutic targeting of TL1A of these patients. Genetic testing has identified protective vs risk alleles in TL1A patients[47,80,93–95]. However, the functional impact of these mutations has not been well-characterized, although much can be inferred from mouse genetic studies, including our own work. For example, TL1A risk alleles that display a loss-of-function phenotype might act functionally similar to our acute colitis models, in which insufficient MNP-derived TL1A impairs proper wound healing after intestinal injury. In this case, treating patients with recombinant TL1A might be a viable therapeutic approach. In contrast, patients with the risk allele displaying a gain-of-function phenotype might act functionally similar to TL1A overexpression models, in which mice develop severe intestinal fibrostenosis[78]. Here, anti-TL1A blocking antibodies might improve clinical outcomes. More work in needed, however, in characterizing the functional role of these TL1A risk alleles in human patients.

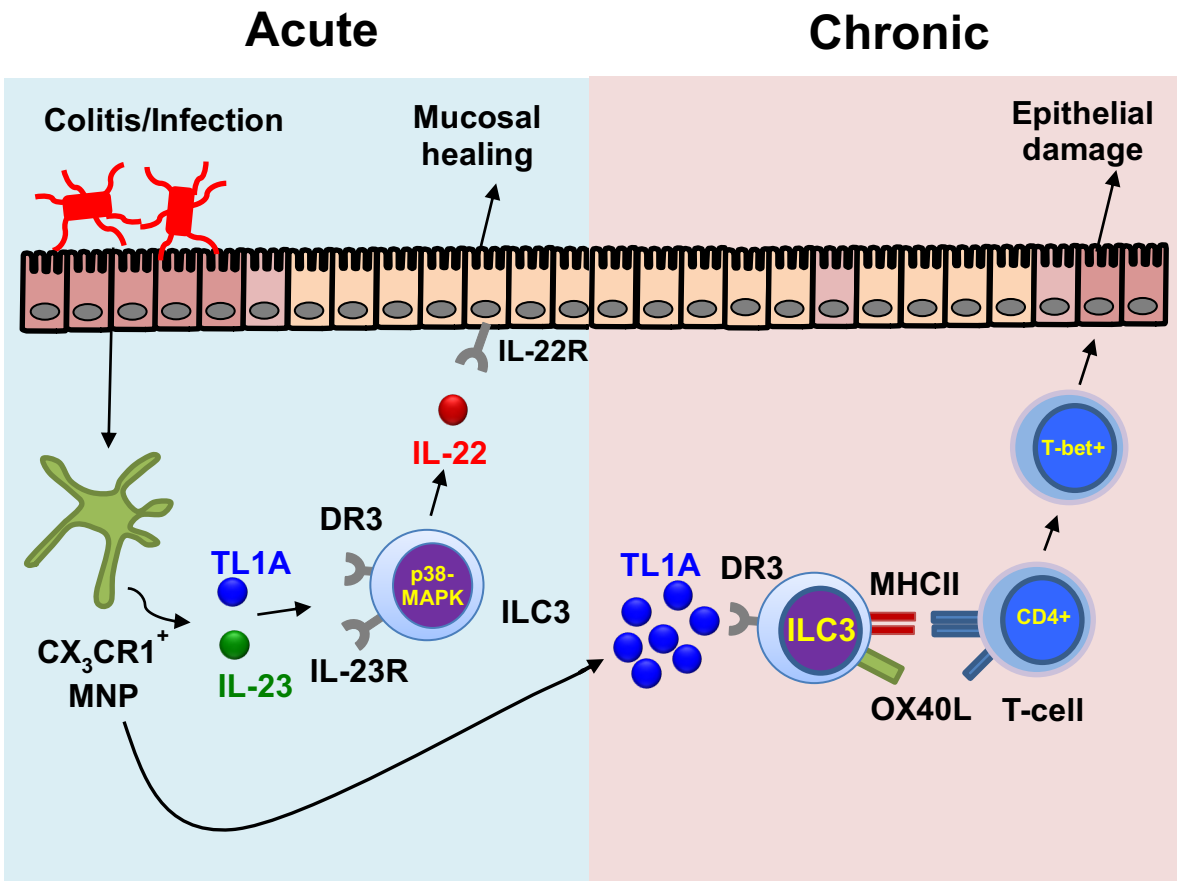

Figure 6.1. A REVISED MODEL: TL1A is a central regulator of Group 3 Innate Lymphoid Cells during colitis. During acute colitis, CX_3CR1^+ MNP-derived TL1A synergizes with IL-23 to promote mucosal healing and restoration of barrier integrity. During chronic colitis, CX_3CR1^+ MNP upregulate TL1A which induces OX40L expression on ILC3, leading to ILC3 promotion of T cell effector functions.

APPENDICES

APPENDIX A: Top 100 differentially expressed genes from global gene expression profiles of media- or TL1A-stimulated sorted Lin^- $CD127^+IL23R^{GFP+}$ ILC3 from *IL23R*$^{GFP/WT}$ mice (scatterplot of global gene expression presented in Figure 4.1B); baseMeanA (media control) and baseMeanB (TL1A stimulated) expression levels presented as transcript reads; p-adjusted value < 0.05 after correction for multiple hypothesis testing. Genes presented in increasing order of p-adj.

Gene ID	baseMeanA (Media)	baseMeanB (TL1A stim)	log2FoldChange	padj
Ccnd2	1221.14	26657.44	4.45	<1.00E-279
Csf2	821.48	100424.88	6.93	<1.00E-279
Egr2	36.39	5998.07	7.36	<1.00E-279
Icam1	2763.12	69350.99	4.65	<1.00E-279
Icosl	1128.74	29201.46	4.69	<1.00E-279
Il22	561.89	83920.99	7.22	<1.00E-279
Iltifb	48.06	6243.81	7.02	<1.00E-279
Ip6k3	270.11	8153.72	4.92	<1.00E-279
Ceacam15	2.26	2664.64	10.2	<1.00E-279
Cxcl3	83.11	24349.6	8.19	<1.00E-279
Gzmc	8.23	2753.4	8.39	<1.00E-279
Ncr1	183.31	5194.1	4.82	1.09E-278
Adamts15	7649.51	461.87	-4.05	4.25E-251
Gadd45b	190.19	4600.7	4.6	5.38E-249
Cxcl16	32.36	4794.66	7.21	3.13E-247
Ccl5	344.89	6004.73	4.12	2.04E-240
Tnfsf11	167.4	4137.94	4.63	4.30E-239
Susd2	51.64	2653.88	5.68	1.91E-234
Serpinb1a	10666.01	649.05	-4.04	7.22E-234
Cxcl2	38.52	2366.86	5.94	1.98E-226
Plat	108.86	3239.27	4.9	3.58E-225

Appendix A (continued).

Gene ID	baseMeanA (Media)	baseMeanB (TL1A stim)	log2FoldChange	padj
Tagap	649.04	8121.85	3.65	1.19E-222
Ikbke	1043.47	10932.23	3.39	4.73E-215
Anxa2	10510.98	81918.85	2.96	1.03E-213
Tnfsf4	2131.64	18004.7	3.08	8.86E-202
Ccdc184	3335.25	25894.73	2.96	9.98E-198
Ehd1	702.87	7467.51	3.41	1.11E-195
Mrpl38	175.31	3291.37	4.23	3.53E-190
Plxnd1	584.65	5979.6	3.35	1.62E-177
Nfkbie	1910.97	14147.59	2.89	5.37E-175
Idi2	0.91	1147.93	10.3	1.48E-171
Fas	29.48	1591.18	5.75	7.89E-168
Nupr1	1674.58	11555.12	2.79	8.07E-158
Pdgfb	568.77	5384.77	3.24	8.05E-156
Glipr2	2853.6	17081.98	2.58	1.75E-148
Lad1	9.56	1135.63	6.89	4.16E-148
Tnip3	1240.84	8460.19	2.77	2.64E-145
S100a10	5023.24	26409.43	2.39	6.72E-137
Xcl1	4.64	954.55	7.69	6.14E-136
Tgm3	2435.05	54.19	-5.49	1.14E-131
Bhlhe40	20551.95	97672.42	2.25	1.27E-131
Blk	1396.83	8510.9	2.61	2.22E-131
Spry2	2388.2	182.77	-3.71	2.91E-130
Hsp90b1	7426.31	36333.66	2.29	5.64E-130
Sqle	952.9	6139.46	2.69	9.04E-126
Pik3r5	77.37	1565.36	4.34	3.28E-124
Rac2	11886.99	54375.89	2.19	5.81E-123
Rcl1	164.75	2076.77	3.66	1.26E-120
Tuba1a	1483.33	8279.48	2.48	5.28E-120
Cd74	272.76	5326.01	4.29	8.40E-119
Rptor	776.3	5041.06	2.7	2.59E-118
Dennd5a	602.99	4776.82	2.99	2.00E-117
Olfr175-ps1	2.26	766.97	8.41	9.97E-117
Gda	83.95	1499.77	4.16	1.39E-114
Slc2a6	468.63	3507.48	2.9	2.79E-114
Il2ra	5138.76	23188.83	2.17	8.51E-114
Rgs2	1669.41	106.02	-3.98	1.17E-113

Appendix A (continued).

Gene ID	baseMeanA (Media)	baseMeanB (TL1A stim)	log2FoldChange	padj
Il27ra	2429.04	11914.05	2.29	1.45E-113
Vash1	10.56	862.97	6.35	1.16E-112
Adap1	73.54	1392.49	4.24	1.40E-111
Stab1	1927.91	9577.29	2.31	1.75E-110
Il1r2	49.79	1206.7	4.6	6.24E-110
Cyp51	1431.97	7515.37	2.39	6.24E-110
Gpnmb	2193.82	77.08	-4.83	5.04E-109
Srgn	7290.6	30940.7	2.09	1.92E-108
Extl1	370.97	2916.39	2.97	2.09E-108
Traf1	7459.45	42964.76	2.53	3.73E-107
Fam189b	2631.82	310.53	-3.08	1.05E-106
Thy1	1733.02	8540.23	2.3	1.95E-106
Madcam1	0	737.47	#DIV/0!	1.01E-105
H2-Aa	1675.77	13819.99	3.04	1.87E-105
Ccl17	44.36	1107.15	4.64	2.85E-104
Phldb1	67.73	1266.53	4.22	9.93E-104
Trf	4194	406.78	-3.37	3.44E-103
Sash3	1333.84	6759.59	2.34	5.80E-103
Sdc1	1319.63	71.44	-4.21	6.03E-103
Lpar6	12309.85	2822.35	-2.12	4.05E-100
Marcksl1	23.79	900.16	5.24	8.02E-100
Cx3cl1	1952.79	29148.84	3.9	1.29E-99
Psme2b	3808.53	15741.25	2.05	2.58E-97
Slc6a7	4623.02	860.76	-2.43	1.09E-95
Abcc1	3253.16	13481.42	2.05	3.34E-95
Slc15a3	1475.96	6873.03	2.22	2.40E-94
Ccdc88a	984.71	5025.37	2.35	5.57E-94
Pdcd1	5628.86	1018.97	-2.47	2.89E-93
Nup62	4554.9	17973.28	1.98	3.70E-93
Ccl22	340.77	2454.13	2.85	1.36E-92
Slc26a11	749.95	11.62	-6.01	3.18E-92
Cep164	1759.31	179.9	-3.29	7.94E-92
Psmb7	1865.31	8100	2.12	7.93E-91
Pdia6	6077.28	22720.56	1.9	3.64E-89
Basp1	795.38	4116.53	2.37	2.47E-88
Meox1	297.15	2184.66	2.88	5.67E-88
Tnfsf9	244.72	1955.21	3	1.78E-87

Appendix A (continued).

Gene ID	baseMeanA (Media)	baseMeanB (TL1A stim)	log2FoldChange	padj
Avil	442.45	2751.78	2.64	2.47E-87
Tnfsf8	1141.18	5248.77	2.2	1.38E-85
Uap1	255.21	1952.2	2.94	9.44E-85
Cpne2	3.19	557.52	7.45	2.78E-84
Slc5a3	316.46	2183.97	2.79	1.48E-83

BIBLIOGRPAPHY

1. Kaplan, G. G. The global burden of IBD: From 2015 to 2025. *Nature Reviews Gastroenterology and Hepatology* (2015). doi:10.1038/nrgastro.2015.150

2. Gevers, D. *et al.* The treatment-naive microbiome in new-onset Crohn's disease. *Cell Host Microbe* (2014). doi:10.1016/j.chom.2014.02.005

3. McGovern, D. P. B., Kugathasan, S. & Cho, J. H. Genetics of Inflammatory Bowel Diseases. *Gastroenterology* (2015). doi:10.1053/j.gastro.2015.08.001

4. Siakavellas, S. I. & Bamias, G. Tumor Necrosis Factor-like Cytokine TL1A and Its Receptors DR3 and DcR3: Important New Factors in Mucosal Homeostasis and Inflammation. *Inflamm. Bowel Dis.* (2015). doi:10.1097/MIB.0000000000000492

5. Aggarwal, B. B. Signalling pathways of the TNF superfamily: A double-edged sword. *Nature Reviews Immunology* (2003). doi:10.1038/nri1184

6. Sethi, G., Sung, B. & Aggarwal, B. B. Therapeutic potential of VEGI/TL1A in autoimmunity and cancer. *Adv. Exp. Med. Biol.* (2009). doi:10.1007/978-0-387-89520-8_15

7. Li, L. *et al.* TNF-like ligand 1A is associated with the pathogenesis of psoriasis vulgaris and contributes to IL-17 production in PBMCs. *Arch. Dermatol. Res.* (2014). doi:10.1007/s00403-014-1497-z

8. Bamias, G. *et al.* Upregulation and nuclear localization of TNF-like Cytokine 1A (TL1A) and its receptors DR3 and DcR3 in psoriatic skin lesions. *Exp. Dermatol.* (2011). doi:10.1111/j.1600-0625.2011.01304.x

9. Wu, N. L. *et al.* EGFR-driven up-regulation of decoy receptor 3 in keratinocytes contributes to the pathogenesis of psoriasis. *Biochim. Biophys. Acta - Mol. Basis Dis.* (2013). doi:10.1016/j.bbadis.2013.05.020

10. Pedersen, A. E. *et al.* Secretion, blood levels and cutaneous expression of TL1A in psoriasis patients. *APMIS* (2015). doi:10.1111/apm.12385

11. Zhang, J. *et al.* Role of TL1A in the Pathogenesis of Rheumatoid Arthritis. *J. Immunol.* (2009).

doi:10.4049/jimmunol.0802645

12. Bamias, G. *et al.* Circulating levels of TNF-like cytokine 1A (TL1A) and its decoy receptor 3 (DcR3) in rheumatoid arthritis. *Clin. Immunol.* (2008). doi:10.1016/j.clim.2008.07.014

13. Cassatella, M. A. *et al.* Soluble TNF-Like Cytokine (TL1A) Production by Immune Complexes Stimulated Monocytes in Rheumatoid Arthritis. *J. Immunol.* (2007). doi:10.4049/jimmunol.178.11.7325

14. Zhou, M., Liu, R., Su, D., Feng, X. & Li, X. TL1A increased the differentiation of peripheral Th17 in rheumatoid arthritis. *Cytokine* (2014). doi:10.1016/j.cyto.2014.04.007

15. Bamias, G. *et al.* Circulating levels of TNF-like cytokine 1A correlate with the progression of atheromatous lesions in patients with rheumatoid arthritis. *Clin. Immunol.* (2013). doi:10.1016/j.clim.2013.03.002

16. Siakavellas, S. I., Sfikakis, P. P. & Bamias, G. The TL1A/DR3/DcR3 pathway in autoimmune rheumatic diseases. *Seminars in Arthritis and Rheumatism* (2015). doi:10.1016/j.semarthrit.2015.02.007

17. Takahashi, M. *et al.* DcR3-TL1A signalling inhibits cytokine-induced proliferation of rheumatoid synovial fibroblasts. *Int. J. Mol. Med.* (2011). doi:10.3892/ijmm.2011.687

18. Ma, Z. *et al.* TL1A increased IL-6 production on fibroblast-like synoviocytes by preferentially activating TNF receptor 2 in rheumatoid arthritis. *Cytokine* (2016). doi:10.1016/j.cyto.2016.04.005

19. Bayry, J. Immunology: TL1A in the inflammatory network in autoimmune diseases. *Nature Reviews Rheumatology* (2010). doi:10.1038/nrrheum.2009.263

20. Meylan, F. *et al.* The TNF-family receptor DR3 is essential for diverse T cell-mediated inflammatory diseases. *Immunity* **29,** 79–89 (2008).

21. Pappu, B. P. *et al.* TL1A-DR3 interaction regulates Th17 cell function and Th17-mediated autoimmune disease. *J. Exp. Med.* **205,** 1049–62 (2008).

22. Targan, S. R. Introductory words about TL1A/DR3. in *Advances in Experimental Medicine and Biology* (2011). doi:10.1007/978-1-4419-6612-4_27

23. Tubak, V. *et al.* Expression of immunoregulatory tumor necrosis

factor-like molecule TL1A in chicken chondrocyte differentiation. *Can. J. Vet. Res.* (2009).

24. Longman, R. S. *et al.* CX_3CR1^+ mononuclear phagocytes support colitis-associated innate lymphoid cell production of IL-22. *J. Exp. Med.* **211,** 1571–83 (2014).

25. Wang, J. *et al.* TL1-A can engage death receptor-3 and activate NF-kappa B in endothelial cells. *BMC Nephrol.* (2014). doi:10.1186/1471-2369-15-178

26. Migone, T. S. *et al.* TL1A is a TNF-like ligand for DR3 and TR6/DcR3 and functions as a T cell costimulator. *Immunity* (2002). doi:10.1016/S1074-7613(02)00283-2

27. Barrett, R. *et al.* Constitutive TL1A expression under colitogenic conditions modulates the severity and location of gut mucosal inflammation and induces fibrostenosis. *Am. J. Pathol.* **180,** 636–49 (2012).

28. Prehn, J. L. *et al.* Potential role for TL1A, the new TNF-family member and potent costimulator of IFN-γ, in mucosal inflammation. *Clin. Immunol.* (2004). doi:10.1016/j.clim.2004.02.007

29. Tung, C. C. *et al.* Combining TNFSF15 and ASCA IgA can be used as a predictor for the stenosis/perforating phenotype of Crohn's disease. *J. Gastroenterol. Hepatol.* (2014). doi:10.1111/jgh.12496

30. Yang, D. H. *et al.* TNFSF15 is an independent predictor for the development of Crohn's disease-related complications in Koreans. *J. Crohn's Colitis* (2014). doi:10.1016/j.crohns.2014.04.002

31. Zheng, L. *et al.* SUSTAINED TL1A (TNFSF15) EXPRESSION ON BOTH LYMPHOID AND MYELOID CELLS LEADS TO MILD SPONTANEOUS INTESTINAL INFLAMMATION AND FIBROSIS. *Eur. J. Microbiol. Immunol. (Bp).* (2013). doi:10.1556/EuJMI.3.2013.1.2

32. Jia, L.-G. *et al.* A Novel Role for TL1A/DR3 in Protection against Intestinal Injury and Infection. *J. Immunol.* (2016). doi:10.4049/jimmunol.1502466

33. Niess, J. H. *et al.* CX3CR1-mediated dendritic cell access to the intestinal lumen and bacterial clearance. *Science* **307,** 254–8 (2005).

34. Diehl, G. E. *et al.* Microbiota restricts trafficking of bacteria to mesenteric lymph nodes by CX(3)CR1(hi) cells. *Nature* **494,**

116–20 (2013).

35. Kamada, N. *et al.* Unique CD14+intestinal macrophages contribute to the pathogenesis of Crohn disease via IL-23/IFN-γ axis. *J. Clin. Invest.* (2008). doi:10.1172/JCI34610

36. Tamoutounour, S. *et al.* CD64 distinguishes macrophages from dendritic cells in the gut and reveals the Th1-inducing role of mesenteric lymph node macrophages during colitis. *Eur. J. Immunol.* (2012). doi:10.1002/eji.201242847

37. Zigmond, E. *et al.* Ly6Chi Monocytes in the Inflamed Colon Give Rise to Proinflammatory Effector Cells and Migratory Antigen-Presenting Cells. *Immunity* (2012). doi:10.1016/j.immuni.2012.08.026

38. Panea, C. *et al.* Intestinal Monocyte-Derived Macrophages Control Commensal-Specific Th17 Responses. *Cell Rep.* **12,** 1314–24 (2015).

39. Satoh-Takayama, N. *et al.* Microbial flora drives interleukin 22 production in intestinal NKp46+ cells that provide innate mucosal immune defense. *Immunity* **29,** 958–70 (2008).

40. Satoh-Takayama, N. *et al.* The Chemokine Receptor CXCR6 Controls the Functional Topography of Interleukin-22 Producing Intestinal Innate Lymphoid Cells. *Immunity* **41,** 776–788 (2014).

41. Prehn, J. L. *et al.* The T cell costimulator TL1A is induced by FcgammaR signaling in human monocytes and dendritic cells. *J. Immunol.* (2007). doi:10.4049/jimmunol.178.7.4033

42. Shih, D. Q. *et al.* Microbial induction of inflammatory bowel disease associated gene TL1A (TNFSF15) in antigen presenting cells. *Eur. J. Immunol.* **39,** 3239–50 (2009).

43. Kamada, N. *et al.* TL1A produced by lamina propria macrophages induces Th1 and Th17 immune responses in cooperation with IL-23 in patients with Crohn's disease. *Inflamm. Bowel Dis.* (2010). doi:10.1002/ibd.21124

44. Schreiber, T. H. *et al.* Therapeutic Treg expansion in mice by TNFRSF25 prevents allergic lung inflammation. *J. Clin. Invest.* (2010). doi:10.1172/JCI42933

45. Meylan, F. *et al.* The TNF-family cytokine TL1A promotes allergic immunopathology through group 2 innate lymphoid cells. *Mucosal Immunol.* **7,** 958–68 (2014).

46. Jostins, L. *et al.* Host-microbe interactions have shaped the genetic architecture of inflammatory bowel disease. *Nature* **491,**

119–24 (2012).

47. Barrett, J. C. *et al.* Genome-wide association defines more than 30 distinct susceptibility loci for Crohn's disease. *Nat. Genet.* (2008). doi:10.1038/ng.175

48. Duerr, R. H. *et al.* A genome-wide association study identifies IL23R as an inflammatory bowel disease gene. *Science* **314,** 1461–1463 (2006).

49. Tremelling, M. *et al.* IL23R Variation Determines Susceptibility But Not Disease Phenotype in Inflammatory Bowel Disease. *Gastroenterology* (2007). doi:10.1053/j.gastro.2007.02.051

50. Lees, C. W., Barrett, J. C., Parkes, M. & Satsangi, J. New IBD genetics: Common pathways with other diseases. *Gut* (2011). doi:10.1136/gut.2009.199679

51. Bianco, A. M., Girardelli, M. & Tommasini, A. Genetics of inflammatory bowel disease from multifactorial to monogenic forms. *World Journal of Gastroenterology* (2015). doi:10.3748/wjg.v21.i43.12296

52. Abraham, C. & Cho, J. H. IL-23 and Autoimmunity: New Insights into the Pathogenesis of Inflammatory Bowel Disease. *Annu. Rev. Med.* (2009). doi:10.1146/annurev.med.60.051407.123757

53. Huang, C. *et al.* Characterization of Genetic Loci That Affect Susceptibility to Inflammatory Bowel Diseases in African Americans. *Gastroenterology* (2015). doi:10.1053/j.gastro.2015.07.065

54. Glas, J. *et al.* rs1004819 is the main disease-associated IL23R variant in German Crohn's disease patients: Combined analysis of IL23R, CARD15, and OCTN1/2 variants. *PLoS One* (2007). doi:10.1371/journal.pone.0000819

55. Einarsdottir, E. *et al.* IL23R in the Swedish, Finnish, Hungarian and Italian populations: Association with IBD and psoriasis, and linkage to celiac disease. *BMC Med. Genet.* (2009). doi:10.1186/1471-2350-10-8

56. Pidasheva, S. *et al.* Functional studies on the IBD susceptibility gene IL23R implicate reduced receptor function in the protective genetic variant R381Q. *PLoS One* (2011). doi:10.1371/journal.pone.0025038

57. Bank, S. *et al.* Polymorphisms in the inflammatory pathway genes TLR2, TLR4, TLR9, LY96, NFKBIA, NFKB1, TNFA, TNFRSF1A, IL6R, IL10, IL23R, PTPN22, and PPARG are associated with susceptibility of inflammatory bowel disease in a Danish cohort. *PLoS One* (2014).

doi:10.1371/journal.pone.0098815

58. Beaudoin, M. *et al.* Deep Resequencing of GWAS Loci Identifies Rare Variants in CARD9, IL23R and RNF186 That Are Associated with Ulcerative Colitis. *PLoS Genet.* (2013). doi:10.1371/journal.pgen.1003723

59. Fraser Cummings, J. R. *et al.* Contribution of the novel inflammatory bowel disease gene IL23R to disease susceptibility and phenotype. *Inflamm. Bowel Dis.* (2007). doi:10.1002/ibd.20180

60. Lappalainen, M. *et al.* Association of IL23R, TNFRSF1A, and HLA-DRB1*0103 allele variants with inflammatory bowel disease phenotypes in the Finnish population. *Inflamm. Bowel Dis.* (2008). doi:10.1002/ibd.20431

61. Liu, J. Z. *et al.* Association analyses identify 38 susceptibility loci for inflammatory bowel disease and highlight shared genetic risk across populations. *Nat. Genet.* (2015). doi:10.1038/ng.3359

62. Sawa, S. *et al.* RORγt+ innate lymphoid cells regulate intestinal homeostasis by integrating negative signals from the symbiotic microbiota. *Nat. Immunol.* **12,** 320–6 (2011).

63. Mortha, A. *et al.* Microbiota-dependent crosstalk between macrophages and ILC3 promotes intestinal homeostasis. *Science* **343,** 1249288 (2014).

64. Bamias, G. *et al.* Expression, Localization, and Functional Activity of TL1A, a Novel Th1-Polarizing Cytokine in Inflammatory Bowel Disease. *J. Immunol.* (2003). doi:10.4049/jimmunol.171.9.4868

65. Ivanov, I. I. *et al.* Induction of intestinal Th17 cells by segmented filamentous bacteria. *Cell* **139,** 485–98 (2009).

66. Sano, T. *et al.* An IL-23R/IL-22 Circuit Regulates Epithelial Serum Amyloid A to Promote Local Effector Th17 Responses. *Cell* (2015). doi:10.1016/j.cell.2015.08.061

67. Viladomiu, M. *et al.* IgA-coated E. Coli enriched in Crohn's disease spondyloarthritis promote TH17-dependent inflammation. *Sci. Transl. Med.* (2017). doi:10.1126/scitranslmed.aaf9655

68. Sonnenberg, G. F., Mjösberg, J., Spits, H. & Artis, D. Snapshot: Innate lymphoid cells. *Immunity* (2013). doi:10.1016/j.immuni.2013.08.021

69. Sonnenberg, G. F. & Artis, D. Innate lymphoid cells in the initiation, regulation and resolution of inflammation. *Nature*

Medicine (2015). doi:10.1038/nm.3892

70. Sonnenberg, G. F. Transcriptionally defining ILC heterogeneity in humans. *Nature Immunology* (2016). doi:10.1038/ni.3413

71. Mjösberg, J. & Spits, H. Human innate lymphoid cells. *J. Allergy Clin. Immunol.* (2016). doi:10.1016/j.jaci.2016.09.009

72. Melo-Gonzalez, F. & Hepworth, M. R. Functional and phenotypic heterogeneity of group 3 innate lymphoid cells. *Immunology* (2017). doi:10.1111/imm.12697

73. Artis, D. & Spits, H. The biology of innate lymphoid cells. *Nature* **517,** 293–301 (2015).

74. Klose, C. S. N. & Artis, D. Innate lymphoid cells as regulators of immunity, inflammation and tissue homeostasis. *Nat. Immunol.* (2016). doi:10.1038/ni.3489

75. Sonnenberg, G. F., Monticelli, L. A., Elloso, M. M., Fouser, L. A. & Artis, D. CD4(+) lymphoid tissue-inducer cells promote innate immunity in the gut. *Immunity* **34,** 122–34 (2011).

76. Ahn, Y. O. *et al.* Human group 3 innate lymphoid cells express DR3 and respond to TL1A with enhanced IL-22 production and IL-2-dependent proliferation. *Eur. J. Immunol.* (2015). doi:10.1002/eji.201445213

77. Awasthi, A. *et al.* Cutting Edge: IL-23 Receptor GFP Reporter Mice Reveal Distinct Populations of IL-17-Producing Cells. *J. Immunol.* (2009). doi:10.4049/jimmunol.0900732

78. Shih, D. Q. *et al.* Inhibition of a novel fibrogenic factor Tl1a reverses established colonic fibrosis. *Mucosal Immunol.* (2014). doi:10.1038/mi.2014.37

79. Kinnebrew, M. A. *et al.* Interleukin 23 Production by Intestinal CD103+CD11b+Dendritic Cells in Response to Bacterial Flagellin Enhances Mucosal Innate Immune Defense. *Immunity* (2012). doi:10.1016/j.immuni.2011.12.011

80. Hedl, M. & Abraham, C. A TNFSF15 disease-risk polymorphism increases pattern-recognition receptor-induced signaling through caspase-8-induced IL-1. *Proc. Natl. Acad. Sci. U. S. A.* **111,** 13451–6 (2014).

81. Bamias, G., Jia, L. G. & Cominelli, F. The tumor necrosis factor-like cytokine 1A/death receptor 3 cytokine system in intestinal inflammation. *Current Opinion in Gastroenterology* (2013). doi:10.1097/MOG.0b013e328365d3a2

82. Withers, D. R. Innate lymphoid cell regulation of adaptive immunity. *Immunology* (2016). doi:10.1111/imm.12639

83. Maizels, R. M. & Withers, D. R. MHC-II: A mutual support system for ILCs and T cells? *Immunity* (2014). doi:10.1016/j.immuni.2014.07.006

84. Hepworth, M. R. & Sonnenberg, G. F. Regulation of the adaptive immune system by innate lymphoid cells. *Current Opinion in Immunology* (2014). doi:10.1016/j.coi.2014.01.013

85. Bando, J. K. & Colonna, M. Innate lymphoid cell function in the context of adaptive immunity. *Nature Immunology* (2016). doi:10.1038/ni.3484

86. Hepworth, M. R. *et al.* Innate lymphoid cells regulate CD4+ T-cell responses to intestinal commensal bacteria. *Nature* (2013). doi:10.1038/nature12240

87. Cortini, A. *et al.* B cell OX40L supports T follicular helper cell development and contributes to SLE pathogenesis. *Ann. Rheum. Dis.* (2017). doi:10.1136/annrheumdis-2017-211499

88. von Burg, N. *et al.* Activated group 3 innate lymphoid cells promote T-cell-mediated immune responses. *Proc Natl Acad Sci U S A* (2014). doi:10.1073/pnas.1406908111

89. Hepworth, M. R. *et al.* Group 3 innate lymphoid cells mediate intestinal selection of commensal bacteria-specific CD4+ T cells. *Science (80-.).* (2015). doi:10.1126/science.aaa4812

90. Xu, M. *et al.* C-MAF-dependent regulatory T cells mediate immunological tolerance to a gut pathobiont. *Nature* (2018). doi:10.1038/nature25500

91. Griseri, T., Asquith, M., Thompson, C. & Powrie, F. OX40 is required for regulatory T cell–mediated control of colitis. *J. Exp. Med.* (2010). doi:10.1084/jem.20091618

92. Souza, H. S., Elia, C. C. S., Spencer, J. & MacDonald, T. T. Expression of lymphocyte-endothelial receptor-ligand pairs, α4β7/MAdCAM-1 and OX40/OX40 ligand in the colon and jejunum of patients with inflammatory bowel disease. *Gut* (1999). doi:10.1136/gut.45.6.856

93. Yamazaki, K. *et al.* Single nucleotide polymorphisms in TNFSF15 confer susceptibility to Crohn's disease. *Hum Mol Genet* (2005). doi:ddi379 [pii]\n10.1093/hmg/ddi379

94. Michelsen, K. S. *et al.* IBD-associated TL1A gene (TNFSFI5) haplotypes determine increased expression of TL1A protein.

PLoS One (2009). doi:10.1371/journal.pone.0004719

95. Kakuta, Y., Kinouchi, Y., Negoro, K., Takahashi, S. & Shimosegawa, T. Association study of TNFSF15 polymorphisms in Japanese patients with inflammatory bowel disease [9]. *Gut* (2006). doi:10.1136/gut.2006.100297